Development of a speed conversion model for the SKM measured wet skid resistance

D. R. van der Bilt

TU Delft Delft University of Technology

Kiwa KOAC

Cover picture: obtained from Kiwa KOAC

Development of a speed conversion model for the SKM measured wet skid resistance

by

D. R. van der Bilt

in partial fulfilment of the requirements for the degree of

Master of Science
in Structural Engineering

at the Delft University of Technology,
to be defended publicly on day April 23, 2019 at 10:30 AM.

Student number:	4155327	
Project duration:	September 3, 2018 - April 9, 2019	
Thesis committee:	Prof. dr. ir. S. M. J. G. Erkens,	Delft University of Technology
	Ir. L.J.M Houben,	Delft University of Technology
	Dr. ir. K. Anupam,	Delft University of Technology
	Dr. ir. O. Copuroglu,	Delft University of Technology
	Dr. ir. J. Groenendijk,	Kiwa KOAC
	Dr. ir. C. A. P. M. van Gurp,	Kiwa KOAC
	Ir. D. van der Ven,	Kiwa KOAC

An electronic version of this thesis is available at http://repository.tudelft.nl/.

TU Delft Delft University of Technology

Kiwa KOAC

Acknowledgements

In front of you lies the thesis on which I have worked the last seven months. This thesis has been written to fulfil the graduation requirements of the Master's degree in Structural Engineering, with a specialisation in Pavement Engineering, at the Delft University of Technology.

I would like to name a few people who helped me during the project and without whom I would never have achieved this result. First of all, I would like to thank everyone from Kiwa KOAC who made it possible for me to perform this research. Jacob Groenendijk, you really took the time to think about the problems I faced and you were always very critical about my thoughts and ideas (in a positive way). I wish you all the best in your recovery. Christ van Gurp, I do not know anyone who is retired and who works that much. Your feedback and quick responses helped raising my thesis to a higher level in only a very short period of time. Dennis van der Ven, thank you for making it possible to write my thesis in cooperation with Kiwa KOAC. During the days I worked in Nieuwegein your positivity and optimism were very motivating. Furthermore, I would like to thank Eelke Vromans and his team for performing additional measurements and helping me with my questions with respect to the measurements.

Besides the people from Kiwa KOAC I also would like to show my gratitude to everyone from the Delft University of Technology who participated in my graduation committee. Lambert Houben, your feedback, especially with respect to the report, is very much appreciated. You always found small mistakes I did not see after reading my own work too much. Kumar Anupam, although I think we sometimes had some difficulties with understanding each other, you were very helpful and critical with respect to the content of my thesis. Furthermore, Oguzhan Copuroglu, thank you for being willing to take place in my graduation committee. Finally, I would like to thank Sandra Erkens for being the chair of my graduation committee. During the meetings you were very sharp in your ideas and feedback which always helped me to make progress after the meetings.

Last but not least I would like to thank my parents for their support and encouragements, not only during this graduation project but during all the years I enjoyed studying and the student life, which will now really come to an end.

D. R. van der Bilt
Amsterdam, April 2019

Summary

Skid resistance is an important parameter for road safety and therefore it is essential to monitor the skid resistance of pavements. In the Netherlands, skid resistance is measured with either the RWS Skid Resistance Tester —measuring the longitudinal friction coefficient— or the Seitenkraft-Messverfahren (SKM) —measuring the sideway friction coefficient. The latter is nowadays the preferred measurement device by Rijkswaterstaat. Skid resistance depends much on the vehicle speed: the higher the speed, the lower the skid resistance. Furthermore, the texture of the surface influences the speed dependency. Because it is not always possible to measure the skid resistance at target speeds set by Rijkswaterstaat, there is a demand for a speed conversion model for the skid resistance measured with the SKM. The objective of this research is therefore formulated as follows: the development of a speed conversion model for the wet skid resistance, measured with the SKM at different speeds, taking into account the macrotexture of the road surface.

The used dataset consists of 718 sections of 100 metre, measured at the Dutch road network. Measurements were performed at 10 different roads with different pavement layers: porous asphalt, concrete pavements, dense pavements and stone mastic asphalt. The mean profile depth of the pavements varies between 0.21 and 1.80 mm. The performed measuring speeds were 40, 60 and 80 km/h, and for few sections 30 km/h.

Three regression methods were performed. Firstly, a multiple linear regression was performed. The datapoints consisted of combinations of two measurements at different speeds on identical 100 metre sections. The second method estimated per 100 metre section a zero speed intercept which was used as a reference point. The third method used multilevel modelling and includes a hierarchical structure.

Concluded was that the multiple linear regression on speed combinations is inappropriate for the objective of this research, because of two reasons: the datapoints are dependent on each other, and information is lost by splitting the 100 metre sections into datapoints with combinations of two measurements. In the second method, problems arise with estimating the zero speed intercept. The third method is most appropriate for this research and the three-level structure fits best on the dataset. The first level contains the individual measurements on the 100 metre sections, performed at different measuring speeds. The second level consists of the 100 metre sections and the third level consist of the roads on which the measurements took place. The obtained model is as follows:

$$\mu_a = \mu_b \cdot e^{(0.00511 - 0.00195 \cdot \mathrm{MPD}) \cdot (V_b - V_a)}$$

μ_a is the converted skid resistance and μ_b is the measured skid resistance at measuring speed V_b. V_a is the desired measuring speed at which μ_a is calculated and MPD is the measured mean profile depth in millimetres.

The standard error of the model on the training data is 0.032 whereas the average change in skid resistance for two datapoints is 0.053. This average change includes conversions over a speed difference from 10 to 40 km/h. From a sensitivity analysis of the macrotexture it was concluded that if no macrotexture can be measured, it is advised to use a different model in which no macrotexture is included. This model is as follows:

$$\mu_a = \mu_b \cdot e^{0.00323 \cdot (V_b - V_a)}$$

Recommendations for further research include among others registering more accurately the type and age of the measured pavements and extending the dataset with measurements performed at low measuring speeds and on curved sections. Furthermore, it is recommended to perform a more comprehensive outlier analysis and to optimise the hierarchical structure.

Contents

List of Figures

List of Tables

Nomenclature

Abbreviations

-2LL	-2 Log Likelihood	
AC	Asphalt Concrete	
ARAN	Automatic Road Analyser	
ASTM	American Society for Testing and Materials	
AT	Ambient Temperature	[°C]
BASt	Bundesanstalt für Straßenwesen, the German Federal Highway Research Institute	
BFC	Braking Force Coefficient	
CAT	Contained Air Temperature	[°C]
CROW	Dutch knowledge platform for infrastructure	
DAC	Dense Asphalt Concrete	
DGD	Dunne Geluidsreducerende Deklaag (Dutch for Thin Silent Surfacing), sometimes called DGAD	
EB	Epoxy Bitumen	
EFI	European Friction Index	
ESDU	Engineering Sciences Data Unit	
FEHRL	Forum of European national Highway Research Laboratories	
HERMES	Harmonisation of European Routine and research Measuring Equipment for Skid resistance of roads and runways	
IFI	International Friction Index	
LFC	Longitudinal Friction Coefficient	
ML	Maximum likelihood estimation	
MPD	Mean Profile Depth	[mm]
MTD	Mean Texture Depth	[mm]
OAB	Open Asfalt Beton (Dutch for Asphalt Concrete)	
PA	Porous Asphalt, also called Open Graded Friction Course	
PCC	Portland Cement Concrete	
PIARC	Permanent International Association of Road Congresses, World Road Association	
PSNG	Percentage Skid Number-speed Gradient	[%]
PSV	Polished Stone Value	
PT	Pavement Temperature	[°C]
REML	Restricted maximum likelihood estimation	
RMS	Root Mean Square of pavement profile	[mm]
RMSE	Root Mean Square Error (standard error of the residuals)	

RWS	Rijkswaterstaat	
SCRIM	Sideway-force Coefficient Routine Investigation Machine	
SFC	Sideway Friction Coefficient	
SKM	Seitenkraft-Messverfahren	
SMA	Stone Mastic Asphalt	
SN	Skid Number	
SR	Slip Ratio	[%]
SWF	Sideway Force	
TD	Texture Depth	[mm]
TW	Measured water temperature	[°C]
VIF	Variance Inflation Factor	
ZOAB	Zeer Open Asfalt Beton (Dutch for Porous Asphalt)	

Greek Symbols

α	Yaw angle of test wheel	[°]
ϵ_{ij}	Error term	
μ	Measured LFC or SFC	[-]
μ_0	Theoretical friction at 0 km/h slip speed, also zero speed intercept	[-]
μ_s	Friction at slip speed S	[-]
μ_V	Skid resistance at measuring speed V	[-]
μ_x	Longitudinal friction coefficient	[-]
μ_y	Sideway friction coefficient	[-]
μ_{30}	Estimated friction coefficient at the reference slip speed	[-]
μ_{datum}	Coefficient of friction at zero ground speed on a dry surface	[-]
μ_{B60}	Slip-speed corrected estimate for the device specific friction coefficient at a slip speed of 60 km/h	[-]
μ_{BS}	Measured friction coefficient with device B at slip speed S	[-]
μ_{peak}	Peak friction level	[-]
$\mu_{R,T}$	SKM skid resistance normalised for temperature and speed	[-]
$\mu_{x,50}$	LFC at 50 km/h	[-]
$\mu_{x,R}$	Predicted LFC at reference speed R	[-]
$\mu_{x,V}$	Measured LFC at measuring speed V	[-]
$\mu_{y,R}$	Predicted SFC at reference speed R	[-]
$\mu_{y,V}$	Measured SFC at measuring speed V	[-]
ρ	Surface contaminant density	[kg/m^3]

Latin Symbols

b_0	Fixed intercept of overall model fitted to the data	
b_1	Fixed effect for predictive variable X_{ij}	
F_L	Longitudinal friction force between the tyre and surface	[N]

F_s	Side friction force between the tyre and surface	[N]
F_t	Total traction force	[N]
F_v^d	Fluid drag force, dependent on vehicle speed	[N]
F_v^u	Fluid uplift force, dependent on vehicle speed	[N]
F_w	Vertical load or weight (1960 N for the SKM)	[N]
F_x	Total resisting forces acting on the wheel	[N]
p	Tyre inflation pressure	[Pa]
r	Coefficient dependent on positive or negative macrotexture	[-]
S	Slip speed	[km/h]
S_0	Speed constant related to tested surface characteristics	[km/h]
S_p	Speed number	[-]
S_R	Reference slip speed	[-]
S_{peak}	Slip speed at the peak friction level	[km/h]
SR_V	SFC measured at speed V, multiplied by 100	[%]
SR_{50}	Skid resistance $\mathrm{SR_s}$ corrected to 50 km/h multiplied by 100	[%]
T_x	Macrotexture measure	[mm]
u_{0j}	Random intercept for group j	
u_{1j}	Random effect for variable X_{ij}, for group j	
V	Measuring speed of the vehicle	[km/h or m/s]
V_p	Average peripheral speed of tyre	[km/h]
V_R	Reference measuring speed	[km/h]
X_{ij}	Predictive variable	
Y_{ij}	Observed value i belonging to group j	
R^2	Coefficient of determination	[-]
SN_0	Zero speed intercept	[-]

1 Introduction

This chapter provides an introduction to the study. Firstly, Section 1.1 gives a background into the topic. After that, Section 1.2 defines the scope of the research. In Section 1.3, the research objective and research questions are posed, followed by the methodology of the research in Section 1.4 and an outline of the report in Section 1.5.

1.1. Background information

Skid resistance is an important parameter for road safety. A road surface needs to be sufficiently skid resistant in order to offset the horizontal forces, that can be present in the contact area between the tyre and road surface. These frictional forces develop during vehicle movements such as steering, braking and accelerating (Vos et al., 2017). Much research showed that if the road surface does not provide enough skid resistance, the risk of accidents increases (e.g. Kogbara et al., 2016 and Fwa, 2017). Skid resistance depends much on the vehicle speed. The higher the speed, the lower the skid resistance. Furthermore, the texture of the surface highly influences the speed dependency.

Because the skid resistance is an important parameter of the road surface, most European countries developed their own skid resistance policies and measuring devices (Vos and Groenendijk, 2009). These policies regulate, for example, how often the skid resistance needs to be measured, which devices should be used, and which target values should be specified to compare the measurement results with. Since countries developed these policies themselves, these policies differ from each other and comparison of the different skid resistance values is not easy (Vos and Groenendijk, 2009).

Rijkswaterstaat (RWS) is the responsible authority for the design, construction, management and maintenance of the main infrastructure facilities in the Netherlands. Until 2013, their own developed RWS Skid Resistance Tester was the device in use for measuring the skid resistance in the Netherlands. Measurements with this device should be performed at 50 or 70 km/h, but often this was not possible, for example at roundabouts. Because besides the speed, also the texture influences the skid resistance, RWS developed a speed conversion model that uses as input whether the asphalt layer is open or dense. However, only taking into account open or dense asphalt layers is often not accurate enough. Therefore, Koac•NPC (now Kiwa KOAC) developed a speed conversion model to convert the skid resistance measured at a speed lower than 50 km/h up to the skid resistance at exactly 50 km/h with the mean profile depth (MPD) as an input parameter representing the surface texture.

In 2013, RWS perceived the idea of changing the skid resistance measuring method. After a comprehensive research to the existing measuring devices, the Netherlands decided to cooperate with Germany and started using the German Seitenkraft-Messverfahren (SKM), a device which measures according to the sideway force (SWF) method (Scharnigg et al., 2016). With the change of measuring device, RWS had to define new target values to compare the measurement results with. These values are defined at measuring speeds of 40, 60 and 80 km/h, which are the standard measuring speeds for the SKM. However, the SKM is a large truck and often it is not possible to perform the measurements at these speeds, such as at roundabouts. Also, during measurements on highways, traffic jams could lower the

maximum possible speed resulting in a measurement at a speed of, for example, 70 km/h. Unfortunately, for the SKM, an accurate speed conversion model does not exist yet. Therefore, in the case of roundabouts, measurements are often still performed with the RWS Skid Resistance Tester. In the case of traffic jams, measurements have to be performed one more time, which evidently costs more money.

Evidently, it would be helpful if measurements could be performed at other speeds than the standard set measuring speeds, which is possible for the RWS Skid Resistance Tester. In Germany, a basic speed conversion model is in use, which applies a linear correlation between the skid resistance of 30 up to 90 km/h. This model does not incorporate the macrotexture, a parameter which does certainly influence the skid resistance. Especially considering that Germany has many dense wearing courses, while in the Netherlands much more open wearing courses are present, a different correlation of skid resistance and speed is expected. Therefore, there is a demand for a research in the subject of a more precise speed conversion model for the skid resistance measured with the SKM.

1.2. Scope

Much research can be done in the theme of speed conversion models for and measuring of skid resistance. This research will purely focus on a conversion model for the wet skid resistance measured with the SKM, with the macrotexture as an influencing parameter, independent of the standards set by Rijkswaterstaat. Furthermore, the correlation between the measured values with the SKM and the RWS Skid Resistance Tester, another actual topic, is considered beyond the scope. Measurements used in the development of the conversion model are limited to the right-hand traffic lane, the traffic lane were measurements are usually performed.

1.3. Research objective and research questions

As becomes clear from Section 1.1, Kiwa KOAC would like to develop a conversion model for the skid resistance measured with the SKM, using the macrotexture as one of the input parameters. With this conversion model it would become easier to perform skid resistance measurements with the SKM, because measurements performed at different speeds could then be used.

The research objective for this study is formulated as follows:

The development of a speed conversion model for the wet skid resistance, measured with the SKM at different speeds, taking into account the macrotexture of the road surface.

In order to achieve this objective a main research question and a couple of sub-questions are posed below. The sub-questions are specific and contribute to the more general main question.

Main question

How can the correlation between the SKM measured skid resistance at different speeds be described, taking into account the macrotexture of the road surface?

Sub-questions

Several sub-questions are formulated, which together should facilitate answering to the main questions.

1. Which factors are of influence on the skid resistance and which should be taken into account in the development of the conversion model?
2. Which kind of road sections could lead to difficulties during measurements with the SKM? Are deviating correlations expected on these sections?
3. What speed conversion models for the skid resistance, used in the Netherlands or used for the SKM, have been developed previously?
4. Which data is needed for developing the model?
5. Which models can be developed in order to, in the end, achieve the best fitted model to represent the correlation between the skid resistance at different speeds?
6. How reliable is the final model?

1.4. Methodology

This research is separated into 4 phases. An overview of the different phases and intermediate steps is provided in Figure 1.1.

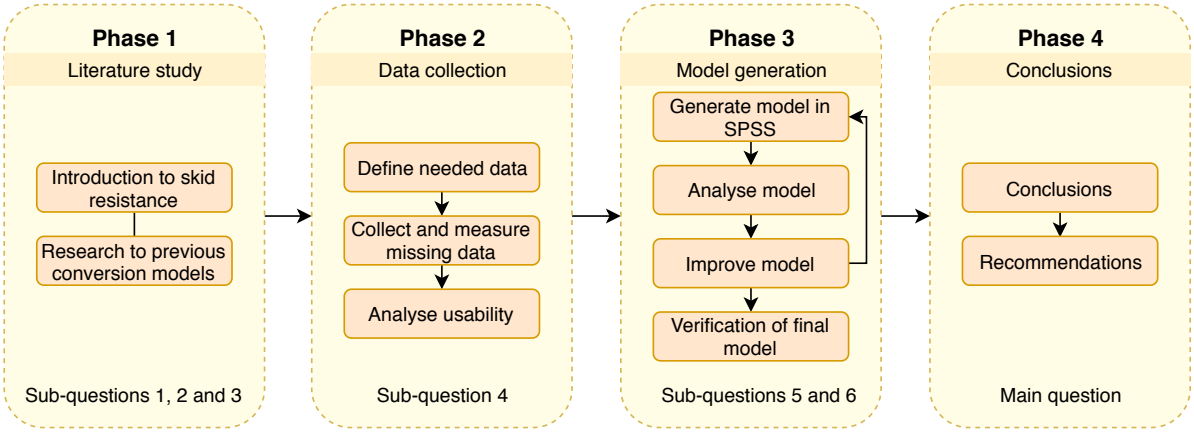

Figure 1.1: Research framework

Sections 1.4.1 to 1.4.4 give an elaborated explanation of the different phases.

1.4.1. Phase 1: Literature study

The first phase consists of an exploratory research and this will be performed with the help of a literature study. The objective of this phase is to fully understand the current situation of the research topic. Primary knowledge about skid resistance is obtained and a study to the conversion models, used or previously developed for skid resistance measurements, is conducted. At the end of the literature study the requirements for the model, which will be generated in a later phase of this study, should be clear.

1.4.2. Phase 2: Data collection

During the second phase, as much data as possible which is needed for the modelling process is obtained. First, a list with requirements of the data will be formed. Secondly, this data will be searched for in the database of Kiwa KOAC. Non available data will be measured (if possible). The obtained data will be prepared for the model generation and analysed according to its usability.

1.4.3. Phase 3: Modelling

The model generation takes place during the third phase. First, a hypothesis about the correlation will be set up. This will be done with the help of the literature research to existing conversion models. Then, with help of SPSS, a conversion model for the skid resistance to different speeds will be generated. Starting with a basic version, an iterative process will follow to obtain a model as precise as possible within the available time. The following models could, for example, be generated:

- considering no macrotexture;
- considering open or dense asphalt;
- considering the MPD as a parameter;
- considering the MPD and positive/negative macrotexture as parameters; and
- considering a straight section, a left and a right curved road section.

In all above, distinction can be made between new and older pavement layers.

After the literature study and the data collection the different models to be generated will be sharpened, because during these phases it will, for example, become clear which road sections are expected to have difficulties and deviating correlations, and which data can be measured.

When the final model is obtained, it will be determined how reliable the final model is. During the literature research, existing models will be analysed. It is expected that at the end of the literature study, it will be clear how to determine the reliability of the generated speed conversion model.

1.4.4. Phase 4: Conclusions

Phase 4 is the final stage of the research. Final conclusions are formulated and recommendations for further research on this topic are given.

1.5. Outline of the report

Figure 1.2 provides an overview of the outline of this report. The literature study is provided in Chapters 2 to 4. Chapter 2 gives an introduction to skid resistance: important aspects and influencing factors of skid resistance are mentioned, whereas Chapter 3 explains more about the two measuring methods for measuring skid resistance which are used in the Netherlands. Chapter 4 focuses on speed conversion models which were previously developed. The model generation is explained in Chapter 5, based on the data as explained in Appendix C. A verification of the final obtained model is given in Chapter 6. Finally, the conclusions of this research and recommendations for further research are given in Chapter 7.

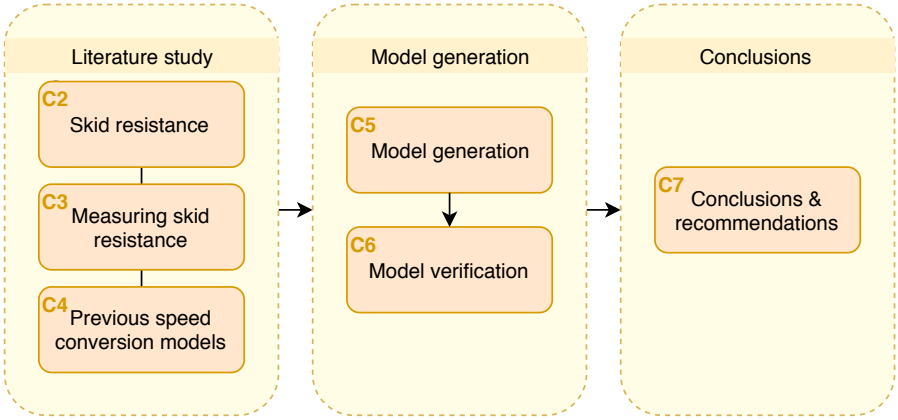

Figure 1.2: Outline of the report

2

Introduction to skid resistance

This chapter provides an introduction into the topic of skid resistance. Section 2.1 gives an explanation of what skid resistance is and explains the principle of how skid resistance is measured. The subsequent paragraphs give more detailed information about some important aspects of skid resistance, which include the effect of pavement texture (Section 2.2), adhesion and hysteresis (Section 2.3) and influencing parameters (Section 2.4). Section 2.5 outlines possible physical explanations for the speed dependency of skid resistance and finally, Section 2.6 gives the conclusions of this chapter.

2.1. What is skid resistance

In order to prevent losing control of a vehicle, horizontal forces are needed which arise from tyre-pavement friction. The tyre-pavement friction coefficient is the ratio of the tangential friction force F between the tyre and surface, which resists the motion, to the perpendicular force F_w, which is the vertical load (Hall et al., 2009 and O'Flaherty, 2002). Tyre-pavement friction depends on many factors, that can be separated into different categories: pavement properties, tyre properties, the interface and other conditions (Mataei et al., 2016, Groenendijk, 2018).

Skid resistance is used to refer to the extent to which the pavement properties contribute to the tyre-pavement friction (Roe et al., 1998), measured under standardised conditions (Vos et al., 2017). The extent to which tyre properties contribute to the tyre-pavement friction is often called grip. Skid resistance can be measured by measuring the tyre-pavement friction coefficient (further indicated in this report by the 'friction coefficient') under standardised conditions. These conditions are set for, for example, the tyre that is used and the interface.

When using dynamic measuring equipment, a measuring wheel that measures the friction force is mounted. These wheels can be mounted in different ways, namely in the direction of travel or under an angle to the direction of travel —the yaw angle. A different friction force is measured with these different mountings, and thus a different friction coefficient is calculated. This is explained in the following two sections.

2.1.1. Longitudinal friction coefficient

The longitudinal friction coefficient (LFC) is of importance when a vehicle is braking, and therefore the LFC is also called the braking friction coefficient (BFC). With help of a wheel mounted in line with the direction of travel the LFC can be measured. The measuring wheel is forced to rotate more slowly than the forward speed of the vehicle, so that a slip speed lower than the vehicle speed arises (Section 2.4.5 explains more about the slip speed). This results in a friction force in the opposite direction of the travel direction of the vehicle. Figure 2.1 shows a simplified diagram of the forces acting on a rotating wheel and Figure 2.2 shows the free body diagram for a wheel measuring the LFC.

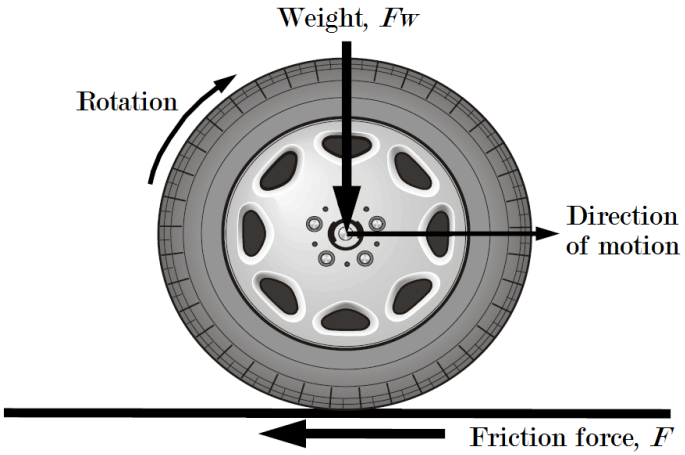

Figure 2.1: Simplified diagram of forces acting on a rotating wheel (Hall et al., 2009)

Figure 2.2: Force-body diagram for the longitudinal friction coefficient (adapted from Flintsch et al., 2012)

The LFC is calculated as:

$$\mu_x = \frac{F_L}{F_w} \tag{2.1}$$

Where:	μ_x	=	Longitudinal friction coefficient	[-]
	F_L	=	Longitudinal friction force between the tyre and surface	[N]
	F_w	=	Vertical load or weight	[N]

2.1.2. Sideway friction coefficient

The sideway friction coefficient (SFC) plays a role when a car is steering. To measure the SFC, a wheel is mounted under an angle to the direction of travel: the yaw angle. The measuring wheel can freely rotate in its longitudinal direction, but this is not the same direction as the vehicle travels. Therefore, the tyre is made to slip over the road surface. The resulting force along the wheel axle is now measured and denoted as the sideway force (Flintsch et al., 2012). This method is called the Sideway Force (SWF) method. The SKM is a device measuring according to the SWF method. Figure 2.3 shows the force-body diagram of a measuring wheel under a yaw angle.

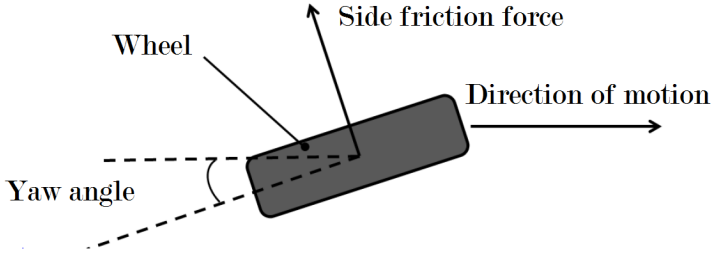

Figure 2.3: Force-body diagram for the sideway friction coefficient (Flintsch et al., 2012)

The SFC is calculated as:

$$\mu_y = \frac{F_s}{F_w} \tag{2.2}$$

Where:				
	μ_y	=	Sideway friction coefficient	[-]
	F_s	=	Side friction force between the tyre and surface	[N]

The friction coefficient is a dimensionless coefficient, hence the units of the vertical force F_w and the horizontal or sideway friction force can be other than Newton, as long as the units are equal.

2.1.3. Devices for measuring skid resistance

In the Netherlands, during the last years, two different devices have been used for measuring skid resistance. The oldest device is the RWS Skid Resistance Tester, introduced in 1959, measuring the LFC. In 2017, the SKM was introduced, a device measuring according to the SWF method (Vos et al., 2017; Kiwa KOAC, 2016).

The original version of the SKM is developed around 1960 in the UK and is called the Sideway-force Coefficient Routine Investigation Machine (SCRIM). This device was already used in several countries, and in the nineties of the previous century Germany constructed the SKM (Derksen, 2017). For the Netherlands, changing the measuring device to the SKM was a step into the direction of standardisation of the devices for measuring skid resistance.

Chapter 3 provides more information about measuring skid resistance.

2.2. Pavement texture

Skid resistance is largely influenced by the pavement texture. The surface texture characteristics are known as microtexture, macrotexture, megatexture, and roughness. The Permanent International Association of Road Congresses (PIARC, the World Road Association) defined the scales of the surface texture according to the wave lengths (see Figure 2.4) of the deviations as follows (Kogbara et al., 2016):

- microtexture: wavelengths from 0 mm to 0.5 mm
- macrotexture: wavelengths from 0.5 mm to 50 mm
- megatexture: wavelengths from 50 mm to 500 mm
- unevenness: wavelengths from 500 mm to 50 m

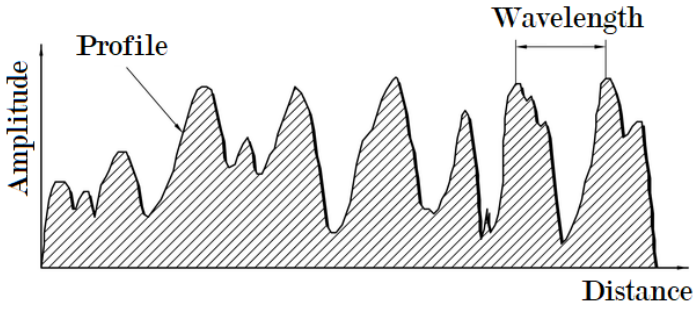

Figure 2.4: Illustration of the wavelength that defines microtexture, macrotexture, megatexture and unevenness (adapted from NEN, 2004)

The megatexture and unevenness are, for example, characterised by potholes, construction deformations due to vehicle loadings (Kogbara et al., 2016) and non-uniform subsoil settlements. The two textures with the smallest wavelengths, microtexture and macrotexture, are the texture characteristics contributing to the friction properties. This is explained in more detail in Sections 2.2.1 and 2.2.2.

2.2.1. Microtexture and macrotexture

Where macrotexture is typically formed by the shape and size of the aggregate particles (Kogbara et al., 2016), microtexture outlines the texture of the stone itself on a microscopic scale. Figure 2.5 shows the difference between the micro and macrotexture.

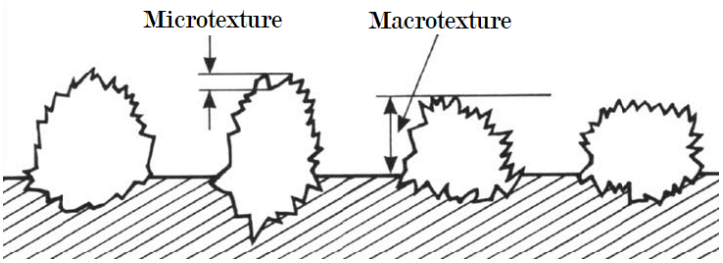

Figure 2.5: Micro and macrotexture of the road surface (Sahhaf and Rahimi, 2014)

The Mean Profile Depth (MPD) is often used as the characterising parameter for the macrotexture, sometimes enhanced with the Root Mean Square (RMS).

The MPD can be defined as the average value of the profile depth over a certain distance, this distance is called the baseline (NEN, 2004). The MPD can then be calculated as the average of the two peaks on the two half baseline minus the profile average, see Figure 2.6.

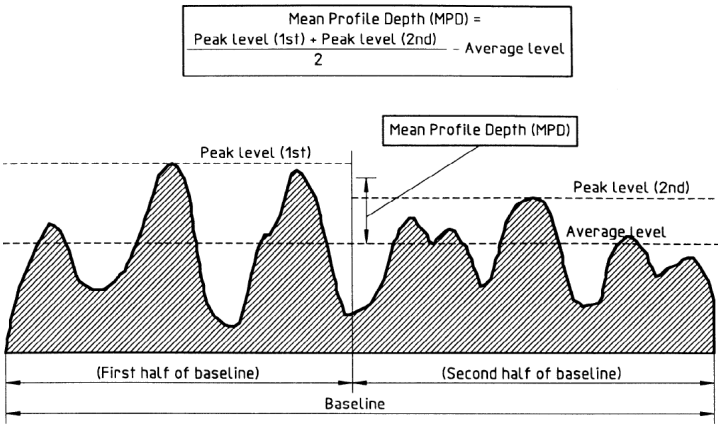

Figure 2.6: Illustration of the MPD (adapted from NEN, 2004)

The MPD quantifies the drainage capabilities of a non-porous pavement surface. For a non-porous surface with a lower MPD, the friction will decrease rapidly with increasing speed (Fuentes, 2009). In case of a porous surface, the drainage is mainly provided by the porosity of the asphalt and the friction decreases less with an increasing speed.

Different methods exist for measuring the MPD; the SKM measures the MPD with a laser. Since the laser covers only a limited scan width, the MPD is a two dimensional measured parameter rather than a three dimensional parameter, although the test result is commonly used as three dimensional information. Important is knowing that during wet measuring conditions this laser does not work properly.

The RMS is a statistical value and outlines how much the measured profile deviates from the MPD (McGhee and Flintsch, 2003). The RMS can be calculated as follows (Fuentes, 2009):

$$RMS = \frac{1}{N-1}\sum_{i=1}^{N} Y(i)^2 \tag{2.3}$$

Where: $Y(i)$ = Elevation of the profile at the ith sample point
N = Sample size

2.2.2. Positive and negative textures

For the macrotexture, a distinction can be made between positive and negative textures. A positive macrotexture is characterised by sharp particles bulging out of the surface (see Figure 2.7a), whilst a negative texture is characterised by a flat surface, with the texture consisting of troughs (see Figure 2.7b) (Groenendijk, 2011).

(a) Positive texture (b) Negative texture

Figure 2.7: Positive and negative macrotextures

When the MPD and RMS of a road section are known, one can determine if the texture is positive or negative (Groenendijk, 2011):

$$\frac{\text{MPD}}{\text{RMS}} > 1.58 : \text{positive macrotexture} \tag{2.4a}$$

$$\frac{\text{MPD}}{\text{RMS}} < 1.58 : \text{negative macrotexture} \tag{2.4b}$$

A positive macrotexture is primarily found in surface treatments of dense wearing courses, a negative macrotexture is characteristic for stone mastic asphalt (SMA) and porous asphalt[1] (PA) layers. With an equal depth of the macrotexture (and an equal microtexture) a positive macrotexture often has a slightly higher skid resistance and a lower speed dependency than the skid resistance of a pavement with a negative macrotexture (Vos et al., 2017).

2.3. Adhesion and hysteresis

The two physical processes of the friction between tyre and road surface are adhesion and hysteresis. Figure 2.8 illustrates these components.

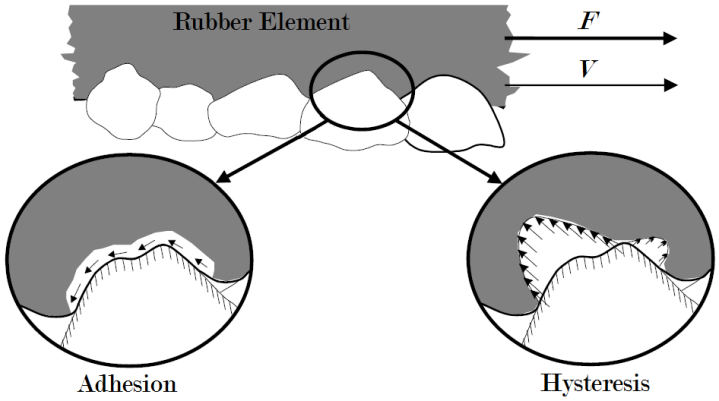

Figure 2.8: Key mechanisms of tyre-pavement friction (adapted from Hall et al., 2009)

As Figure 2.8 shows, particularly the microtexture of the surface contributes to adhesion. The adhesion force is developed at molecular level and is a function of their surface free energy components (Al-Assi and Kassem, 2017). A force arises due to an interface shear strength over a certain contact

[1] In Dutch: Zeer Open Asfalt Beton (ZOAB), dubbellaags ZOAB, and sometimes, but less often, Dunne Geluidsreducerende Deklagen (DGD or DGAD, Dutch for thin silent surfacing)

area. Therefore, the adhesion friction is dominant for smooth surfaces under dry conditions and at low speeds. When a water film is present on a pavement, the microtexture is covered with this water film and therefore adhesion is not dominant at wet surfaces. On wet and rough-textured pavements, hysteresis becomes dominant (Hall et al., 2009).

Figure 2.9 shows the stress-strain diagrams for both elastic (Figure 2.9a) and viscoelastic (Figure 2.9b) behaviour of a material. Hysteresis is caused by tyre deformations due to the pavement macrotexture. Because rubber is a viscoelastic material, the tyre does not immediately revert to its original state after the excitation is released —in contrary to elastic materials. A certain delay is present between the stress release and the deformation to its original state. This delay is called hysteresis and is accompanied by a dissipation of heat, which is an energy loss (Michelin, 2001). The energy loss leaves a frictional force which increases the tyre-pavement friction (Hall et al., 2009). Thus, the higher the energy dissipation, the higher the skid resistance.

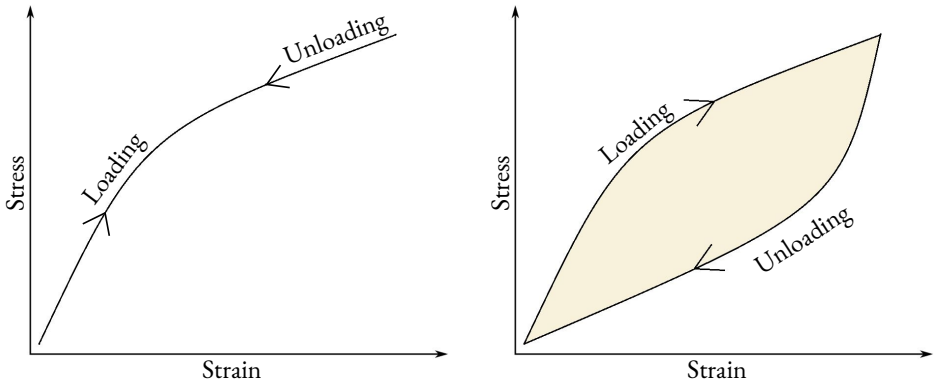

(a) Stress-strain diagram of an elastic material: the material immediately reverts to its original state after the stress is released.

(b) Stress-strain diagram of a viscoelastic material: a delay is present between the stress release and the deformation to its original state, indicated by the shaded area. The larger the shaded area, the larger the hysteresis and the more energy is dissipated.

Figure 2.9: Stress-strain diagrams for elastic and viscoelastic materials, showing the hysteresis loss for a viscoelastic material.

The total friction force F is the sum of the two forces developed due to adhesion and hysteresis (Hall et al., 2009).

2.4. Factors influencing skid resistance and its measurements

Tyre-pavement friction is influenced by many factors. When considering skid resistance, one tries to measure the contribution of the road surface to the tyre-pavement friction, meaning keeping all other factors constant and often at standardised conditions. When discussing factors influencing skid resistance, one should distinct factors influencing the slipperiness of the road surface, measured by the skid resistance, and factors influencing skid resistance *measurements*. Factors influencing the slipperiness of the road surface are factors relating to the pavement properties, whereas factors influencing skid resistance measurements are all other factors influencing the friction coefficient.

Standardised conditions are set for factors influencing these measurements, however, if the experienced conditions differ from the standardised conditions, this could influence the measured value of the skid resistance. In the ideal situation, the influences of these deviating circumstances would be exactly known such that the skid resistance under standardised conditions can be calculated from the measured skid resistance.

The factors influencing skid resistance and its measurements can be separated into several categories (Mataei et al., 2016, Groenendijk, 2018), as is shown below. Some of these factors are already explained in previous sections, because knowledge of these aspects is needed for understanding the basics of skid resistance. Other influencing factors are elaborated in more detail in the following sections.

- Pavement properties
  - Micro and macrotexture (Section 2.2.1)
  - Porosity: not separately explained, because it correlates with other factors such as the micro and macrotexture or wet and dry conditions
  - Age (Section 2.4.6)
- Interface
  - Wet and dry skid resistance (Section 2.4.1)
  - Layer thickness (also explained in Section 2.4.1)
  - Properties of the interface (viscosity, density)
  - Contaminants (Section 2.4.2)
- Measurement conditions
  - Temperature (Section 2.4.3)
  - Vehicle speed (Section 2.4.4)
  - Slip ratio and yaw angle (Section 2.4.5)
  - Slip speed (Section 2.4.5)
- Tyre properties (Section 2.4.7)
  - Tyre size, pattern and tread depth
  - Inflation pressure and wheel loading
  - Rubber properties (e.g. hardness, stiffness)

Because the measurements are performed under standardised conditions, care should be taken that measurements comparing skid resistance at different speeds should be performed with all other influencing factors, such as tyre conditions, kept as constant as possible. Temperature is also a desirable factor to keep constant, but this is of course not a parameter that can be kept constant. Therefore, for temperature a correction factor is applied.

2.4.1. Wet and dry conditions

A distinction should be made between wet and dry skid resistance. Dry skid resistance is measured at dry conditions, whilst wet skid resistance is, as the name indicates, measured at wet conditions. At dry conditions there is contact between the pavement layer and tyre, whereas at wet conditions the water acts as an interface between the pavement and tyre. A car driver can experience both wet and dry conditions in real life, thus it is important to know which of the two is critical.

In wet conditions, the tyre needs to drain the water through its profile and through the pavement macrotexture and porosity. The more water standing on or running over the road, the more problems a tyre can have with draining this water. Compared to dry conditions, a very thin water film decreases already significantly the skid resistance, as is shown in Figure 2.10. At a water layer thickness of 2-3 mm, the skid resistance will reach its minimum, after which the skid resistance can slightly increase with an increasing water layer thickness. However, Welleman (1977, as cited in Groenendijk (2015)) states that this is not real tyre-pavement friction but water drag, hence this does not contribute to steering and breaking manoeuvres.

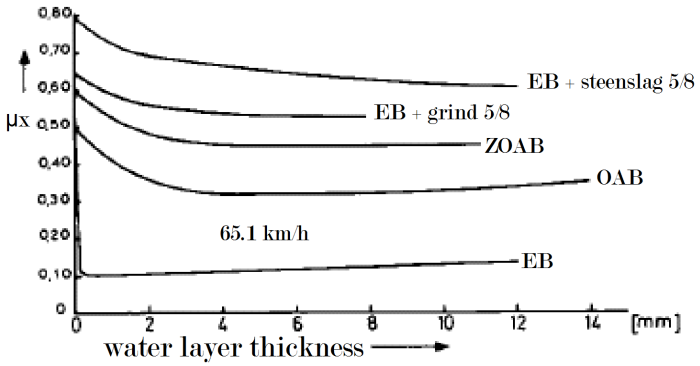

Figure 2.10: Wet friction coefficient μ_x as a function of the water layer thickness for a speed of 65.1 km/h and 5 different pavement layers (Welleman (1977), as cited in Groenendijk (2015))

The different pavement layers shown in Figure 2.10 are:

- epoxy bitumen + chippings 5/8 (EB + steenslag 5.8): pavement with a high micro and macro texture,
- epoxy bitumen + gravel 5/8 (EB + grind 5.8): pavement with a high macro texture and a lower micro texture than EB + steenslag 5.8,
- porous asphalt (ZOAB): pavement with a lower macro texture than the first two, but with a high porosity,
- asphalt concrete (OAB, Open Asfalt Beton): pavement with less porosity and less macrotexture than the ZOAB layer, and
- epoxy concrete, not gritted (EB): dense pavement with a smooth surface.

As can be observed in the graph, the lower the microtexture of the surface, the lower the starting value of the friction coefficient. Furthermore, the pavement with the highest macro textures (EB + steenslag, EB + grind and ZOAB) have the smallest decline in skid resistance.

Moore (1966, as cited in Flintsch et al. (2012)) proposed the Three Zone Concept to better understand the concept of wet friction. This three zone concept is shown in Figure 2.11.

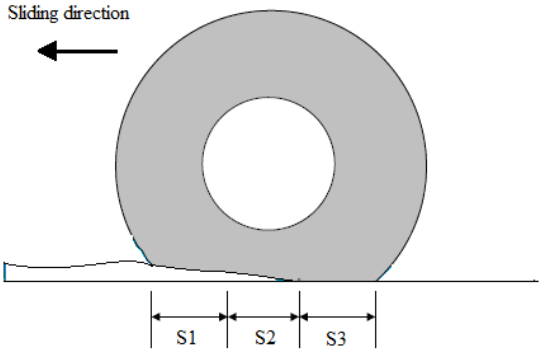

(a) The three zones: in zone 1 there is pressurised drainage of water, zone 2 is the visco-dynamic zone and zone 3 is the dry contact zone

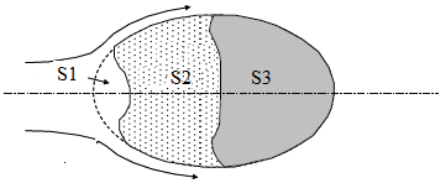

(b) Top view of the three zone concept at low vehicle speed

Figure 2.11: Three zone concept of Moore, (Moore (1966), as cited in Flintsch et al. (2012))

The next sections give an explanation of the different zones.

Zone 1: pressurised drainage of water

In the first zone, the water is drained by the macrotexture of the pavement. The rougher the surface, the more water is dispersed. If not all water is dispersed by the macrotexture, the design of the tyre tread plays an important role as drainage channel. The viscosity and velocity gradient of the water film play an important role for the developed friction. In zone 1, an uplift force of the water is present. If this uplift force generated on the tread is equal to the wheel loading, hydroplaning can occur (Michelin, 2001). However, this only occurs under extreme circumstances (Browne (1975), as cited in Fenghua (2013)).

Zone 2: visco-dynamic zone

In zone 2, the combined zone, some uplift pressure is present, but not as significant as in zone 1. Generally, the microtexture is responsible for draining the water (Flintsch et al., 2012).

Zone 3: actual contact zone

In zone 3, dry contact between the tyre and road surface is obtained. Both adhesion and hysteresis play a role (Flintsch et al., 2012).

If the pavement has a large macrotexture and porosity, the drainage capacity of the road will be larger and less water is left over for the tyre to drain, which means the wet skid resistance will be larger. In most situations the wet skid resistance is critical for the purpose of safety (Vos et al., 2017) and therefore usually the wet skid resistance is measured. Therefore, when skid resistance is mentioned in this thesis without specifying wet or dry conditions, the wet skid resistance is meant.

2.4.2. Contaminants

Besides water, other materials can act as lubricant between the pavement surface and tyre. These contaminants —such as sand, salt and lubricating oil— form a coating over the pavement layer and therewith decrease the value of skid resistance (Lubis et al., 2018). Lubis et al. showed with help of the British Pendulum Tester that both flexible and rigid pavements decreased in skid resistance after applying contaminants, varying from 20% up to 50%. For rigid pavements this decrease was slightly higher (approximately 1-2%) than for flexible pavements.

2.4.3. Temperature

Many literature sources show that temperature has a significant effect on the skid resistance. Especially the temperature of the thread area is important and the contained air temperature (CAT) —the temperature of the air inside the tyre's air chamber— is an indicator of this temperature. Besides the CAT one can distinguish pavement temperature (PT), ambient (air) temperature (AT), and the water temperature used in wet friction measurements.

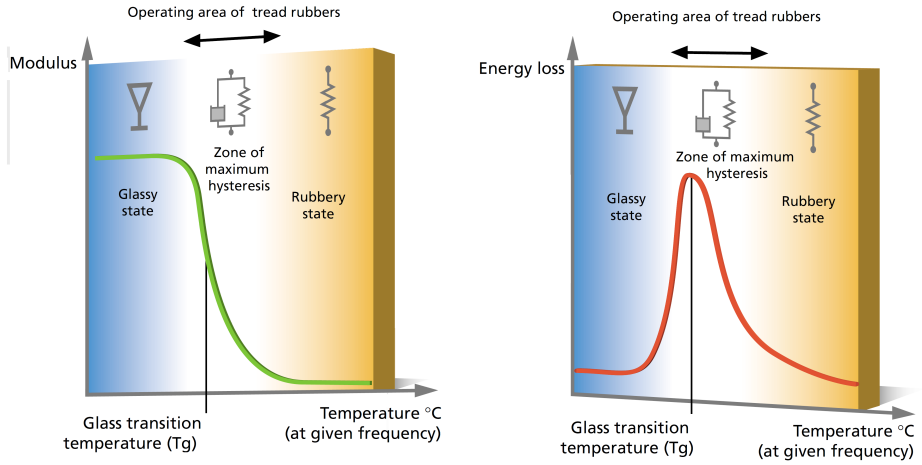

(a) Modulus (b) Energy loss

Figure 2.12: Influence of temperature on the energy loss and modulus (Michelin, 2001)

Figure 2.12 shows the influence of the rubber tyre temperature on the modulus and energy loss. Because of the visco-elastic behaviour of rubber, friction decreases with increasing temperature (Fuentes, 2009). The hysteresis component of friction mainly depends on the rubber stiffness (Anupam et al., 2013). With an increasing temperature, due to the visco-elastic behaviour of rubber, the rubber stiffness decreases. Rubber resilience increases and hysteresis losses become smaller, which combined give a reduced skid resistance (Kogbara et al., 2016). Therefore, during winter the skid resistance of a wet road surface is often larger than during summer (Hosking and Woodford, 1976a).

Anupam et al. (2013) list many researchers who investigated the influence of temperature on the skid resistance. These researchers concluded that in general, a higher temperature lowers the skid resistance. Anupam et al. (2013) also showed with help of a thermomechanical friction model that a higher PT, AT and CAT would always result in a lower hysteresis friction for a given pavement surface and a given tyre slip ratio. Srirangam (2015) cited from previous research (Oliver (1980), Jayawickrama and Thomas (1981), Hill and Henry (1981) and Hosking (1992)) that both AT and PT significantly influence the temperature of the tyre, which in turn influences the skid resistance, whilst the water temperature has a negligible effect on the measured friction coefficients.

Bazlamit and Farhad Reza (2005) recommended that skid numbers obtained at any arbitrary temperature should be normalised with respect to, for example, a value at a reference temperature. Nowadays, when measuring skid resistance with the SKM, a temperature correction for the PT and water temperature is applied according to the TP Griff-StB (SKM) (see Equation (4.17)). Remarkable is that Srirangam (2015) cited from previous research that the water temperature has a negligible effect on the measured friction coefficient, whereas the TP Griff-StB (SKM) applies a correction factor for the water temperature. This correction factor followed from practical research and might be explained by the fact that the water temperature could influence the temperature of the tyre or the CAT, due to which the skid resistance does change.

Temperature effects on skid resistance is an actual theme of research and is beyond the scope of this research. However, during the data analysis temperature variations should be taken into account. A correction factor for deviating temperature circumstances will be used to compare skid resistance measurements converted to the same reference temperatures. The corrections of TP Griff-StB (SKM)

will be applied, which corrects the water and pavement temperature to a 'standard' temperature of $20°C$. However, as shown in this section, temperature influence is an actual topic of research. The accuracy of the applied temperature correction is therefore not taken into further consideration.

2.4.4. Vehicle speed

As mentioned in the introduction, the vehicle speed has a large influence on the friction coefficient. The friction coefficient is highest for both dry and wet conditions at a low speed, whereas at increasing speed the friction coefficient will decrease —especially for wet roads (Vos et al., 2017). This can be explained by the fact that during wet conditions and at an increasing speed, the tyre needs to drain more water per second and therefore the tyre can loose the contact with the pavement (Groenendijk, 2011). Because the macrotexture can help the drainage of water, as explained in Section 2.4.1, the extent to which the wet friction coefficient decreases with an increasing speed mainly depends on the macrotexture. On the other hand, the macrotexture primarily defines the level of friction at low speeds (Mataei et al., 2016). Figure 2.13 illustrates the decrease of the friction coefficient with an increasing speed for different textures.

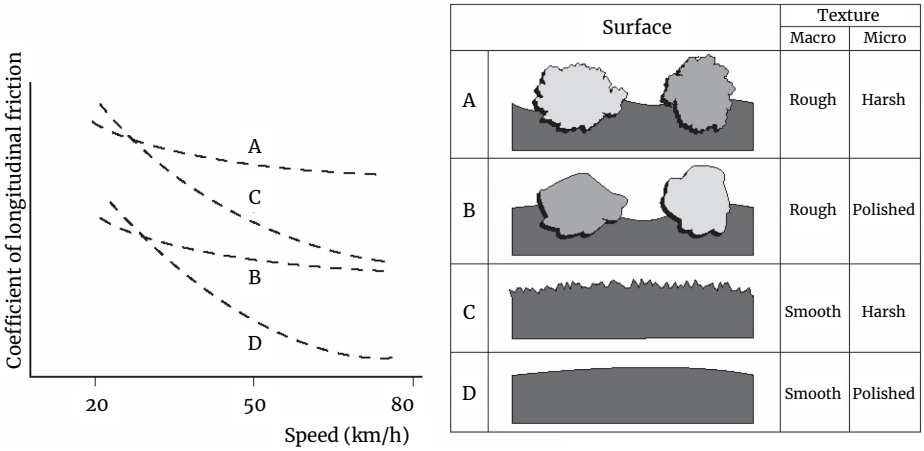

Figure 2.13: Speed dependency and effect of micro and macrotexture on the friction coefficient (PIARC World Road Association (2003), as cited in Wilson (2006))

Mechanisms behind effect of increased vehicle speed

This section explains several mechanisms which could cause the change in skid resistance with an increasing speed.

- **Three Zone Concept for increased vehicle speed**

The three zone concept of Moore is discussed in Section 2.4.1. Besides Figures 2.11a and 2.11b, Moore (1966, as cited in Fenghua (2013)) gave a top view of the three zone concept with an increased vehicle speed, as is shown in Figure 2.14.

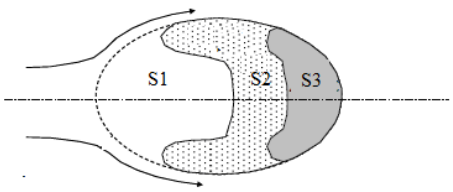

Figure 2.14: Top view of three zone concept with high vehicle speed (Moore (1966), as cited in Flintsch et al. (2012)). Compared to the low vehicle speed as shown in Figure 2.11b, the area of S1 increased and the areas of S2 and S3 decreased.

Clear differences can be seen between Figures 2.11b and 2.14. Zone 1 is larger for a higher speed,

indicating a larger wet area in front of and under the tyre, and thus a larger area where an uplift force of the water on the tyre works. A larger part of the vertical force is offset by the uplift force of the water, indicating a smaller vertical force acting on zone 3, where the adhesion and hysteresis forces arise. This gives a lower skid resistance. At a certain vehicle speed, the vehicle will fully loose its contact with the pavement and hydroplaning occurs. This can result from a too shallow tyre profile, a too thick water film or a too high vehicle speed —or a critical combination (Anupam, 2012; Flintsch et al., 2012). The slip ratio is now uncontrolled and braking traction and directional control stability is prevented (Anupam, 2012).

The main hypothesis in this study is that the mechanism described above is predominantly responsible for the decreased skid resistance at increasing speeds. However, another mechanisms gives an alternative hypotheses.

- **Increased excitation frequency**

Another effect of an increased vehicle speed is the increased excitation frequency. At low vehicle speeds the tyre deforms slowly and the rubber behaves reasonably elastic. The tyre has enough time to revert to its original state before the subsequent excitation. Its hysteresis is low and so is the hysteresis component of the skid resistance. However, when increasing the vehicle speed and thus the excitation frequency, there is more hysteresis and thus more energy is dissipated (Srirangam, 2015), which results into a higher skid resistance. Figure 2.15 shows the change in energy loss and modulus for an increasing frequency.

The higher amount of dissipated energy is in the form of heat therefore, because of the increased hysteresis at increasing speed, the tyre is heated up. This, in turn, decreases the hysteresis friction, as explained in Section 2.4.3. This phenomenon would be higher for larger macrotextures, because a larger macrotexture generates a larger hysteresis energy dissipation. Also, it would be stronger for pavements with a higher draining capacity, because this will decrease the cooling effect of the water. It is assumed that the decline in skid resistance due to the increased heat is dominant and that therefore increasing the vehicle speed decreases the skid resistance.

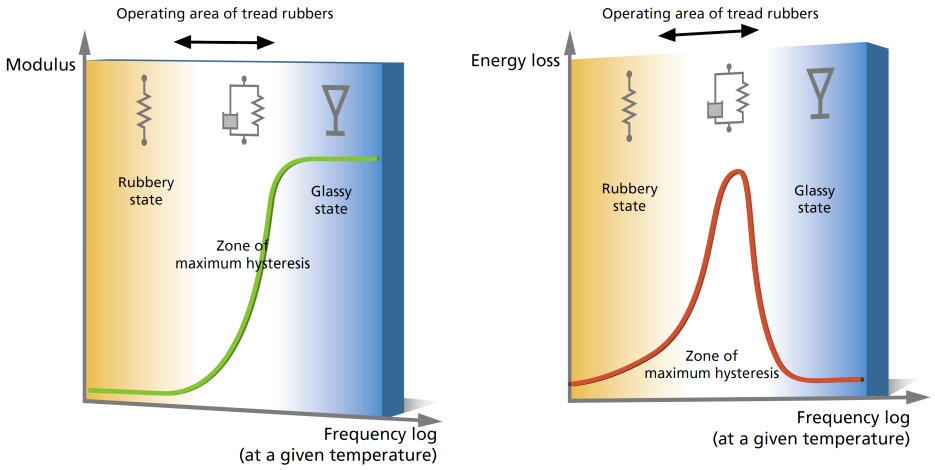

(a) Modulus (b) Energy loss

Figure 2.15: Influence of excitation frequency on the energy loss and modulus (Michelin, 2001)

2.4.5. Slip speed and slip ratio

When measuring the LFC, a sliding process of the tyre by application of a braking force is simulated (Kogbara et al., 2016). The measuring wheel is partly blocked such that it rotates with a lower speed than that of the vehicle, and therefore it slides over the surface. The slip ratio expresses how much the measuring wheel slides over the surface and can be expressed as (Kogbara et al., 2016):

$$SR = \frac{V - V_p}{V} \cdot 100 = \frac{S}{V} \cdot 100 \tag{2.5}$$

Where:	SR	=	Slip ratio	[%]
	V	=	Measuring speed of the vehicle	[km/h]
	V_p	=	Average peripheral speed of the tyre	[km/h]
	S	=	Slip speed	[km/h]

Some measuring devices work with a fully locked measuring wheel. This implies that the slip speed S is equal to the vehicle directional speed V, and the peripheral speed of the tyre V_p is 0 km/h. In case of the RWS Skid Resistance Tester, the slip ratio is 86%, thus, the peripheral speed of the tyre V_p is 14% of the vehicle directional speed V.

The skid resistance of a road surface changes at different slip ratios, as is shown in Figure 2.16. With an increasing slip ratio up to 10-20%, the friction coefficient rapidly increases. At a certain percentage, a maximum skid resistance is reached. While increasing the slip ratio up to a fully-locked measuring wheel, the friction coefficient declines. On wet pavements this decline is bigger than on dry pavements and the difference between the peak friction and the full sliding friction can go up to 50% of the peak friction coefficient (Hall et al., 2009). The extent to which the coefficient of friction decreases after the maximum is reached depends, besides on the applied slip ratio, in particular on the macrotexture (Vos and Groenendijk, 2009).

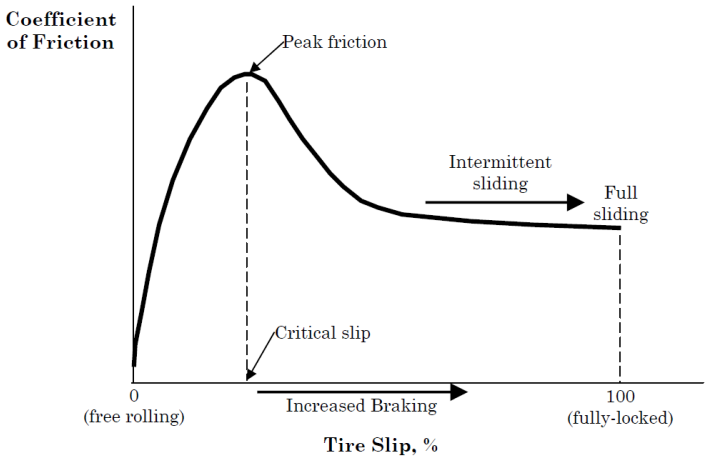

Figure 2.16: Pavement friction versus tyre slip (Henry, 2000)

When measuring the SFC, no slip is applied on the measuring wheel, but the measuring wheel is set at a yaw angle α. However, many developed speed conversion models (Chapter 4) used the *slip speed* as determining factor. Therefore, for the SFC, a 'slip speed' of $sin(\alpha) \cdot V$ was considered.

2.4.6. Age of the surface

The effect of the age of the surface can be separated into short-term and long-term effects. During the first few months up to a year after construction, the interface is vulnerable to changes which consequently changes the skid resistance. It can increase or decrease more than for older asphalt layers. On the long-term, polishing of the aggregates changes the texture of the pavement. As a result of polishing, the skid resistance will decrease. Monitoring the skid resistance of pavements occurs with the purpose of detecting (on time) poor skid resistance due to various factors, among which polishing. This section explains more about changes of the skid resistance on the short-term.

One may distinguish if the pavement layer is gritted after construction or not. Gritting means that the new wearing courses are covered with fine material to improve the skid resistance. In case of a gritted pavement layer, passing vehicles will remove most of the grit during the first months and the skid resistance will decrease. A thin layer of bitumen can, if not removed together with the grit, remain on

the surface while convering the aggregates. If this is the case, both the wet and dry skid resistance are temporarily lower. The dry skid resistance can now be critical —especially for locked wheel braking— and the phenomenon contributing to this deviating dry skid resistance is bituplaning, caused by bitumen being melted by locked-wheel braking (Vos et al., 2017). After some months, the top layer of bitumen is worn and the skid resistance finally increases to its 'normal' skid resistance.

In case of non-gritted wearing courses, the aggregates of the wearing course are covered with a thin layer of bitumen and bituplaning can occur directly after construction. That is why often the road sign 'New road surface, longer braking distance' is placed along new wearing courses. After some months, the top layer of bitumen is worn off and the wearing course has its 'normal' skid resistance (Vos et al., 2017).

Dense asphalt layers such as dense asphalt concrete (DAC) are always gritted. SMA layers are sometimes gritted but not always. Porous wearing courses are often applied in the Netherlands. For this type of wearing courses, one firstly assumed that gritting reduced the air voids content in porous asphalt, hence the porous wearing courses were not gritted (Vos et al., 2017). However, reducing the amount and size of the gritting material solved this problem, hence nowadays also PA layers are often gritted with fine grit material.

During this research it is important to take into account the initial skid resistance which can fluctuate over a short period of time. One cannot assume that all road surfaces measured by Kiwa KOAC are older than 1 year, although RWS demands skid resistance measurements with the SKM only for pavements older than one year (Rijkswaterstaat, 2017). The ages of the road surfaces are not recorded and often not known while performing the measurements, and furthermore road surfaces could have been recently treated with rejuvenators as preventative maintenance, which reduces the skid resistance for up to 1 year (Army and Air Force, 1988).

2.4.7. Tyre characteristics

Tyre properties have a significant influence on the skid resistance. For different measuring techniques, standards are set for the usage of tyres to prevent variations in the measurements because of deviating tyre properties.

Tyre profile

The tyre profile is an important factor when considering friction on contaminated (e.g. wet) pavement surfaces. If a surface is contaminated the macrotexture partially disappears, because the texture is filled with contaminants. In this situation, the tyre profile provides a drainage system to evacuate contaminants (Fuentes, 2009). Therefore, bald tyres have lower skid resistance than tyres with full profile depth. Tyres with deeper treads offer better frictional characteristics especially at higher speeds, because more water can be drained than in case of bald tyres (Anupam, 2012).

Profile wear has only small effect on the average friction coefficient until the profile is about 80% worn, after which it drops rapidly. Higher wear ultimately results in lower skid resistance (Srirangam, 2015). Hall et al. (2009) states that studies reported a decrease in wet friction of 45 to 70 percent for fully worn tyres compared to new ones. When measuring skid resistance a smooth tyre is recommended because in this situation the skid resistance measurement will only be influenced by the drainage capabilities of the texture of the pavement, and not by the tyre profile (Fuentes, 2009).

Inflation pressure

Tang et al. (2017) performed a research to the influencing parameters on braking distance with help of a finite element model. It was concluded that with an increasing inflation pressure —between 150 and 250 kPa— the breaking distance increased as well, thus the skid resistance decreased. An increase of inflation pressure leads to a decrease of contact area between the tyre and pavement, which reduces the braking force. For a 100% slip ratio this effect was stronger than for a 20% slip ratio. A decreased vehicle loading decreases the contact area between the tyre and pavement and therefore this can also have the effect of a reducing braking force.

2.5. Physical explanation for the speed dependency of skid resistance

As Chapter 4 will show, many conversion models for skid resistance have been developed in the past. Many of these conversion models are empirical models obtained by regressions of measurements performed for the corresponding research. This section outlines possible physical explanations which could explain the relation between the speed dependency of the skid resistance and pavement macrotexture.

2.5.1. Dissipated energy

This section investigates the possible relationship between the dissipated energy and skid resistance at different speeds. As explained in Section 2.3, adhesion and hysteresis are two physical mechanisms providing friction forces between the tyre and road surface. In wet circumstances hysteresis is the governing component. Therefore this section considers the dissipated energy due to hysteresis.

The mathematical explanation of the friction component caused by hysteresis is very complicated and much research has been performed on this topic. Srirangam (2015) presented a 3D thermo-mechanical tyre-pavement interaction model in a finite element framework and expressed the total energy dissipation as:

$$W = \sum_{i=1}^{m} \int_0^T \sigma_i \cdot \dot{\epsilon}_{vi} dt \tag{2.6a}$$

$$\sigma_i = E_i \epsilon_{ei} = E_i \int_0^t e^{-\frac{E_i}{\eta_i}(t-s)} \dot{\epsilon}(s) ds \tag{2.6b}$$

$$\dot{\epsilon}_{vi} = \frac{1}{\tau_i} \epsilon_{ei} = \frac{1}{\tau_i} \int_0^t e^{-\frac{1}{\tau_i}(t-s)} \dot{\epsilon}(s) ds \tag{2.6c}$$

Where:	W	=	Total energy loss per tyre revolution	[-]
	T	=	Time for one tyre revolution	[-]
	σ_i	=	Component related to the stress	[-]
	$\dot{\epsilon}_{vi}$	=	Component related to the change of strain	[-]

The parameter corresponding to vehicle speed is T, which is the time needed for one tyre revolution. If the radius of the tyre would be known, T can be obtained from the vehicle speed. The circumference of the tyre is $2 \cdot \pi \cdot r$, hence $T = \frac{2 \cdot \pi \cdot r}{V}$. If V will linearly increase, T will linearly decrease with the same rate. Because both the stress and strain components (σ_i and $\dot{\epsilon}_{vi}$) have a negative e-power, a decreasing T will imply a larger value for the stress and strain component of the energy loss, following the exponential curve.

2.5.2. Volume of water

As described in Section 2.4.4, having a higher velocity means that more water per second must be drained, especially on non-porous asphalt layers. Also, the larger the speed, the higher the upward water pressure in the front area of the vehicle wheel. A smaller vertical force from the vehicle is now acting on the third zone, where hysteresis and adhesion forces arise.

The extent to which the area of the first zone increases with an increasing vehicle speed depends on many factors, such as the thickness of the water layer, the macrotexture and the used tyres. During skid resistance measurements, most of these factors are kept constant. The macrotexture, however, is not constant. The size of the macrotexture might have an influence on the increase of the upward water pressure with an increasing vehicle speed, which in turn influences the skid resistance. However, this is a very complicated physical process and one cannot answer easily the question how the macrotexture influences this process. Therefore, this is left outside the scope for this research.

2.6. Conclusions

From the literature study on skid resistance and its influencing factors, some important aspects became clear. Besides insight into skid resistance in general, it became clear that during the development of the conversion model for the SKM used in the Netherlands, some aspects must be considered. Conclusions, based on the literature study given in this chapter, are:

- A distinction should be made between the LFC and SFC. Different forces are used to calculate these coefficients. Possibly also the speed dependency differs for these two coefficients, hence care should be taken when analysing prior developed speed conversion models.
- The macrotexture, which can be expressed in the MPD (possibly extended with RMS), has a large influence on the skid resistance and especially on its speed dependency.
- With an SKM the macrotexture is measured in terms of the MPD. This measurement cannot be accomplished accurately during wet measuring conditions. When analysing the data, care should be taken that the MPD measurements are performed under dry conditions.
- Positive and negative macrotextures possibly influence the speed dependency of the wet skid resistance. A positive macrotexture can be defined as having a MPD/RMS value larger than 1.58, whereas a negative macrotexture can be defined as having a MPD/RMS smaller than 1.58.
- Temperature has a significant influence on the skid resistance. For the SKM, a temperature correction formula exists. During the model generation, the raw measured skid resistance must be corrected for temperature fluctuations in order to make the measurements comparable.
- The vehicle speed has a large influence on the skid resistance and multiple explanations for this relation exists. In this study the main hypothesis is that at higher speeds the wet skid resistance decreases because of the higher volume of water per second which needs to be drained. However, one might discuss which of the mechanisms is governing for which situations.
- The skid resistance of new asphalt layers fluctuates much. Possibly, for new asphalt layers, a different correlation exists than for older asphalt layers.
- Besides the speed, age and temperature, many other factors influence the skid resistance. These are not taken into account in the model generation. However, one should not forget these influencing parameters because they could cause deviating measurements if they are not kept constant while measuring.

3

Measuring skid resistance

Measurements of skid resistance can be accomplished with static or dynamic equipment. Static devices measure the skid resistance at one specific location, after which the device should be moved to another location. Dynamic devices measure the skid resistance continuously over a distance.

The sections below describe two devices recently used in the Netherlands. Section 3.1 explains how the RWS Skid Resistance Tester works, a device measuring de LFC. Section 3.2 gives more information about the SKM, a device measuring the SFC.

Table 3.1 gives an overview of the devices.

Table 3.1: Devices for measuring the skid resistance used in the Netherlands

Device	Measures	Measuring speed	Slip	Angle of wheel
RWS Skid Resistance Tester	LFC	50/70 km/h	86%	-
SKM	SFC	40/60/80 km/h	-	20°

Besides the properties mentioned in the table, also the types and sizes of the tyres used for the RWS Skid Resistance Tester and the SKM differ. These are not specified in further detail because this is considered irrelevant for the speed conversion model.

3.1. RWS Skid Resistance Tester

3.1.1. Working principle

The RWS Skid Resistance Tester (see Figure 3.1) consists of a trailer fitted with a test wheel. To this test wheel a slip ratio of 86% is applied, which means the rotational velocity of the wheel is 14% of the velocity of the trailer. The test wheel is loaded with a 200 kilograms mass and a water layer with a thickness of 0.5 mm is sprayed in front of the test wheel, for measuring the wet skid resistance. With a standard measuring speed of 50±2.5 or 70±3.5 km/h, the longitudinal friction force between the test wheel and the road surface is measured. The location of the measurements is normally in the right wheel path, as Figure 3.1 shows. If this is not possible, the location of measuring should be noted.

Figure 3.1: The RWS system (Kiwa KOAC, 2015)

3.1.2. Calculation of friction coefficient

The wet coefficient of friction can now be defined as the ratio of the horizontal frictional force and the vertical applied load as in Equation (2.1) (Vos et al., 2017).

If the measurements cannot be performed at the standard measuring speeds, for example on roundabouts, a measuring speed lower than 50 km/h can be used, and the indicative skid resistance at the speed of 50 km/h can be estimated with help of a speed conversion model developed by Kiwa KOAC (see Section 4.9) (Kiwa KOAC, 2015). Besides the speed correction, some corrections for seasonal and temperature influences are applied in order to obtain the friction coefficient which needs to meet the requirements.

3.2. SKM

There are two SWF devices which are widely used, namely the German SKM and the British SCRIM. The working principle of these devices is roughly identical. In the Netherlands the German SKM is used. Specifications of the measuring devices and principles are stated in the German Technical Specifications, the 'Technische Prüfvorschriften für Griffigkeitsmessungen im Staßenbau Teil: Seitenkraftmessverfahren (SKM)' (TP Griff-StB (SKM)). The following sections present a description of the SKM as used by Kiwa KOAC.

3.2.1. Working principle

Figures 3.2a and 3.2b show photographs of the SKM used bij Kiwa KOAC. The measuring equipment is incorporated in a truck. At the right side of the truck, a measuring wheel is mounted in between the rear and front wheels. This wheel is set at a yaw angle of 20° to the direction of travel of the vehicle. The measuring speed should be 40, 60, or 80 km/h, chosen by the client. On the test wheel a load of 1960 ± 10 N is applied and a water layer with a thickness of 0.5 mm is sprayed in front of the measuring wheel.

(a) SKM device (b) Measuring wheel

Figure 3.2: Photos of the SKM device (Kiwa KOAC, 2016)

3.2.2. Calculation of friction coefficient

The equation for calculating the friction force as given by Kiwa KOAC (2016) is equal to Equation (2.2). If the measurement was not performed at one of the prescribed vehicle speeds (40, 60 or 80 km/h), a speed correction should be applied. Currently, Equation (4.16) is used to apply a speed correction. Furthermore, a temperature correction is applied as in Equation (4.17).

3.2.3. Measuring curved sections

Research showed that the yaw angle has an influence on the level of the measured SFC. Hosking and Woodford (1976b) state that the effect of increasing the yaw angle is increasing the level of the measured SFC and at a certain angle the SFC has reached its maximum and it does not increase further. For lower values of the SFC, this critical angle is smaller than for higher values of the SFC, as can be seen in Figure 3.3.

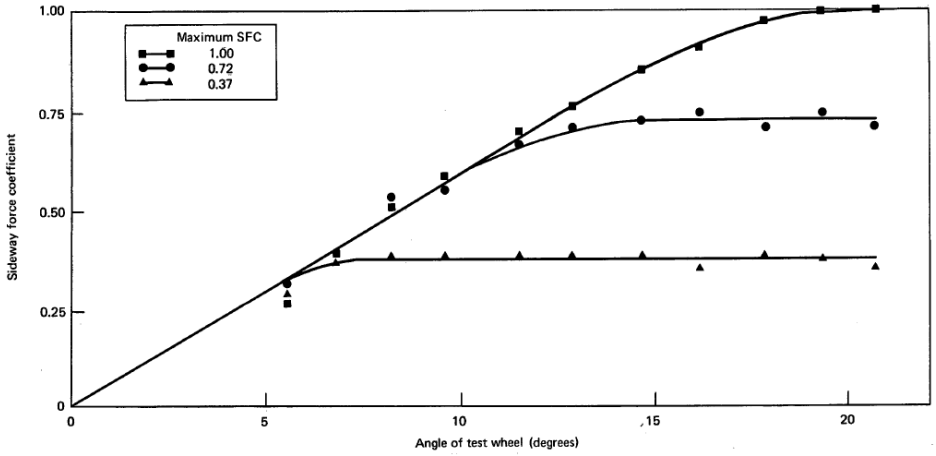

Figure 3.3: Relation between the SFC and the yaw angle of the test wheel (Hosking and Woodford, 1976b)

However, Day (2014) gives a different graph than Hosking and Woodford (1976b) and declares that for every yaw angle a limit of the available tyre/road adhesion can be found, and that the maximum possible SFC only occurs at a specific yaw angle (around 6-12°). After the SFC has reached its maximum, it will decline with increasing yaw angle.

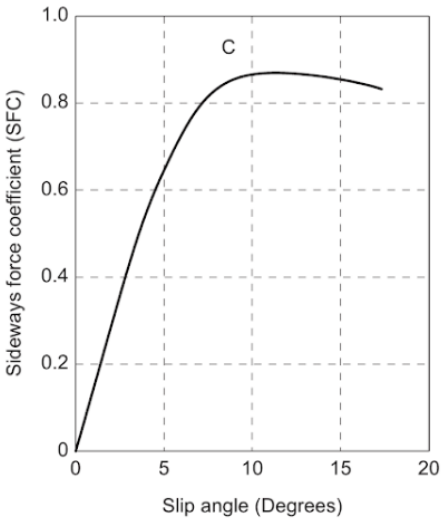

Figure 3.4: Relation between the SFC and the yaw angle of the test wheel (Day, 2014)

Although Hosking and Woodford (1976b) and Day (2014) give different relationships for the yaw angle and SFC, attention should be paid to the yaw angle of the measuring wheel when measuring curved sections with the SKM. For curves directed towards the left, the yaw angle is 'reduced' because the front wheels are turned into the same direction of the measuring wheel.

For right curved sections, the yaw angle is 'increased' because the front wheels are rotated into the opposite direction of the yaw angle. Figures 3.5a and 3.5b illustrate the change in yaw angle for left and right turns.

According to Hosking and Woodford (1976b), when decreasing the yaw angle, a reduction in the measured SFC could be found, whilst according to Day (2014) an increase could be measured. For an increasing ywa angle, there would be no difference according to Hosking and Woodford (1976b) whereas Day (2014) declares that the SFC might decrease further.

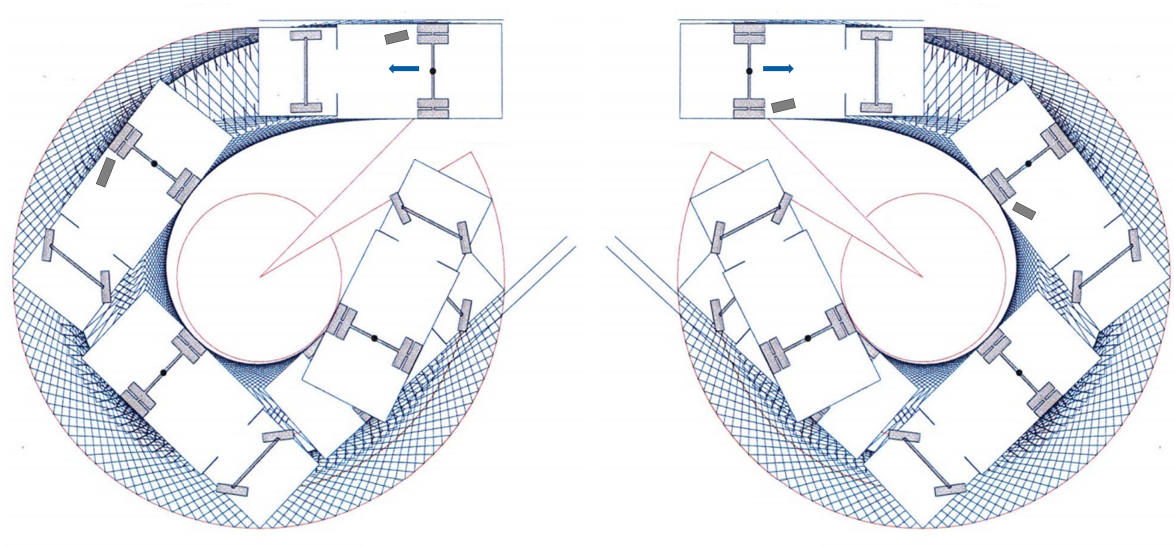

(a) Left curve (b) Right curve

Figure 3.5: Illustrations of SKM measuring device in curves (Vroomans, 2016)

The question whether the measured SFC can be compared to the set target values is beyond the scope of this research. However, it is not known whether the speed dependency will be different for measurements performed at curved sections compared to straight sections.

As shown in Figure 3.6, Anupam et al. (2014) found with help of a finite element model, like Hosking and Woodford (1976b), a declining increase in the friction coefficient for an increasing yaw angle.

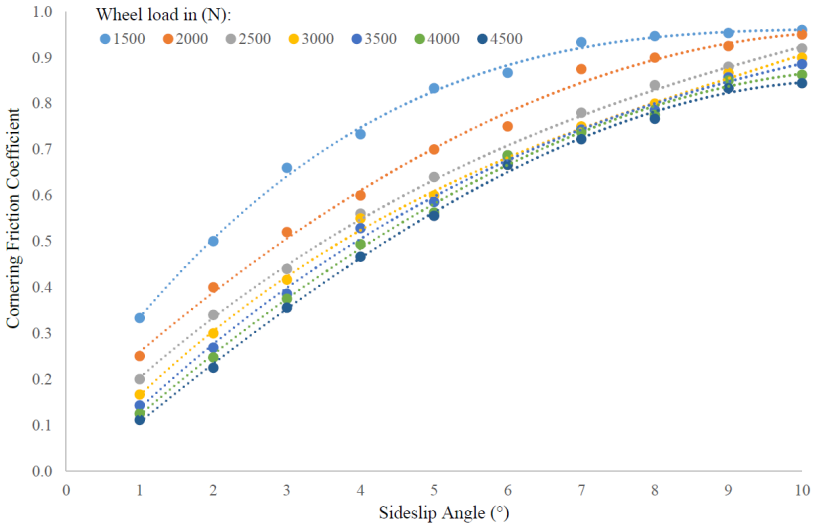

Figure 3.6: Cornering Friction Coefficient vs. Yaw angle (Anupam et al., 2014)

Furthermore, Anupam et al. (2014) investigated the speed dependency of the cornering friction coefficient for different side-slip angles. A decreasing correlation was found —thus, the higher the speed the lower the cornering friction coefficient. In terms of percentages, they found 25% to 54% decrease of the cornering friction coefficient with an increase in speed of 50 km/h within 1° to 10° slip angle. The results are plotted in Figure 3.7.

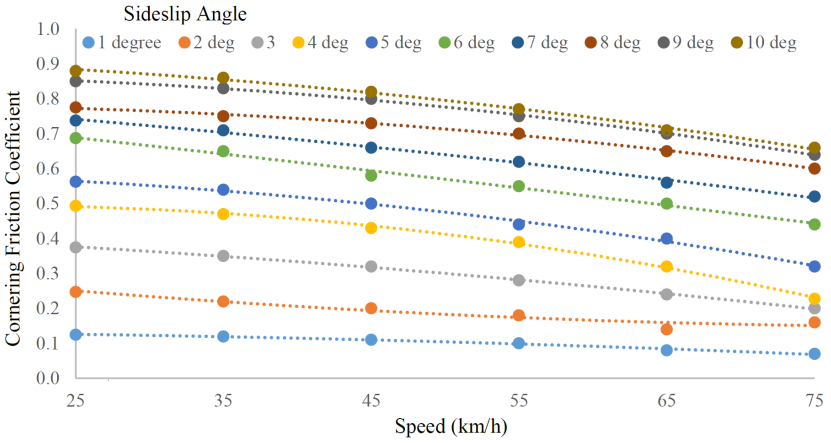

Figure 3.7: Cornering Friction Coefficient vs. Speed (Anupam et al., 2014)

The lines in Figure 3.7 show that the speed dependency increases slightly with increasing yaw angle. One should note that the yaw angle of the SKM is 20°, which is not included in this graph.

3.3. Conclusions

This chapter provides information about two different measurement methods of the friction coefficient. Conclusions, based on this chapter, are:

- With the RWS Skid Resistance Tester the LFC is measured, whereas with the SKM the SFC is measured.
- When measuring the LFC, a slip ratio is applied on the measuring wheel. This slip ratio influences the friction coefficient. Therefore, when analysing the previously developed speed conversion models, one should take into account whether the slip speed or vehicle speed is used as an input

parameter and if the LFC or SFC is used as friction coefficient.

- With the SKM, when measuring curves to the left the yaw angle is slightly decreased whereas when measuring curves to the right the yaw angle is slightly increased. The smaller the radius, the larger the change in yaw angle.
- A change in yaw angle could change the speed dependency of the measured SFC. Therefore, sharp curves can have an influence on the speed dependency of the skid resistance measured with the SKM. Although this influence is expected not being significant, in the development of the model, this influence should not be neglected.

4

Previously developed speed conversion models for the skid resistance

The speed dependent characteristic of skid resistance was observed and reported already in the 1930s (Fwa, 2017). Much research was performed into the development of speed conversion models for the skid resistance. The motivating reasons were different. For example, Vos (2008) formulated a speed conversion model for the RWS-Skid resistance measurements from 50 km/h to 70 km/h. The reason behind his research was that the standard measuring speed was increased from 50 km/h to 70 km/h, and therefore the threshold values and requirements needed to be adapted. Groenendijk (2011) performed his research for the same reason as Vos. Another motivating reason for obtaining a correction for the speed was the harmonisation of skid resistance measurements. Harmonisation provides a way of making comparisons between the different approaches used in different countries or between different measuring techniques in a consistent manner (Vos and Groenendijk, 2009). In this situation, the speed conversion is one of the needed steps in order to obtain comparable values for the skid resistance.

Table 4.1 gives an overview of conversion models developed in different researches[1]. In Sections 4.1 to 4.12 these models are presented[2]. Section 4.13 compares some of the presented models.

[1] Limited to: models used in The Netherlands and models developed for the SFC (also outside the Netherlands)

[2] In the descriptions of the models, the symbols noted could differ from the symbols given in the sources. The purpose of these adaptions is to prevent confusion caused by the same symbol used for different terms, or the other way around, by different symbols used for the same terms. The original formulas can be found in Appendix A.

Table 4.1: Overview of different speed conversion models for the skid resistance

Research	Measurement device	Slip speed or vehicle speed	Possible speed conversions	LFC or SFC	Relation of μ to speed	Influence of macro texture
Hosking and Woodford	SCRIM	Vehicle	From 30-50 km/h to 50 km/h	SFC	Linear	-
Penn state Model	US locked wheel tester	Slip	-	LFC	Exponential	PSNG
Rado Model	Different devices	Slip	-	LFC	Exponential	shape factor C
PIARC Model	Different devices	Slip	From different speeds to 60 km/h	Both	Exponential	Various
Koac WMD	RWS Skid Resistance Tester	Vehicle	Between 30-90 km/h	LFC	Exponential	MPD and positive/negative macrotexture
ESDU	Different devices	Vehicle	-	LFC	Quadratic	MPD (indirect)
FEHRL Hermes	Different devices	Slip	From different speeds to 30 km/h	Both	Exponential	MPD
E. Vos	RWS Skid Resistance Tester	Vehicle	From 50 to 70 km/h and vice versa	LFC	Linear	Open / dense
Koac•NPC	RWS Skid Resistance Tester	Vehicle	From 20-50 km/h to 50 km/h	LFC	Exponential	MPD
SCRIM conversion	SCRIM	Vehicle	From 25-85 km/h to 50 km/h	SFC	Quadratic	-
TP Griff-StB (SKM)	SKM	Vehicle	From different speeds to 40/60/80 km/h	SFC	Linear	-
BASt	SKM	Vehicle	From different speeds to 40/60/80 km/h	SFC	Linear	MPD

4.1. Hosking and Woodford (1976)

Hosking and Woodford (1976b) investigated several factors affecting SCRIM measurements of which one was the speed. Not a speed conversion model was developed, but a model with which the skid resistance under certain circumstances could be calculated.

4.1.1. Experimental setup

- Measurements were performed with the SCRIM.
- A test wheel was used with a standardised 3.00x20 tyre under a yaw angle of 20 degrees to the direction of travel.
- Measurements were performed on the motorway M40 in the UK.
- The bituminous surfaces were gritted with aggregates having a polished stone value (PSV) between 60 and 75 and a texture depth varying from 0.5 to 2.5 mm.
- The section was tested 5 times in both directions at measuring speeds of 16, 32, 48, 64 and 80 km/h.
- All the work was done in one day and therefore the temperature influence was kept minimal.
- The water supply had a mean film thickness of 1.1 $\pm$ 0.1mm on a smooth road.

4.1.2. Developed model

Multiple regression analysis of the mean values of SFC gave the following relationships (Hosking and Woodford, 1976b):

In the direction of trafficking:

$$\mu_{y,V} = 0.015 \cdot \mathrm{PSV} + 0.028 \cdot \mathrm{TD} - 0.0027 \cdot V - 0.286 \tag{4.1a}$$

In the opposite direction of trafficking:

$$\mu_{y,V} = 0.014 \cdot \mathrm{PSV} + 0.026 \cdot \mathrm{TD} - 0.0025 \cdot V - 0.200 \tag{4.1b}$$

Where:	$\mu_{y,V}$	=	Calculated SFC at measuring speed V	[-]
	PSV	=	Polished-stone value of aggregate	[-]
	TD	=	Texture depth of surfacing measured with the sand Patch method	[mm]

V = Measuring speed of vehicle [km/h]

This is not a conversion model, but a model to calculate, based on certain texture and speed input parameters, the corresponding SFC. However, for obtaining these equations, Hosking and Woodford (1976b) investigated the effect of different measuring speeds on the skid resistance. This effect appeared to be almost similar for both measuring directions, respectively 0.0027 and 0.0025 units per km/h difference in measuring speed. For practical purposes, Hosking and Woodford (1976b) advised to apply a correction of 0.01 units for each 4 km/h —which equals a correction of 0.0025 units for each km/h— if the measuring speed is lower than the standard measuring speed of 50 km/h. They mentioned that for speeds lower than 30 km/h the accuracy of this correction declines.

Reliability

No information about the reliability or accuracy of this model is given in the work of Hosking and Woodford (1976b).

4.2. Penn State Model (1978)

The Penn State Model is one of the first models bearing in mind the speed dependent characteristic of skid resistance. This model was developed by researchers at the Pennsylvania State University (Fwa, 2017) and describes the relationship of friction μ_x to the slip speed S (Henry, 2000).

4.2.1. Experimental setup

- Measurements were performed according to E274-77 of the American Society for Testing and Materials (ASTM). This implies[3] a locked wheel device with a grooved tyre (E501), a water film of 0.56 mm, a wheel load of 4286 N and a tyre pressure of 165 kPa.
- 20 test sections located in West Virginia were measured in July 1976.
- All data was obtained at the same time and therefore seasonal effects such as temperature and rain were considered to be negligible and therefore excluded.
- The sections were measured at measuring speeds of 48, 64, 80 and 96 km/h.
- Twelve tests were made at each speed of which the measured values were averaged .

4.2.2. Developed model

Leu and Henry (1978) developed the following equation:

$$\mathrm{SN} = \mathrm{SN}_0 \cdot e^{-\frac{\mathrm{PSNG}}{100} \cdot S} \tag{4.2}$$

Where:
SN = Skid number (= $100 \cdot \mu_x$) [-]
SN_0 = Zero speed intercept [-]
PSNG = Percentage skid number-speed gradient [%]
S = Slip speed [km/h]

SN_0 is the skid resistance estimated with the British Pendulum Test (Fwa, 2017) and is called the zero speed intercept. Leu and Henry (1978) suggested that this parameter was correlated to the microtexture, whereas the PSNG is a parameter related to the macrotexture. PSNG is a parameter obtained by curve fitting with inputs of skid resistance measurements made at three or more speeds (Fwa, 2017).

Reliability

No information about the reliability or accuracy of this model is found.

4.3. Rado Model (1994)

Rado modelled the slip behaviour as in Figure 2.16 with the following formula (Henry, 2000):

[3] As given in E274-79, a renewed version of E274-77

$$\mu_S = \mu_{peak} \cdot e^{-\left[\frac{ln(S/S_{peak})}{C}\right]} \tag{4.3}$$

Where:	μ_S	=	Friction coefficient at slip speed S	[-]
	μ_{peak}	=	Peak friction level	[-]
	S_{peak}	=	Slip speed at the peak friction level	[km/h]
	C	=	Shape factor	[-]
	S	=	Slip speed	[km/h]

S_{peak} is typically about 15 percent of the vehicle speed and Rado found C to be related to the harshness of the texture, this parameter is closely related to the speed number S_p in the PIARC model(Leandri and Losa, 2015). Equation (A.3) can be used to determine the whole friction curve $\mu(S)$ for a braking process from free rolling to the locked wheel state (Leandri and Losa, 2015).

An example of the Rado model is shown in Figure 4.1, the curve of this figure resembles Figure 2.16.

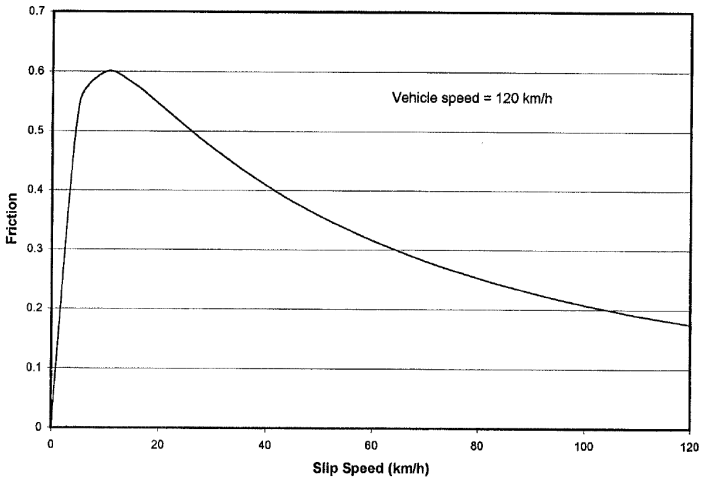

Figure 4.1: Rado model (Henry, 2000)

Above the peak friction value, the Rado Model is similar to the Penn State Model and the models depend on the pavement characteristics (Henry, 2000). The Rado Model is not intended tu be used for converting the skid resistance between different measuring speeds, but for calculating the skid resistance at a certain used slip speed, because S_{peak}, C and μ_{peak} are constant numbers in the formula. However, because later research is based on Rado's work, this model is addressed in this research.

Reliability

No information about the reliability or accuracy of this model is found.

4.4. PIARC Model (1995)

The PIARC International Experiment was conducted to compare and harmonise texture and skid resistance measurements performed with different devices (Henry et al., 1995). Section 4.4.1 presents the setup of the experiment whereas Section 4.4.2 explains how the model is developed, which can be applied on various devices. Section 4.4.3 tries to analyse the PIARC model for SCRIM devices into more detail.

4.4.1. Experimental setup

47 different measuring systems participated the PIARC project. These measuring systems came from sixteen different countries. These systems measured 67 different parameters —33 texture parameters and 34 friction parameters (Henry et al., 1995).

The friction was measured with SWF, fixed slip and locked wheel measurements. Because different friction devices were used, measurements were performed under different conditions. For example, some measurements were performed with PIARC ribbed tyres, whereas others were performed with PIARC smooth tyres. Measuring devices from the US do not use PIARC tyres but ASTM tyres, which can also be smooth or ribbed. The RWS Skid Resistance tester is the Dutch device used in the PIARC experiment. From Germany, a version of the British SCRIM was used.

Texture was measured with both stationary and dynamic equipment and expressed in variables such as the RMS, MPD and the mean texture depth (MTD).

Measurements were performed in September and October of 1992. A variety of test sites was used. In total 28 Belgium tracks —2 at an airfield, 4 at a race track and 22 on public roads— and 26 Spanish tracks —8 at airfields and 18 on public roads— were used. As a requirement, approximately 75% of the sites should be asphalt concrete (AC) whereas 25% should be portland cement concrete (PCC). However, it is not known if this requirement was fulfilled. Each measurement was repeated one time at each speed. The different measuring speeds were 30, 60 and 90 km/h.

4.4.2. Developed model

During the experiment a model was developed according to the procedure presented in Figure 4.2. The skid resistance (μ_{BS}) measured with a certain measuring device B at a certain slip speed S is first converted to the skid resistance (μ_{B60}) for the same device B at the reference slip speed which is defined at 60 km/h. This is followed by a conversion for the skid resistance measured with device B to the skid resistance (μ_{60}) measured with reference device A. The first step is the important step for this research because this step contains the speed conversion. Therefore, the second step is not analysed in depth.

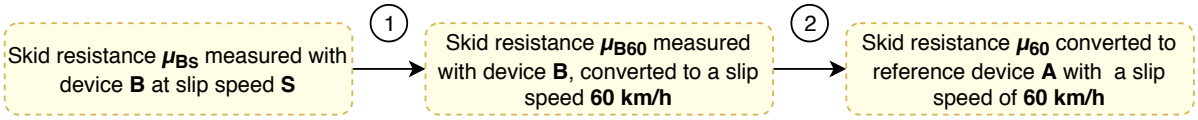

Figure 4.2: Framework of PIARC model

The first step of the PIARC model consists of two parts: firstly, the speed number S_p, which indicates the texture dependency, is determined. This is followed by a second formula that calculates the friction coefficient at a standard slip speed of 60 km/h, μ_{B60}. The speed number is calculated as follows (Henry et al., 1995):

$$S_p = a + b \cdot T_x \tag{4.4}$$

Where:	S_p	=	Speed number	[-]
	a	=	Constants for any texture device	[-]
	b	=	Constants for any texture device	[1/mm]
	T_x	=	Macrotexture measure	[mm]

T_x can be measured as the MTD measured by the sand patch method, or the MPD measured by a laser device (Fwa, 2017). For example, ASTM adopted the following relationship for S_p (ASTM E1960-98, 2015):

$$S_p = 14.2 + 89.7 \cdot \text{MPD} \tag{4.5}$$

In which the MPD is measured according to ASTM E1854. Henry et al. (1995) developed a model, based on the Penn State Model, to convert the measured friction at slip speed S to a friction coefficient at a slip speed of 60 km/h as follows:

$$\mu_{B60} = \mu_{BS} \cdot e^{\frac{S-60}{S_p}} \tag{4.6}$$

Where:	μ_{B60}	=	Slip-speed corrected estimate for the device specific friction coefficient at a slip speed of 60 km/h		[-]
	μ_{BS}	=	Measured friction coefficient with device B at slip speed S		[-]
	S	=	Slip speed		[km/h]
		=	V	for locked wheel	
		=	$V \cdot$ SR/100	for fixed slip testers	
		=	$V \cdot \sin(\alpha)$	for SFC	
			where α = yaw angle of test wheel		[°]

With the values μ_{60} (estimate of the "true" friction index measured at 60 km/h for the standard measuring device A) and S_p, PIARC proposed the International Friction Index (IFI) as IFI(μ_{60}, S_p). With help of the IFI it is now possible to estimate the friction coefficient at any speed (Henry et al., 1995) for the standard measuring device. This is considered not relevant for this research and therefore it is not described into further detail.

In Equation (4.6) there are no device specific parameters, only S_p depends on the type of texture device. Instead of the vehicle speed, the slip speed is used and the model assumes a comparable correlation for the different devices when considering slip speed. When measuring with the SKM no slip is applied but a yaw angle. The difference between the LFC and SFC is addressed by converting the yaw angle to a slip ratio of sin(20) = 34%. However, this does possibly not eliminate all differences (Vos and Groenendijk, 2009).

4.4.3. PIARC model for SCRIM Devices

In the research of PIARC, 8 different SCRIM devices participated. All of these used a smooth tyre and had a yaw angle of 20°. See Table 4.2 for an overview of the used SCRIM devices.

Table 4.2: SCRIM devices used in the PIARC research (Table 1, Henry et al., 1995)

Device ID	Device name (country)	Measuring speed [km/h]
C3B	Flemish Scrim (B)	30, 60, 90
C3E	CEDEX SCRIM (E)	30, 60, 90
C6E	MOPT SCRIM (E)	30, 60, 90
D1E	SCRIM (D)	40, 60, 90
D2	SCRIM-GEOCISA (E)	30, 60, 80
D3	SCRIM (F)	30, 60, 90
D4	SUMMS (I)	30, 60, 80
D5	SCRIMTEX (UK)	30, 60, 90

From this table, it seems that device D1E is the device used in Germany. However, it is unknown how much the current German SKM deviates from the 1994 German SCRIM. What we are actually interested in, are the a and b values used for the macrotexture measurements. These do not depend on the skid resistance measuring device but on the macrotexture measuring device. PIARC gives some combinations of texture equipment and skid resistance measuring devices, but unfortunately no texture measuring equipment is provided for the D1E. The only SCRIM devices presented in this table (table 2, Henry et al., 1995), are D2 and D5. However, these devices measure the macrotexture as the MTD, thus makes the a and b parameters unusable for this research. Three different devices measuring the MPD are used in the PIARC research, which are A2, A4 and A5. Table 4.3, below, provides information about these texture measuring devices.

Table 4.3: Values for a and b for different texture measuring devices (adapted from table 2 and 24, Henry et al., 1995)

Device ID	Texture device (country)	Measurements	V	a	b
A2	VTI Mobile Profilometer (S)	RMS, ETD, TDMA, MPD	34	14.235	89.720
A4 (1)	CRR Mobile Profilometer (B)	MPD, RMS	18	11.502	69.133
A4 (2)	CRR Mobile Profilometer (B)	MPD, RMS	36	9.229	83.230
A4 (3)	CRR Mobile Profilometer (B)	MPD, RMS	72	42.256	139.203
A5	CRR Stationary Profilometer (B)	MPD, RMS	0	9.741	81.676

As Table 4.3 shows, different values for a and b were used for the A4 device depending on the measuring speed. The different values for a and b for all given texture devices were compared by calculating the S_p for MPD values ranging from 0.1 to 2.0 mm.

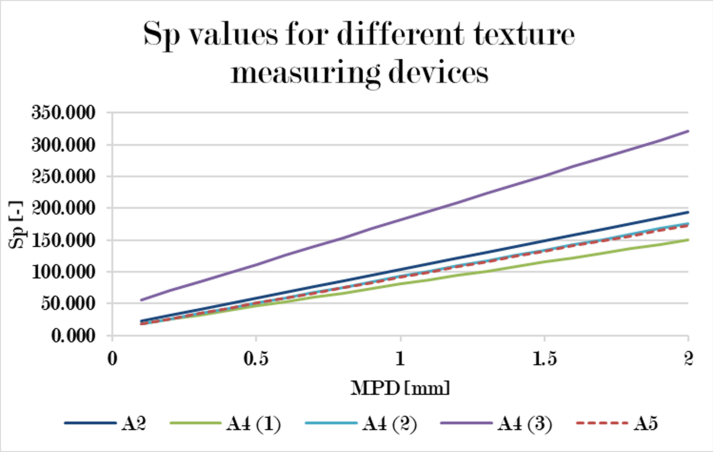

Figure 4.3: Comparison of different formulas for S_p, the speed number in the PIARC model

Figure 4.3 clearly shows that the values for S_p calculated with the a and b according to texture devices A2, A4 (1), A4 (2) and A5 are roughly similar, whereas A4 (3) shows a much larger value for Sp. The a and b values for A4 (3) are much larger than for the other texture devices. This might be due to the measuring speed, which is 72 km/h for A4 (3), whilst for the other devices it is limited to 36 km/h.

Furthermore, Figures 4.4 and 4.5 visualise the skid resistances, measured between 25 and 80 km/h, with a reference skid resistance of 0.4 at 60 km/h. The two graphs differ in the macro texture, which is 0.5 mm in Figure 4.4 and 1.5 mm in Figure 4.5.

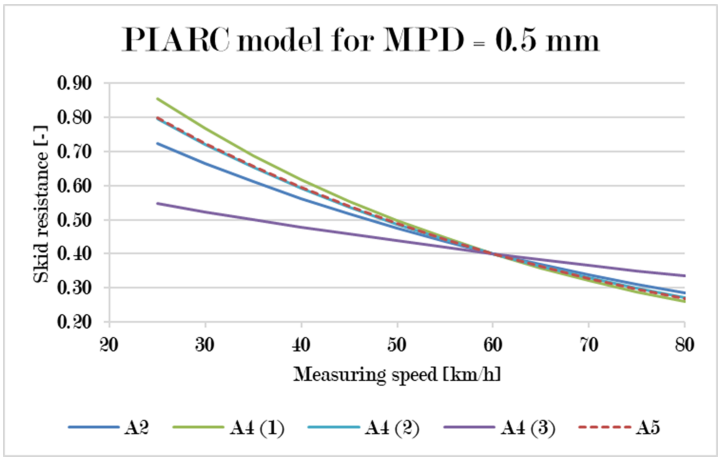

Figure 4.4: Comparison of the PIARC model for different texture devices, with a reference skid resistance of 0.4 at 60 km/h and an MPD of 0.5 mm

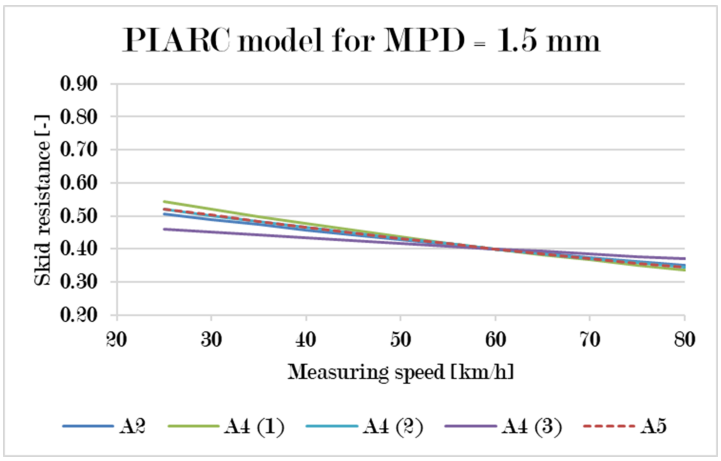

Figure 4.5: Comparison of the PIARC model for different texture devices, with a reference skid resistance of 0.4 at 60 km/h and an MPD of 1.5 mm

Figures 4.4 and 4.5 show very clear the impact of the MPD: a larger MPD implies a much smaller speed dependency. Furthermore, A4 (2) and A5 give approximately equal conversions, which could have been expected due to very similar values for a and b.

Reliability

Dr. James C. Wambold performed an analysis on accuracy of the model developed by PIARC and Vos and Groenendijk (2009) gave a summary of this analysis. This analysis is moreover performed on the overall PIARC model, and not only on the speed corrections. Furthermore, Vos and Groenendijk (2009) mentioned that it was not fully clear to them what was meant with all the given calculated values (contributing to the accuracy of the PIARC model). Therefore, at this moment, no steps were set to dive deeper in the accuracy analysis of the PIARC model.

4.5. KOAC•WMD (1999)

In 1999, Koac•WMD (now Kiwa KOAC) performed skid resistance and macro texture measurements for the CROW (Dutch knowledge platform for infrastructure). At that moment, a model existed for the speed dependency of the skid resistance, but this model was developed based on a limited number of texture variations. Therefore, CROW asked Koac•WMD to verify and improve the existing model on different asphalt layers with a variation of micro and macrotextures (Wennink, 2000).

4.5.1. Experimental setup

- Test tracks of the BASt (Die Bundesanstalt für Straßenwesen, the German Federal Highway Research Institute), on a former Russian airport 50 kilometres south of Berlin, were used. In total, 46 test tracks were constructed with a variety of pavement types.
- AC, PCC and mastic asphalt are the main groups of pavement types. With respect to the AC layers, most were dense layers and some layers were made with porous asphalt. Most of the mastic asphalt layers were gritted with both fine and coarser material.
- The MPD of the tested tracks varied between 0.08 and 2.60 mm.
- The texture was measured with the Automatic Road Analyser (ARAN), a device which measures the MPD with help of a laser. The applied measuring speed of the ARAN was approximately 15 km/h.
- Skid resistance measurements were performed with the RWS Skid Resistance Tester, which measures the LFC.
- A smooth PIARC-tyre (165 R 15) with a tyre pressure of 200±10 kPa and a load of 1960 N was used.
- In front of the measuring wheel a water film with a thickness of 0.5mm and a width of minimum 0.15m was jetted.
- Measurements were performed at 30, 50, 70 and 90 km/h and three times for each measuring speed.

4.5.2. Developed model

With help of SPSS and TableCurve a model was developed for the conversion between varying measuring speeds. Firstly, the shape of the model was defined as in Equation (4.7) (Wennink, 2000):

$$\mu_{x,R} = \mu_{x,V} \cdot e^{(B \cdot (V_R - V))} \tag{4.7}$$

Where:	$\mu_{x,R}$	=	Predicted LFC at reference speed V_R	[-]
	$\mu_{x,V}$	=	Measured LFC at measuring speed V	[-]
	B	=	Parameter dependent on texture	[-]
	V_R	=	Reference measuring speed	[km/h]

B is a parameter dependent on the texture of the surface. MPD is the best variable to predict the value for B and furthermore it became clear that for positive textures (at least gritted pavements) factor B is slightly larger, hence gritted pavements (for equal MPD values) are less speed dependent. B can be expressed as (Wennink, 2000):

$$B = -0.00533 + 0.003073 \cdot ln(\text{MPD}) + r \tag{4.8}$$

Where:	r	=	0	if MPD/RMS $<$ 1.5805 (negative texture)	[-]
		=	0.001682	if MPD/RMS $>$ 1.5805 (positive texture)	[-]

Considering that speed and wet skid resistance have a negative correlation, which should follow from Equation (4.7), one can calculate that for positive textures the model is valid up to a maximum MPD of 3.28 mm and for negative textures the model is valid up to a maximum MPD of 5.67 mm.

4.6. ESDU (2003)

The Engineering Sciences Data Unit (ESDU) company developed a statistical method which represents and relates the braking performances of aircraft and ground-test machines in wet conditions (Balkwill and mitchell (2000), as cited in van Es et al., 2004). The method was developed to apply on measurements performed on natural wetted surfaces, and the Dutch working group on runway friction evaluated

investigated if the ESDU approach could also be used to correlate the friction measurements of devices that apply a water layer in front of the measuring wheel (van Gurp, 2005).

4.6.1. Experimental setup

The experimental setup for ESDU and the model evaluation was as follows (van Es et al., 2004, van Gurp, 2005):

- The measuring devices (measuring the LFC) included in the evaluation study were as follows (van Gurp, 2005):
  - griptester, 14.5% slip
  - ROAR, 15% slip
  - mu-meter Mk 6, no slip but a yaw angle of 15°
  - skiddometer BV11, 15% slip
  - sarsys Friction Tester Saab 9-5, 15% slip
  - ASFT Sharan #1, 15% slip
  - RAW Trailer (RWS Skid Resistance Tester), 86% slip
  - ASFT Sharan #2, 15% slip
- All devices sprayed a water film with a thickness of 1.0 mm in front of the measuring wheel.
- 30 surfaces used for the PIARC experiment were selected to use for this evaluation. These surfaces had a range of macrotexture depths which were representative fro airfields.
- Measurements from the PIARC experiments on these 30 surfaces were used. This included MPD measurements measured with the CRR Stationary profilometer.

4.6.2. Developed model

The ESDU method is as follows (van Gurp, 2005):

$$\mu_V = \frac{\mu_{\text{datum}}}{1 + \beta \frac{o.5\rho V^2}{p}} \tag{4.9}$$

Where:	μ_V	=	Skid resistance at measuring speed V	[-]
	μ_{datum}	=	Coefficient of friction at zero ground speed on a dry surface	[-]
	β	=	Empirical variable	[-]
	ρ	=	Surface contaminant density	[kg/m^3]
	V	=	Measuring speed	[m/s]
	p	=	Tyre inflation pressure	[Pa]

The empirical variable β is device specific and can be calculated form the measured skid resistance of a wetted surface. Therefore, skid resistances measured at equal vehicle speeds with different measuring devices can be compared.

From the evaluation it was concluded that the ESDU method can be used for correlating the output of different measuring devices that spray a water layer in front of the measuring wheel. The advantage above previous developed models (such as the PIARC Model (1995)) is that the ESDU method accounts for random uncertainties to which all skid resistance measuring devices are subjected (van Es et al., 2004).

4.7. FEHRL Hermes project (2006)

In the early 2000s, the Forum of European national Highway Research Laboratories (FEHRL) conducted a research called Harmonisation of European Routine and research Measuring Equipment for Skid resistance of roads and runways (HERMES)). The aim of this research was to promote harmonisation of skid resistance measurements (Vos and Groenendijk, 2009). During the project the European Friction

Index (EFI) was developed. This is a scale for the skid resistance, comparable to the IFI, but now developed on European level.

4.7.1. Experimental setup

- Fifteen skid resistance measuring devices and eight texture-measuring devices were used in the HERMES project. The most relevant devices that took part in the project are the RWS Skid Resistance Tester and three types of the SCRIM. The setup conditions for these devices were as follows:
  - RWS Skid Resistance Tester: 86% fixd slip, PIARC smooth tyre at 200 kPa, water film with a thickness of 0.5 mm
  - SCRIM CEDEX: yaw angle of 20°, SCRIM smooth tyre at 350 kPa, water film with a thickness of 0.5 mm
  - SCRIM MET: yaw angle of 20°, SCRIM smooth tyre at 350 kPa, water film with a thickness of 0.5 mm
  - SCRIM TRL: yaw angle of 20°, SCRIM smooth tyre at 350 kPa, water film with a thickness of 0.5 mm at 50 km/h and 0.25mm at 90 km/h.
- Skid resistance measuring devices measured either the SFC or the LFC, with slip ratios from 14% up to 100% (locked wheel).
- Eight different texture meters were used in the project, among which the ARAN operated in the Netherlands.
- Different test locations were defined and at each test location the selected devices measured at three different measuring speeds: 30 km/h, 90 km/h and an intermediate speed that corresponded to the standard measuring speed of this device.
- Many test sections consisted of a concrete pavement, however, some pavements consisted of for example PA, DAC or SMA.

4.7.2. Developed model

The formula developed by the Hermes project is based on Equation (4.6). To focus more on the devices used in Europe, the texture depth values were recalculated according to the new ISO-standard for the calculation of the MPD (ISO 13473-1:1997 (1997), as cited in Descornet et al. (2006)). A further difference to the PIARC is that the formulae developed by the Hermes project used a reference slip speed of 30 km/h instead of 60 km/h.

FEHRL Hermes developed the formulae as follows (Vos and Groenendijk (2009) and Descornet et al. (2006)):

$$\mathrm{EFI} = B \cdot \mu_{30} \tag{4.10a}$$

$$\mu_{30} = \mu \cdot e^{\frac{S - S_R}{S_0}} \tag{4.10b}$$

$$S_0 = a \cdot \mathrm{MPD}^b \tag{4.10c}$$

Where:	a, b, B	=	Device specific parameters	[-]
	μ	=	Measured LFC or SFC	[-]
	μ_{30}	=	Estimated friction coefficient at the reference slip speed, which is set to 30 km/h	[-]
	S_R	=	Reference slip speed, set to 30 km/h	[km/h]
	S_0	=	Speed constant related to tested surface characteristics	[km/h]

S_p is a parameter depending on the surface characteristics and a and b depend on the texture meter. Parameter B is to convert the skid resistance of a certain device to the skid resistance measured with a reference device. Thus, B depends on the used skid resistance meter. Therefore, Equation (4.10b) is the conversion model to convert a measured skid resistance to the skid resistance at another speed.

Descornet et al. (2006) developed a second regression because the first model was not very accurate. This model contained an extra input parameter, namely the slip ratio. The HERMES approximation for this curve is as follows:

$$\mu_s = \mu_0 \cdot e^{-\frac{S}{S_0}^3} = \mu_0 \cdot e^{-(\frac{S}{117 \cdot (\mathrm{MPD})^a \cdot (\mathrm{SR})^{0.9}})^3} \tag{4.11}$$

Where:

μ_s	=	Friction at slip speed S	[-]
μ_0	=	'Theoretical' friction at 0 km/h slip speed	[-]
S_0	=	Speed constant	[km/h]
a	=	Device specific constant	[-]

Reliability

In 10% of the cases did the model stemming from Equations (4.10a) and (4.10c) not fit to the experimental data. The majority of these deviations was found in measurements on porous asphalt and/or measurements with a low slip ratio (<20%) (Vos and Groenendijk, 2009). Therefore, the second model was developed. The model according to Equation (4.11) showed less deviations to the data, but still it was not very accurate.

4.8. E. Vos (2008)

Vos (2008) performed his research commissioned by the RWS. In 2010, the standard measuring speed for the RWS Skid Resistance Tester was raised from 50 km/h to 70 km/h (Vos et al., 2017) and therefore the skid resistance measured at a speed of 50 km/h needed to be converted to the skid resistance of the same road section at a speed of 70 km/h.

4.8.1. Experimental setup

- 17 road sections were measured, of which 7 were constructed with porous asphalt (ZOAB) and 10 with dense asphalt (DAC). In total, this gave 41 sections with a length of 1 hectometre. Measurements were performed 4 times, twice per measuring speed (50 and 70 km/h).
- Sections were consciously selected on having a skid resistance close to the intervention level (the target values defined by RWS).
- Measurements were performed with the RWS SKid Resistance tester, which measures the LFC.
- In front of the measuring wheel a water film with a thickness of 0.5mm and a width of 0.15m was jetted.
- The tyre used was the PIARC 1998 measuring tyre, which is a smooth tyre.

4.8.2. Developed model

Vos (2008) generalised his results on PA and DAC to a distinction between open and dense wearing courses and he found that there was, with this distinction, a good correlation between the measured skid resistance at 50 km/h and 70 km/h. Equations (4.12a) and (4.12b) show the found correlations.

$$\text{For open asphalt: } \mu_{x,70} = \frac{42}{45} \cdot \mu_{x,50} \ (= 0.993 \cdot \mu_{x,50}) \tag{4.12a}$$

$$\text{For dense asphalt: } \mu_{x,70} = \frac{39}{44} \cdot \mu_{x,50} \ (= 0.886 \cdot \mu_{x,50}) \tag{4.12b}$$

Reliability

The model of (Vos, 2008) was only based on 41 sections of one hectometre, which is not very extensive. Furthermore, no information about the reliability or accuracy of this model is given in the work of (Vos, 2008).

4.9. Koac•NPC (2009)

Koac•NPC (now Kiwa KOAC) developed a conversion model for the skid resistance measured with the RWS Skid Resistance Tester at a measuring speed between 20 and 50 km/h, to the skid resistance at 50 km/h. This conversion model was developed because sometimes measuring at the speed of 50 km/h, for example on roundabouts or bicycle paths, was not possible. These type of sections can be measured with a maximum speed of approximately 30 km/h only. The experimental setup is not known. The conversion model is given in Equation (4.13).

$$\mu_{x,50} = \mu_{x,V} \cdot e^{(V-50)\cdot(0.01222-0.00668\cdot \mathrm{MPD})} \tag{4.13}$$

Where:				
	$\mu_{x,50}$	=	LFC at 50 km/h	[-]
	$\mu_{x,V}$	=	LFC measured at measuring speed V below 50 km/h	[-]

A second model was developed in cases where the MPD could not be measured, for example during rain. In this situation, Equation (4.14) can be used, with is slightly less accurate than Equation (4.13).

$$\mu_{x,50} = \mu_{x,V} \cdot e^{0.00734\cdot(V-50)} \tag{4.14}$$

Reliability

No information about the reliability or accuracy of this model is known.

4.10. SCRIM Model

In the UK, the SCRIM is used for measuring the SFC. The Design Manual for Roads and Bridges gives a speed conversion for measuring speeds varying from 25 to 85 km/h to a reference speed of 50 km/h using the following equation (Highways England, 2015):

$$SR_{50} = SR_V \cdot \frac{-0.0152 \cdot V^2 + 4.77 \cdot V + 799}{1000} \tag{4.15}$$

Where:				
	SR_{50}	=	SFC corrected to 50 km/h, multiplied by 100	[%]
	SR_V	=	SFC measured at speed V, multiplied by 100	[%]

(Roe et al., 1998) performed a research to the influence of texture depth of high and low speed skidding resistance. Roe et al. concluded that a quadratic equation provided the best representation for the relationship between friction and speed measured with a smooth tyre. This research could be the origin of the quadratic formula of Equation (4.15), but this not certain.

4.11. TP Griff-StB (SKM) (2007)

In the German TP Griff-StB (SKM) (Arbeitsgruppe Infrastrukturmanagement, 2007), the technical document which prescribes all requirements regarding measurements with the SKM device, the speed conversion is given as:

$$\mu_{y,R} = \mu_{y,V} + \frac{V - V_R}{20} \cdot 0.05 \tag{4.16}$$

Where:				
	$\mu_{y,R}$	=	Predicted SFC at reference speed R	[-]
	$\mu_{y,V}$	=	Measured SFC at measuring speed V	[-]
	V_R	=	Reference measuring speed (40, 60 or 80 km/h)	[km/h]

This formula is possibly derived from the statement that a decrease in speed will have the effect of increasing the measured SFC by 0.01 for each 4 km/h reduction in speed (Hosking and Woodford, 1976b), since $\frac{4}{20} \cdot 0.05 = 0.01$.

Equation (4.16) can be used when the measuring speed is at most 10 km/h lower or higher than the reference speed. This means that the following speed intervals can be used to convert to the mentioned reference speeds:

40 km/h:	30 km/h	$<$	V	$<$	50 km/h
60 km/h:	50 km/h	$<$	V	$<$	70 km/h
80 km/h:	70 km/h	$<$	V	$<$	90 km/h

Besides correcting the speed, also a temperature correction is applied according to Equation (4.17).

$$\mu_{R,T} = \mu_R + (TW - 20°C) \cdot 0.002/°C + (PT - 20°C) \cdot 0.0012/°C \tag{4.17}$$

Where:				
	$\mu_{R,T}$	=	SKM skid resistance normalised for temperature and speed	[-]
	TW	=	Measured water temperature	[°C]
	PT	=	Measured temperature of the pavement	[°C]

Reliability

Equation (4.16) is a linear relation between skid resistances at different speeds, not taking into account the macrotexture of the surface. Because in much previous research it turned out that the macrotexture is an important parameter to consider, it is plausible that Equation (4.16) is not very accurate. Derksen (2017) wrote that for practical reasons the German approach is used for the conversion in the Netherlands, which might already indicate the inaccuracy of the conversion model.

4.12. BASt (2012)

On behalf of the BASt, Bürckert et al. (2012) performed a research to the influence of pavement textures on SKM measurements. They concluded that the speed-dependency is influenced by the surface macro texture and that even the micro texture should be considered, because the combination of macro and micro texture is essential. Bürckert et al. (2012) mentioned also that unknown temperature effects appeared which could not be explained in the time of their research.

4.12.1. Experimental setup

- Measurements were performed with the SKM, measuring the SWF, according to the TP Griff-StB (SKM).
- Smooth SWF tyres of 3x20 inch were used with a tyre pressure of 2.5 $\pm$ 0.1 bar.
- In front of the measuring wheel a water film with a thickness of 0.5 mm and a width of 80 mm was jetted.
- Measurements were performed on a 5 km long section of the the German Motorway A24.
- The surface type is unknown, but it had an MPD between 0.72 and 1.47 mm.
- The skid resistance was measured at measuring speeds of 40, 60, and 80 km/h.

4.12.2. Developed model

Bürckert et al. (2012) proposed a speed correlation formula which was an elaboration of Equation (4.16). This formula takes the surface texture into account:

$$\mu_{y,R} = \mu_{y,V} + \frac{V - V_R}{20} \cdot (0.120 - 0.062\frac{1}{mm} \cdot \text{MPD}) \tag{4.18}$$

This formula is obtained by a regression of data points with on the x-axis the macrotexture and on the y-axis the $\Delta\mu_y/\Delta V$ (thus, the average decline in skid resistance per km/h difference in measuring speed). This is, like the model of Equation (4.16), a linear equation once the macrotexture is set. The larger the macrotexture, the smaller the slope of the regression line and thus the less speed dependent the skid resistance will be.

Reliability

The coefficient of determination (R^2) for Equation (4.18) obtained by a regression of the data is 0.672. This is interpreted as the proportion of the variance in the dependent variable ($\Delta\mu_y/\Delta V$) that is predictable from the independent variable (macrotexture) (StatTrek, 2018). However, the regression was made based on a limited variation of pavement textures and compositions and therefore the formula cannot be generalised (Bürckert et al., 2012).

4.13. Comparison of speed conversion models for the SFC

It is difficult to compare the different speed conversion models for the SFC, because different reference speeds and input parameters are used. This section attempts to make a comparison and obtain an indication of how the speed conversion models differ from each other.

4.13.1. TP Griff-StB (SKM) and BASt

Equations (4.16) and (4.18) are equal for an MPD of 1.129 mm, this value is obtained by solving:

$$0.120 - 0.062\frac{1}{mm} \cdot \text{MPD} = 0.05 \tag{4.19}$$

As can be seen from the example in Table 4.4, the correction of Equation (4.16) (TP Griff) is smaller than the correction of Equation (4.18) (BASt) for MPD values smaller than 1.129 mm, which means:

- A correction to a *higher* reference speed: the converted value of TP Griff is larger than the converted value of the BASt.
- A correction to a *lower* reference speed: the converted value of TP Griff is smaller than the converted value of the BASt.

Furthermore, Table 4.4 shows that for MPD values larger than 1.129, the correction of Equation (4.16) is larger than the correction of Equation (4.18), which means:

- A correction to a *higher* reference speed: the converted value of TP Griff is smaller than the converted value of the BASt.
- A correction to a *lower* reference speed: the converted value of TP Griff is larger than the converted value of the BASt.

Table 4.4: Comparison between conversion models of the TP Griff-StB (SKM) and the BASt. A measured SFC of 0.5 at respectively 50 or 70 km/h is converted to an SFC at 60 km/h.

Measuring speed	Measured SFC	MPD	TP Griff converted SFC	BASt converted SFC	Correction TP Griff	Correction BASt
50	0.5	1	0.475	0.471	-0.025	-0.0290
70	0.5	1	0.525	0.529	0.025	0.0290
50	0.5	1.5	0.475	0.487	-0.025	-0.0135
70	0.5	1.5	0.525	0.514	0.025	0.0135

It is undesirable that a speed correction model results into a too high value for the converted SFC, because in this situation the converted value of a SFC could probably meet the standards whilst in reality it would not. However, no clear conclusions can be drawn from the comparison above. In some situations, the TP Griff gives a higher value of the converted SFC and in some situations the BASt does.

Figure 4.6 gives a visualisation of the comparison between the conversion models of the BASt and TP Griff. In this figure the following is shown:

- The reference skid resistances are given at 40 at 60 km/h and are 0.6 and 0.5 respectively.

- The reference skid resistances are converted to the 'measured' skid resistances, which are 30 to 50 km/h (for the reference skid resistance at 40 km/h) and 50 to 70 km/h (for the reference skid resistance at 60 km/h).
- Three values of the MPD have been used as input, namely 0.5, 1.0 and 1.5 mm.

The figure shows values for skid resistances at certain speeds in combination with a certain macrotexture (for the BASt), which would give a reference skid resistance μ_R of 0.6 at 40 km/h or 0.5 at 60 km/h.

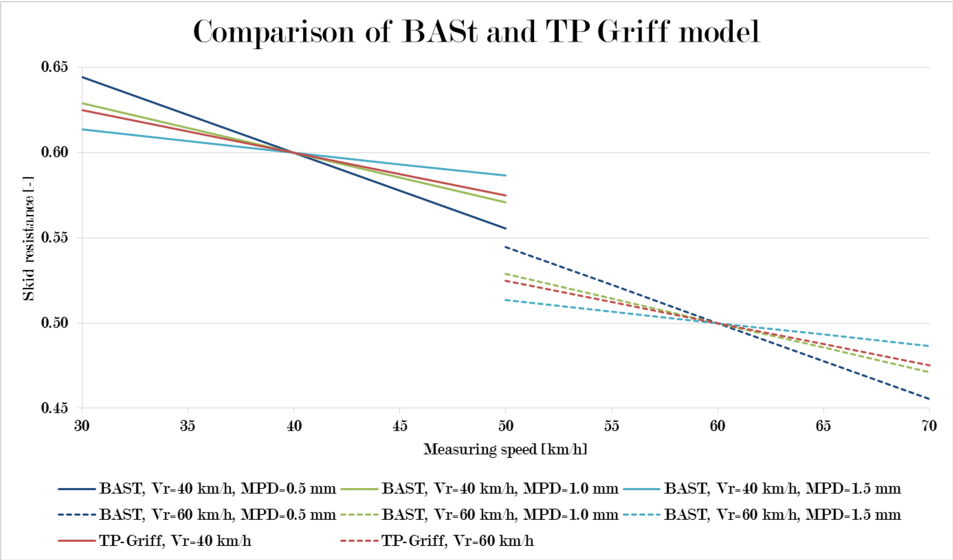

Figure 4.6: Comparison of conversion models BASt and TP Griff-StB (SKM). A reference skid resistance of 0.6 measured at 40 km/h or 0.5 measured at 60 km/h is converted over a speed difference of 10 km/h.

From the figure it becomes clear that the larger the macro texture is, the less speed dependent the skid resistance for the BASt conversion model will be. This matches with the theory that a larger macrotexture provides a drainage system and makes the skid resistance less speed dependent, because at higher speeds the macrotexture will help to drain off the water.

4.13.2. TP Griff and SCRIM

A first difference of Equations (4.15) and (4.16) (respectively the SCRIM model and the TP Griff model) is that the SCRIM model gives a relative correction, whilst the TP Griff model provides an absolute correction. This means, the SCRIM model is of the shape $\mu_R{=}\mu_V \cdot X$, whereas the TP Griff model is of the shape $\mu_R{=}\mu_V + X$.

The two models are compared with fictitious skid resistance measurements. A reference speed of 50 km/h is used, because this is the reference speed for the SCRIM. This is not a reference speed for the TP Griff, but because the TP Griff provides a linear model, it is assumed that a different reference speed can be used to compare the different conversion models —as long as the corrections are limited to 10 km/h. With a a reference speed of 50 km/h and a skid resistance at 50 km/h, the values for the skid resistance at the measuring speeds from 40 to 60 km/h can be calculated.

For Table 4.5 a reference skid resistance of 0.5 is used, for Table 4.6 a reference skid resistance of 0.7 is used. As can be seen from the examples:

- For smaller SFC values the corrections calculated according to Equation (4.15) are higher than for larger SFC values.
- For the SCRIM model, the average correction in SFC per km/h declines when the measuring speed increases, whilst for the TP Griff this stays 0.0025.
- Only at very high skid resistances the correction of the SCRIM will be equal or smaller than the correction applied by TP Griff. In Table 4.6 this is the case for a measured value of 0.73 by the

SCRIM at a measuring speed of 40 km/h. However, for the other measuring speeds, the correction applied by the SCRIM is always smaller. As 0.7 is already quite high, this indicates that in most of the situations the SCRIM model will give a smaller correction for the SFC.

Table 4.5: Comparison of SCRIM and TP Griff-StB (SKM) conversions. The given corrections are corrections to converd from the corresponding measuring speed to a reference skid resistance of 0.5 at a reference speed of 50 km/h.

Measuring speed	**SCRIM, μ50=0.5**	**TP Griff, μ50=0.5**	**Correction SCRIM**	**Correction TP Griff**	**Correction SCRIM per km/h**	**Correction TP Griff per km/h**
40	0.518	0.525	-0.018	-0.025	-0.0018	-0.0025
45	0.509	0.513	-0.009	-0.013	-0.0017	-0.0025
50	0.500	0.500	0.000	0.000		
55	0.492	0.488	0.008	0.013	0.0015	0.0025
60	0.485	0.475	0.015	0.025	0.0015	0.0025

Table 4.6: Comparison of SCRIM and TP Griff-StB (SKM) conversions. The given corrections are corrections to converd from the corresponding measuring speed to a reference skid resistance of 0.7 at a reference speed of 50 km/h.

Measuring speed	**SCRIM, μ50=0.7**	**TP Griff, μ50=0.7**	**Correction SCRIM**	**Correction TP Griff**	**Correction SCRIM per km/h**	**Correction TP Griff per km/h**
40	0.725	0.725	-0.025	-0.025	-0.0025	-0.0025
45	0.712	0.713	-0.012	-0.013	-0.0024	-0.0025
50	0.700	0.700	0.000	0.000		
55	0.689	0.688	0.011	0.013	0.0021	0.0025
60	0.679	0.675	0.021	0.025	0.0021	0.0025

Figure 4.7 visualises the difference for the two conversion models. For this figure, a reference skid resistance of 0.5 and 0.7 at a reference speed of 50 km/h is calculated to the corresponding skid resistances for measuring speeds of 40 to 60 km/h. Figure 4.7 shows that for the reference skid resistance of 0.7, the outcome of the models are more similar than for the reference skid resistance of 0.5.

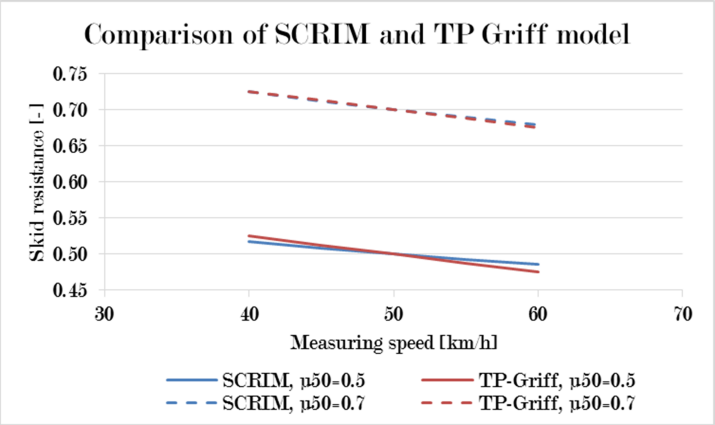

Figure 4.7: Comparison of conversion models SCRIM and TP Griff-StB (SKM). A reference skid resistance of 0.5 or 0.7 measured at 50 km/h is converted to a skid resistance at 40 and 60 km/h.

In Figure 4.8a the SCRIM model is given for a wider variety of measuring speeds, because this model can be used for speeds varying between 25 and 85 km/h. As one can see, the model of the SCRIM follows slightly the curve of Figure 4.8b.

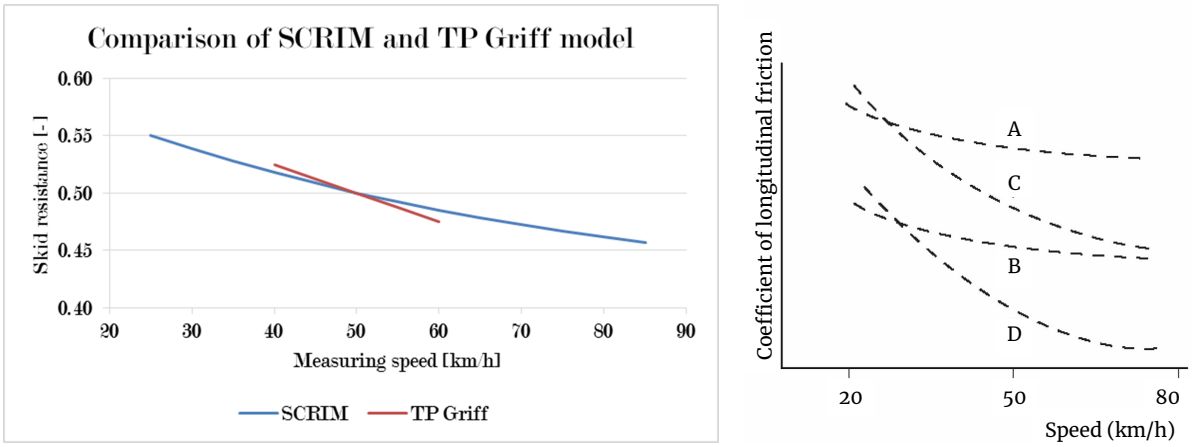

(a) (b)

Figure 4.8: On the left: comparison of conversion models SCRIM and TP Griff-StB (SKM). On the right: speed dependency of friction coefficient (copy of Figure 2.13)

4.13.3. TP Griff-StB (SKM), PIARC and BASt

A comparison between the PIARC Model, the BASt model, and the conversion formula used in the TP Griff-StB (SKM) was performed by plotting graphs of the formulas in which a reference skid resistance of 0.4 at 60 km/h is used in combination with an MPD of 0.5 mm (Figure 4.9) and 1.5 mm (Figure 4.10).

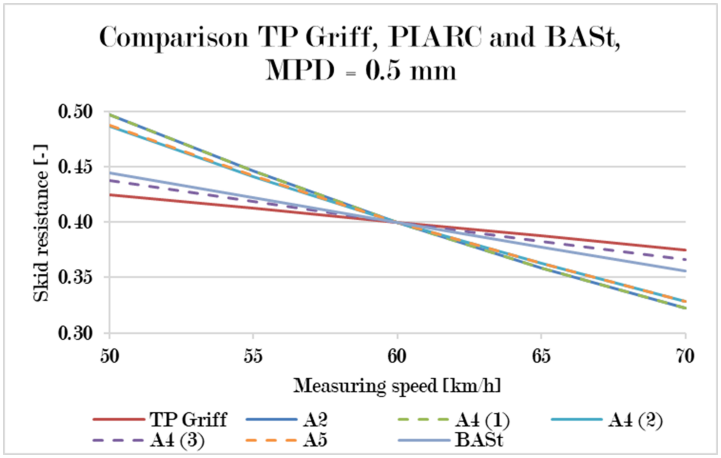

Figure 4.9: Comparison of TP Griff-StB (SKM), PIARC and BASt for an MPD of 0.5 mm. A skid resistance of 0.4 at 60 km/h is converted to skid resistances at 50 and 70 km/h.

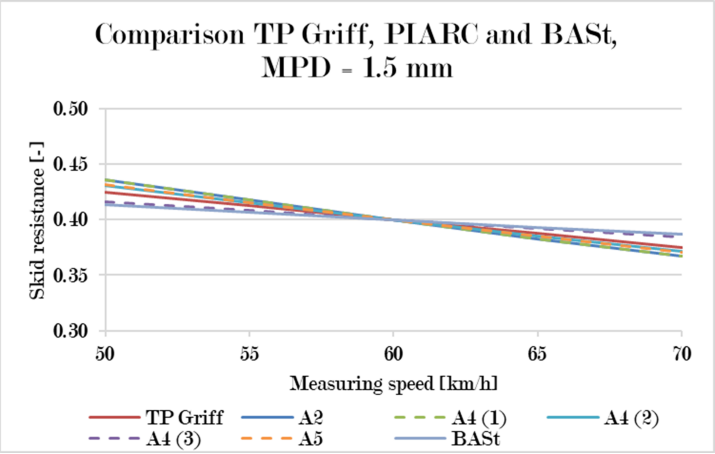

Figure 4.10: Comparison of TP Griff-StB (SKM), PIARC and BASt for an MPD of 1.5 mm. A skid resistance of 0.4 at 60 km/h is converted to skid resistances at 50 and 70 km/h.

The graphs clearly show that, for an MPD of 0.5 mm, the lines are less close to each other than for an MPD of 1.5 mm. As expected, because 1.129 (see Section 4.13.1) is between the two used macrotextures, for a MPD of 0.5 mm the BASt applies a larger correction whilst for an MPD of 1.5 mm the TP Griff-StB (SKM) applies a larger correction. The model with a and b values for texture device A4 (3) matches the values obtained by TP Griff-StB (SKM) and BASt. This may indicate that the values for a and b of A4 (3) fit best to the texture device used in the SKM. The PIARC formula would then become:

$$\mu_{B60} = \mu_{BS} \cdot e^{\frac{S-60}{42.256+139.203 \cdot MPD}} \tag{4.20}$$

However, one should note that A4 (3) is the device of which the a and b parameters are most divergent comparing to the other texture meters (see Table 4.3). Therefore, the values of a and b for the SKM remain doubtful.

4.14. Conclusions

Based on the analysis of previous speed conversion models and some comparisons between the models, some conclusions can be drawn:

- Forms of models that exist are:
  - linear formulas, which add or subtract a factor to the measured skid resistance (Hosking and Woodford (1976), TP Griff-StB (SKM) (2007));
  - linear formulas, that multiply the measured skid resistance with a certain factor (E. Vos (2008));
  - quadratic formulas, which multiply the measured skid resistance with a factor (SCRIM Model);
  - exponential formulas (Penn State Model (1978), PIARC Model (1995), KOAC•WMD (1999), FEHRL Hermes project (2006), Koac•NPC (2009)).
- Most of the models use an exponential relationship. Possibly, this fits best the speed dependent behaviour of skid resistance.
- Some models use the texture, or a parameter dependent on the texture, as input. The macrotexture is used in the PIARC Model (1995), KOAC•WMD (1999), Koac•NPC (2009), and BASt (2012)). E. Vos (2008) makes a distinction between open and dense pavements, and the FEHRL Hermes project (2006) uses a speed parameter related to tested surface characteristics.
- BASt (2012) extended the model of TP Griff-StB (SKM) (2007) and incorporates the fact that the skid resistance is less speed dependent on a road with a larger macrotexture. This model still

uses a linear function. For a macrotexture of 1.129, BASt (2012) and TP Griff-StB (SKM) (2007) are equal.

- The plot of the SCRIM model looks more equal to Figure 2.13 than the TP Griff-StB (SKM) model, but no macrotexture is used in this formula. Also, this formula always converts to a speed of 50 km/h, which is not the purpose of the conversion model in this research. Therefore, this model might not be extendable to a model that takes into account macrotexture and which can convert the skid resistance to different reference speeds.
- It is not known which a and b should be applied in the S_p of the PIARC Model (1995) for the SKM. Based on a comparison with TP Griff-StB (SKM) (2007) and BASt (2012) for different values of the MPD, the conclusion can be drawn that the texture device A4 (3) with a=42.256 and b=139.203 fits best in the other conversion models.
- For most models, no evaluation of the accuracy or reliability of the model is given or found in the consulted literature.

5

Model generation

This chapter describes the regression analysis performed on the data. An overview of the available data is given in Appendix C, as well as some graphs visualising the dataset and a short repeatability analysis. Furthermore, the analysis as described in this chapter is performed on approximately 75% of the total available data, the other 25% of observations are used to verify the model.

Section 5.1 describes the set-up of the performed analysis for the model generation. The predictive variables and the used methods are concisely described. The performed methods are elaborated in detail in Sections 5.2 to 5.4 and Section 5.6 gives the final conclusions of the model generation.

5.1. Set-up of analysis

From the literature review and experiences in measurements it became clear that the skid resistance is assumed to decline with an increasing measuring speed. In previously developed conversion models often a curvilinear —exponential— relationship is assumed between the speed and skid resistance, whereas in fewer models a linear relationship is assumed. Therefore, initially, two different models are formulated for the regression analysis:

$$\mu_a = \mu_b + C_0 + C_1 \cdot var_1 + C_2 \cdot var_2 + ... + C_n \cdot var_n \tag{5.1a}$$

$$\mu_a = \mu_b \cdot e^{C_0 + C_1 \cdot var_1 + C_2 \cdot var_2 + ... + C_n \cdot var_n} \tag{5.1b}$$

Equation (5.1a) shows the linear relationship and Equation (5.1b) shows the exponential relationship. $C_1, ..., C_n$ are the regression coefficients and $var_1, ..., var_n$ are the predictive variables.

5.1.1. Predictive variables

Equations (5.1a) and (5.1b) show the models which are used for the regression analysis, in which $C_1, ..., C_n$ are the regression coefficients and $var_1, ..., var_n$ are the predictive variables.

From previous research, predictive variables are selected and some new possible predictive variables are added. The following variables are used in the analysis:

- $V_b - V_a$
- MPD$\cdot(V_b - V_a)$
- $ln(\text{MPD}) \cdot (V_b - V_a)$
- $\frac{\text{MPD}}{\text{RMS}} \cdot (V_b - V_a)$
- $\frac{\text{MPD}}{\text{RMS}} \cdot (V_b - V_a)$ as a dummy variable:
  - $(V_b - V_a)$ if $\frac{\text{MPD}}{\text{RMS}} > 1.58$
  - 0 if $\frac{\text{MPD}}{\text{RMS}} < 1.58$

- 1-$\frac{V_b}{V_a}$: this variable is not included in previous research but will be investigated in this regression analysis. Often it is assumed that at a lower speeds the skid resistance declines more with increasing the speed than at higher speeds. Therefore, it is investigated whether the relative change in speed works as a predictive variable.
- MPD·$(1 - \frac{V_b}{V_a})$
- $\frac{\text{MPD}}{\text{RMS}} \cdot (1 - \frac{V_b}{V_a})$
- $ln(\text{MPD}) \cdot (1 - \frac{V_b}{V_a})$

Replicate measurements of skid resistance at the same measuring speed should ideally result in the same value of skid resistance. For this reason a model set-up was chosen in which all predictive variables combined with their regression coefficients were to be regarded as a multiplication of $V_a - V_b$ or $1 - \frac{V_b}{V_a}$. This implies that the intercept (C_0) should be set to zero.

In general, a decline in skid resistance is expected with an increasing speed. This means that if $V_b - V_a$ would be included, this variable would have a positive coefficient (if V_a is smaller than V_b, a higher skid resistance is expected. Since $V_b - V_a$ is positive the coefficient must be positive as well). Furthermore, a larger MPD is expected to diminish the speed dependency, thus the coefficients of MPD·$(V_b - V_a)$ and $ln(\text{MPD}) \cdot (V_b - V_a)$ are expected to be negative. For the other predictive variables, such as MPD/RMS·$(V_b - V_a)$ it is more difficult to set up an hypothesis about the sign of the regression coefficient.

In the analysis, all variables with $(V_b - V_a)$ are divided by 100. The regression coefficients are very small and by dividing the variables by 100 the constants become larger. This makes no difference in the correlations and the calculated regression constants, besides that they must be divided by 100 after the regression. In this report, all regression constants are already divided by 100 and thus the models shown are based on the variables above, and not on the variables divided by 100.

5.1.2. Performed regression methods

The regression analysis is performed according to three different methods, which are as follows:

- The first method is a multiple linear regression, performed on data consisting of combinations of two skid resistance measurements with corresponding measurement speeds. This method is explained in Section 5.2.
- The second method is based on the estimation of a zero speed intercept. This zero speed intercept is then used in the linear regression analysis to predict μ_a based on the μ_0. This method is clarified in Section 5.3.
- The third method uses multilevel modelling and this method is elaborated in Section 5.4.

5.1.3. Comparison of regression methods: RMSE

For the obtained models, the standard error of the residuals (Root Mean Square Error, RMSE) is calculated according to the equation as follows:

$$RMSE = \sqrt{\frac{\sum_1^n (\mu_{pred,i} - \mu_{measured,i})^2}{n}} \tag{5.2}$$

This standard error of the residuals is used to compare the models obtained by the different regression methods. The RMSE has the same unit as the dependent variable, and to obtain comparable values of the RMSE, it must be calculated in the same datasheet. Therefore, the datasheet of the first regression method, which is explained in the next section, is used for calculating the RMSE for all obtained models.

5.2. Method 1: multiple linear regression performed on speed combinations

The first method is a multiple linear regression performed on combinations of two measurements, consisting a measuring speed and a corresponding value for the skid resistance. The comprehensive theory

behind a multiple linear regression analysis can be found in Section B.2.

5.2.1. Explanation of method

The objective of this research is to develop a model which can convert a skid resistance measurement at a certain measuring speed B to a skid resistance at a different measuring speed A. Therefore, the data, which mostly consists of three measurements per 100 metre section, is split into multiple observations with two measurements per observation. If the measurement speeds for a road section were 40, 60, and 80 km/h, three observations are composed consisting of measurements performed at 40 and 60 km/h, 40 and 80 km/h, and 60 and 80 km/h with the corresponding measured values of the skid resistance. The structure of the data is presented in Table 5.3, and this matches the input needed for the models as in Equations (5.1a) and (5.1b). The structure of the data is explained in more detail in Section C.2.2.

Table 5.1: Structure of datasheet for regression method 1 - multiple linear regression

Unique code for 100 metre section	V_a	V_b	μ_a	μ_b	**MPD**	**RMS**	**... other information**
1	40	60	μ_{40}	μ_{60}			
1	40	80	μ_{40}	μ_{80}			
1	60	80	μ_{60}	μ_{80}			

Both a linear and exponential relationship can be investigated with this method. In case of a linear relationship, a regression will be performed on:

$$\mu_a - \mu_b = C_1 \cdot var_1 + C_2 \cdot var_2 + ... + C_n \cdot var_n \tag{5.3}$$

In case of the exponential relationship, the regression will be performed on:

$$ln\left(\frac{\mu_a}{\mu_b}\right) = C_1 \cdot var_1 + C_2 \cdot var_2 + ... + C_n \cdot var_n \tag{5.4}$$

Therefore, some extra variables are calculated and added to the datasheet:

- Variables to be predicted:
  - $\mu_a - \mu_b$
  - $ln\left(\frac{\mu_a}{\mu_b}\right)$
- Possible predictive variables: as in Section 5.1.1

Various regressions on the data were performed. First, a stepwise (forward) regression with all possible predictive variables was performed on both a linear and exponential model, to see which variables fit best on the dataset. Thereafter, several regressions were performed with combinations of predictive variables. For the combination of variables that gives the best outcome, a more comprehensive output was generated, making it possible to detect and select outliers and highly influential observations. Finally, a regression without outliers was performed to see whether this would give a large difference compared to the regression with all data included in for example the standard error of the residuals (Root Mean Square Error, RMSE).

5.2.2. Analysis of data

This section outlines the obtained results with the analyses performed as explained in the previous section. The executed analyses are:

- stepwise regression on multiple variables
- regressions on combinations of variables, and
- outlier analysis.

Stepwise regression on multiple variables

A forward stepwise regression was performed for a linear and exponential model with all predictive variables as in Section 5.1.1. With a stepwise regression, a regression starts with one predictive variable and in each step another predictive variable is added. The process is stopped when adding a new variable did not generate a significant improvement.

The included variables for the exponential model per step are:

1. $\frac{\text{MPD}}{\text{RMS}} \cdot (1 - \frac{V_b}{V_a})$
2. MPD$\cdot(1 - \frac{V_b}{V_a})$
3. $\frac{\text{MPD}}{\text{RMS}} \cdot (V_b - V_a)$
4. $1 - \frac{V_b}{V_a}$
5. $ln(\text{MPD}) \cdot (1 - \frac{V_b}{V_a})$
6. $V_b - V_a$

For the linear model the included variables are slightly different:

1. $\frac{\text{MPD}}{\text{RMS}} \cdot (1 - \frac{V_b}{V_a})$
2. MPD$\cdot(1 - \frac{V_b}{V_a})$
3. $\frac{\text{MPD}}{\text{RMS}} \cdot (V_b - V_a)$
4. $\frac{\text{MPD}}{\text{RMS}} \cdot (V_b - V_a)$ as a dummy variable
5. MPD$\cdot(V_b - V_a)$
6. Removal of: MPD$\cdot(1 - \frac{V_b}{V_a})$
7. $1 - \frac{V_b}{V_a}$
8. $ln(\text{MPD}) \cdot (V_b - V_a)$
9. MPD$\cdot(1 - \frac{V_b}{V_a})$

The first three steps include similar predictive variables for the linear and exponential model. Thereafter, the included variables are sometimes different. For the exponential model, $ln(\text{MPD}) \cdot (V_b - V_a)$, MPD$\cdot(V_b - V_a)$ and MPD/RMS$\cdot(V_b - V_a)$ as a dummy variable were not included. For the linear model, $V_b - V_a$ and $ln(\text{MPD}) \cdot (1 - \frac{V_b}{V_a})$ are not included.

By analysing the output of these regressions, feasible combinations of variables were formulated for the regressions on combinations of predictive variables. Import information is given by the variance inflation factor (VIF), which can indicate multicollinearity (see Section B.2.2). Combining too many of the possible predictive variables gives high a high VIF because many variables depend on each other. A high VIF arises when the following variables are combined within one model:

- $\frac{\text{MPD}}{\text{RMS}} \cdot (V_b - V_a)$ and $\frac{\text{MPD}}{\text{RMS}} \cdot (1 - \frac{V_b}{V_a})$
- $\frac{\text{MPD}}{\text{RMS}} \cdot (V_b - V_a)$ and $V_b - V_a$
- MPD$\cdot(1 - \frac{V_b}{V_a})$ and $ln(\text{MPD}) \cdot (1 - \frac{V_b}{V_a})$

Regressions on combinations of variables

An overview of the performed regressions is shown in Table 5.2. The table shows the included variables, the values of the VIF, the R^2 and the RMSE for both the exponential and linear relationship. Important is that in SPSS the R^2 for a regression through the origin is calculated differently than for a regression with an intercept, and therefore the value for R^2 seems higher than it in reality is. Furthermore, the RMSE for the exponential and linear models are in other units (for the exponential model it is given in $ln\left(\frac{\mu_a}{\mu_b}\right)$, whereas for the linear model the RMSE is given in $\mu_a - \mu_b$). The R^2 is therefore used to

compare the exponential and linear models, and the RMSE is used to compare models with different variables within the exponential or linear equation.

Table 5.2: Overview of performed regressions with combinations of predictive variables

Regression	Included variables	Highest VIF	Exponential		Linear	
			R^2	RMSE	R^2	RMSE
1	$V_b - V_a$, MPD·$(V_b - V_a)$, MPD/RMS·$(V_b - V_a)$	32.0	0.805	0.043	0.797	0.029
2	MPD/RMS·$(V_b - V_a)$	-	0.746	0.049	0.741	0.033
3	$V_b - V_a$, MPD/RMS·$(V_b - V_a)$	22.0	0.746	0.049	0.742	0.033
4	$V_b - V_a$, MPD/RMS·$(1 - V_b/V_a)$	12.0	0.723	0.055	0.709	0.038
5	$V_b - V_a$, MPD·$(V_b - V_a)$	7.7	0.780	0.046	0.763	0.031
6	$V_b - V_a$, MPD·$(1 - V_b/V_a)$	7.4	0.768	0.047	0.749	0.032
7	1-Vb/Va, MPD·$(1 - V_b/V_a)$	7.8	0.776	0.046	0.765	0.031
8	MPD/RMS·$(V_b - V_a)$, 1-Vb/Va	18.0	0.747	0.049	0.741	0.033
9	MPD·$(V_b - V_a)$, MPD/RMS·$(V_b - V_a)$	5.5	0.788	0.045	0.786	0.030
10	MPD·$(1 - V_b/V_a)$, MPD/RMS·$(1 - V_b/V_a)$	5.3	0.782	0.046	0.766	0.030
11	$V_b - V_a$	-	0.720	0.055	0.707	0.037
12	ln(MPD)·$(V_b - V_a)$, MPD/RMS·$(V_b - V_a)$	1.1	0.792	0.045	0.782	0.030
13	ln(MPD)·$(1 - V_b/V_a)$, MPD/RMS·$(1 - V_b/V_a)$	1.1	0.777	0.046	0.767	0.031
14	ln(MPD)·$(V_b - V_a)$, Vb-Va	1.1	0.766	0.047	0.747	0.032
15	$V_b - V_a$, ln(MPD)·$(1 - V_b/V_a)$	1.1	0.766	0.047	0.748	0.032
16	$1 - V_b/V_a$, MPDMPD·$(V_b - V_a)$	6.7	0.761	0.048	0.751	0.032

For all performed regressions, the exponential models give higher values of R^2 than the linear regressions. Therefore, in the further analysis, only the exponential models are considered. Furthermore, regressions with the variables multiplied by $V_b - V_a$ fit better than regressions for the same variables multiplied by $1 - \frac{V_b}{V_a}$ (for example, model 5 fits better than model 6).

One can see that not all models fulfil the requirement of having a VIF lower than 10. Only considering models with predictive variables multiplied by $V_b - V_a$, the exponential models with a VIF lower than 10 that have the lowest values for the RMSE are:

- Model 5, including variables $V_b - V_a$ and MPD·$(V_b - V_a)$
- Model 9, including variables MPD·$(V_b - V_a)$ and $\frac{\text{MPD}}{\text{RMS}} \cdot (V_b - V_a)$
- Model 12, including variables $ln(\text{MPD}) \cdot (V_b - V_a)$ and $\frac{\text{MPD}}{\text{RMS}} \cdot (V_b - V_a)$

Models with these variables fit best to the dataset. From a statistical point of view, the last model of these three fits best. However, the differences in the standard errors are very small (0.046 versus two times 0.045), and therefore simplicity of the model is preferred. For this reason, the comprehensive output for performing an outlier analysis is generated for the regression with $V_b - V_a$ and MPD·$V_b - V_a$ as predictive variables.

Outlier analysis

A more comprehensive output was generated from the regression performed with $V_b - V_a$ and MPD·$V_b - V_a$ as predictive variables. With this output, it is possible to detect outliers and highly influential points. Observations were considered to be outliers when they had a residual value more than three times the average residual. Furthermore, plots of the Cook's distance and the Centrered Leverage Value were generated, in which high values indicate highly influential points.

Only four observations are detected as outliers, of which three belong to the road HOV1 (Concrete). The plots of the Cook's Distance and Centered Leverage Values are shown in Figures 5.1 and 5.2.

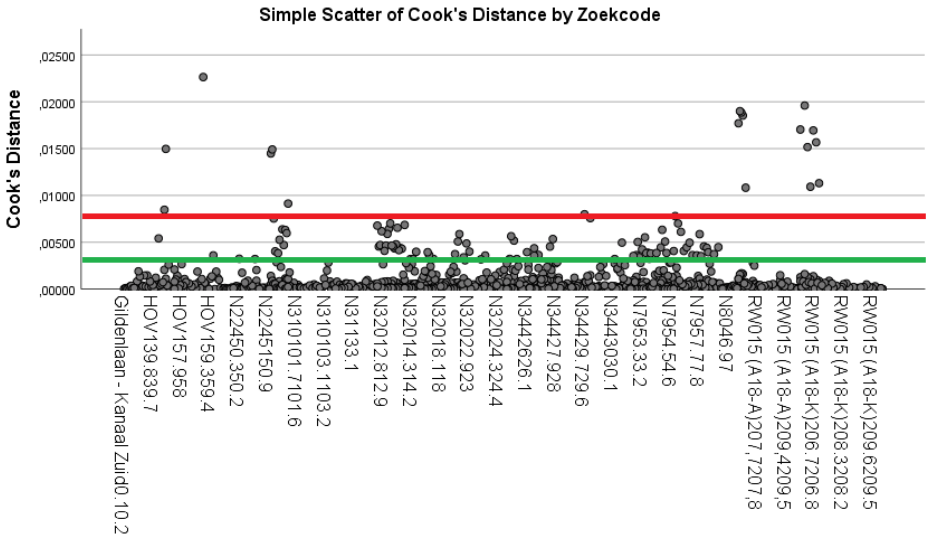

Figure 5.1: Plot showing the Cook's Distance for all observations. On the x-axis the unique codes per 100 metre section are given (not all names are displayed on the x-axis). Dots close to each other on the x-axis therefore often correspond to the same road. The green line indicates 4/n, the red line indicates 10/n.

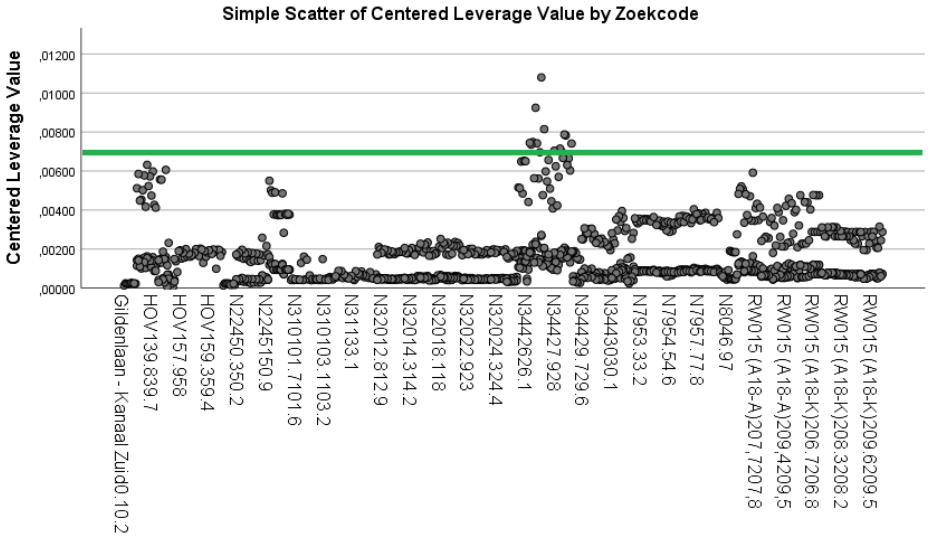

Figure 5.2: Plot showing the Centered Leverage Value for all observations. On the x-axis the unique codes per 100 metre section are given (not all names are displayed on the x-axis). Dots close to each other on the x-axis therefore often correspond to the same road. The green line indicates 5*p/n.

Karadimitriou and Marshall (2018) propose comparing the Cook's Distance to 4/n where n is the number of observations. This line is indicated by the green line in Figure 5.1. Many observations would then be indicated as having a (too) high Cook's Distance. Because in literature no strict cut-off values are found, but moreover suggestions, the cut-off limit was increased to 10/n (coinciding with the red line). With this limit, 22 observations were marked with a high Cook's distance of which one was already detected as an outlier. For the Centered Leverage Value, Karadimitriou and Marshall (2018) propose comparing these values to $\frac{5 \cdot p}{n}$, where p is the number of predictive variables and n is the number of observations. This gives the green line in Figure 5.2, and with this limit only 5 observations were marked as having a high Centered Leverage Value. In total, 29 observations were marked as outliers or highly influential points.

First of all, a new stepwise regression was performed without observations marked as outliers or highly

influential points, with all available predictive variables. The same variables were included as in the stepwise regression, and an extra regression was performed in which MPD/RMS·$(V_b - V_a)$ was in cluded as a dummy variable. The outliers did not change the included predictive variables much. Furthermore, a new regression was performed with only $V_b - V_a$ and MPD·$(V_b - V_a)$ as predictive parameters, to see whether the model would improve compared to the model with these variables on all data. The obtained models are as follows:

$$ln\left(\frac{\mu_a}{\mu_b}\right) = 0.00560 \cdot (V_b - V_a) - 0.00263 \cdot \text{MPD} \cdot (V_b - V_a) \tag{5.5a}$$

$$ln\left(\frac{\mu_a}{\mu_b}\right) = 0.00586 \cdot (V_b - V_a) - 0.00285 \cdot \text{MPD} \cdot (V_b - V_a) \tag{5.5b}$$

Equation (5.5a) is the model based on all data and Equation (5.5b) is the model based on the data without outliers and highly influential points. The corresponding values for the RMSE given in SPSS are respectively 0.046 and 0.043, which is a very small improvement. It is not known *why* these observations are marked as deviating observations. Spikes (physical errors during the measurements, giving very deviating values for μ) are filtered out because many measurements are taken on one 100 metre section and these are averaged. Furthermore, at this stage, it is not possible to exclude observations based on a choice different than for a statistical motivation. Because the regression coefficients differed very little and the RMSE did not increase much, it was decided to not make a distinction in the subsequent regressions between 'normal' observations, outliers or highly influential points.

5.2.3. Conclusions of multiple linear analysis on speed combinations

Variables giving best outcomes

In the final model $V_b - V_a$ and MPD·$(V_b - V_a)$ were used as predictive parameters. Although these variables did not give the highest RMSE, the differences compared to other models were very small. Therefore, preference was given to use the most 'simple' parameters, ie. the parameters that are most logical to use and that are not transformed.

Final model

The final model obtained with the multiple linear regression is:

$$\mu_a = \mu_b \cdot e^{(0.00560 - 0.00263 \cdot \text{MPD}) \cdot (V_b - V_a)} \tag{5.6}$$

This model is obtained with a multiple linear regression performed on all data, including observations selected as outliers or highly influential points. When applying this model in the datasheet with speed combinations, an RMSE of 0.032 is obtained.

Outliers

For the regression with predictive variables $V_b - V_a$ and MPD·$(V_b - V_a)$ the outliers were selected and a new regression was performed based on the dataset without outliers. The RMSE of the regression did not improve much and the regression coefficients did not change and therefore, in the further regression analysis, outliers are not treated.

Limitations of method

When performing the regression analysis with the multiple linear regression, only two datapoints per observation are taken into account. However, three of the measurement combinations belong to one and the same road section. By splitting the data into observations with two measurements, this inter-dependency information is being lost. SPSS considers each pair of measurements separately and does not know that three of these observations belong to the same 100 metre section.

Furthermore, one of the assumptions of a linear regression is that all observations must be independent (see Section B.2.1). This can be examined with help of the Durbin Watson statistic, which is given in the output of a linear regression. For the final model, this statistic has a value of 0.5, which does indicate autocorrelations and thus implies that the observations are not independent. Although time, which is often an indication of dependency of the data, does not play a role in this model, the

observations are not independent. For one 100 metre section, three datapoints exist. These three data points are dependent on each other, because the same measurements appear in multiple observations. Therefore, three datapoints for one 100 metre section are dependent. Together with the limitation of the lost information as explained in the previous paragraph, this makes the multiple linear regression inappropriate for the objective of this research.

5.3. Method 2: linear regression with zero speed intercept

The second regression method is based on the idea of a zero speed intercept, as is also used by Leu and Henry (1978). Where the multiple linear regression (method 1) did loose the information that multiple observations were measured on one 100 metre section, this method tries to avoid this loss by estimating a zero speed intercept μ_0 which is equal for observations on similar 100 metre sections. The zero speed intercept is considered to be related to pavement microstructure. Physically it is the friction between tyre and pavement interface at zero sliding speed.

5.3.1. Explanation of method

This method assumes an intercept value at a measuring speed of 0 km/h, of which two examples are shown in Figure 5.3. Every 100 metre section has a different intercept value. The extrapolation is a mathematical step and ignores the stick-slip effect which occurs when a fully or partially locked tyre starts moving.

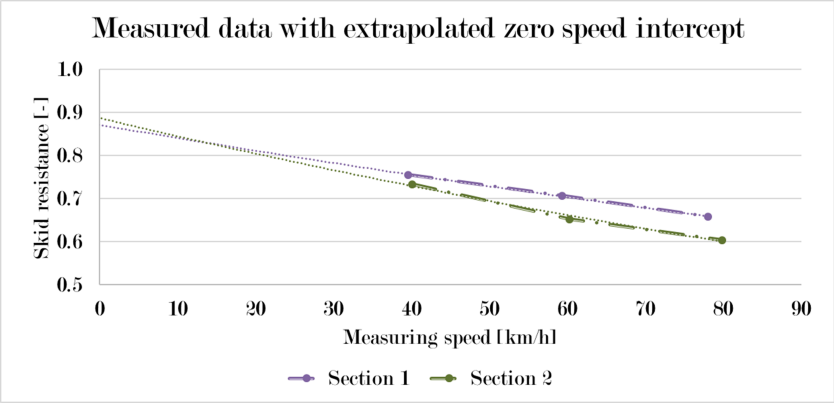

Figure 5.3: Two measured 100 metre sections with an extrapolation to their 'zero speed' intercept

A speed intercept which fits the data must be estimated. After determining the μ_0, a regression analysis can be performed to determine the skid resistance dependent on the predictive variables and the estimated μ_0.

In brief, this method contains of two steps:

1. determining μ_0 and adding this value to the dataset, and
2. performing a multiple linear regression on the dataset including μ_0.

The dataset for the final regression as in step 2 contains one measurement per observation with a fitted μ_0. The structure of the dataset is as follows:

Table 5.3: Structure of datasheet for regression method 2 - zero speed intercept

Unique code for 100 metre section	V_a	μ_a	μ_0	**MPD**	**RMS**	**... other information**
1	40	μ_{40}	μ_0			
1	60	μ_{60}	μ_0			
1	80	μ_{80}	μ_0			

5.3.2. Step 1: determination of zero speed intercept

The μ_0 is determined according to two different methods:

1. Obtaining μ_0 with help of a functional approach developed by Chu and Fwa (2017);
2. Determine μ_0 with help of a regression in SPSS.

Determining the zero speed intercept according to a functional approach

Chu and Fwa (2017) developed a functional approach for determining skid resistance threshold states of porous pavements. In this approach, a finite element simulation model for the computation of skid resistance is included. The final output of this simulation analysis is the skid resistance μ at speed v defined by (Chu and Fwa, 2017):

$$\mu_v = \frac{F_x}{F_w} = \left[\frac{F_t + F_v^d}{F_w}\right] = \left[\frac{\mu_0 \cdot (F_w - F_v^u) + F_v^d}{F_w}\right] \tag{5.7}$$

Where:	μ_v	=	Skid resistance at speed V	[-]
	F_x	=	Total resisting forces acting on the wheel	[N]
	F_t	=	Total traction force	[N]
	F_w	=	Vertical wheel load (1960 N for the SKM)	[N]
	F_v^u	=	Fluid uplift force, dependent on vehicle speed	[N]
	F_v^d	=	Fluid drag force, dependent on vehicle speed	[N]
	μ_0	=	Zero speed intercept	[-]

The last formula of Equation (5.7) was used to estimate the values for μ_0. In this formula, F_v^u and F_v^d depend on the vehicle speed. The higher the vehicle speed, the larger F_v^u and F_v^d. Therefore, the unknown parameters are:

- μ_0
- F_{30}^u, F_{40}^u, F_{60}^u, F_{80}^u
- F_{30}^d, F_{40}^d, F_{60}^d, F_{80}^d

For reason of simplification, all measuring speeds were assumed to be performed at exactly 30, 40, 60 and 80 km/h. In reality, the measuring speeds can be for example 42 or 58 km/h as well.

The exact solution of these unknowns cannot be determined. However, with the solver function in excel, estimating the variables including μ_0 is possible. The approach is as follows:

- All unknown variables above are added to the dataset, and are initially set to random, but plausible, values. μ_0 is set to a number between 0 and 1, the drag forces are very small (for example, 0.1 kN) and the uplift forces can be large (for example, 1000 kN).
- For each observation, the μ_{pred} (predicted skid resistance according to Equation (5.7)) is calculated.
- The absolute difference between the predicted and the measured skid resistance is calculated and the sum of the errors is determined.
- The excel solver can determine an optimal solution taken into account predetermined constraints. The solver is focused on minimising the sum of the errors, such that Equation (5.7) predicts the skid resistance most accurate. The given constraints are:
  - $\mu_0 > \mu_{max}$, in which μ_{max} is the highest measured skid resistance for the observations for which the μ_0 is calculated
  - $F_{30}^u < F_{40}^u$
  - $F_{40}^u < F_{60}^u$
  - $F_{60}^u < F_{80}^u$
  - $F_{30}^d < F_{40}^d$

  - $F_{40}^d < F_{60}^d$
  - $F_{60}^d < F_{80}^d$
- The solver determines all unknowns such that the error of the predictions is minimal given the constraints. This gives an estimation of μ_0. This μ_0 is added to the dataset, after which the second step of this regression method can be performed.

The value for μ_0 is different for each 100 metre section, however, it is not possible to use the solver for determining the μ_0 for each separate 100 metre section. Multiple measurements are needed in order to make an adequate estimation. Therefore, several zero speed intercepts were estimated:

- μ_0 equal for the whole dataset:
  - μ_0 based on 100% of the data: $\mu_{0,total,100,solver}$
  - μ_0 based on 25% of the data: $\mu_{0,total,25,solver}$
- μ_0 different per road:
  - μ_0 based on 100% of the data, per road: $\mu_{0,road,100,solver}$
  - μ_0 based on 25% of the data, per road: $\mu_{0,road,25,solver}$

Thus, in total, 4 values for μ_0 ($\mu_{0,total,100,solver}$, $\mu_{0,total,25,solver}$, $\mu_{0,road,100,solver}$, $\mu_{0,road,25,solver}$) were added to the dataset. These values were used in the multiple linear regression in step 2.

Determining zero speed intercept with regressions in SPSS

Besides the functional approach, μ_0 was estimated with help of SPSS. A regression was performed on:

$$ln(\mu_a) = C_0 + C_1 \cdot V_a + C_2 \cdot \text{MPD} \cdot V_a \tag{5.8}$$

After which $\mu_0 = e^{C_0}$.

With this approach, per 100 metre section, three different values for μ_0 were estimated:

- One μ_0 for the whole dataset: $\mu_{0,total,SPSS}$. The regression was performed as in Equation (5.8).
- One μ_0 for every road[1]: $\mu_{0,road,SPSS}$. Separate regressions in SPSS were performed per road on:

  $$ln(\mu_a) = C_{0,m} + C_{1,m} \cdot V_a + C_{2,m} \cdot \text{MPD} \cdot V_a \tag{5.9}$$

  Then: $\mu_{0,m} = e^{C_{0,m}}$, with m the different roads.
- One μ_0 for every road separated into subsections: $\mu_{0,subsection,SPSS}$. The roads were visually divided into more subsections of roughly equal levels of skid resistance (see for an example Figure 5.4). Then, μ_0 was determined per subsection by performing separate regressions in SPSS per subsection on:

  $$ln(\mu_a) = C_{0,m,n} + C_{1,m,n} \cdot V_a + C_{2,m,n} \cdot \text{MPD} \cdot V_a \tag{5.10}$$

  Then: $\mu_{0,m,n} = e^{C_0}$, with m the different roads and n the different subsections.

[1] Every road consists of one pavement type except one road, for this road a few sections had another pavement layer. In the determination of μ_0, no distinction was made between these two pavement types.

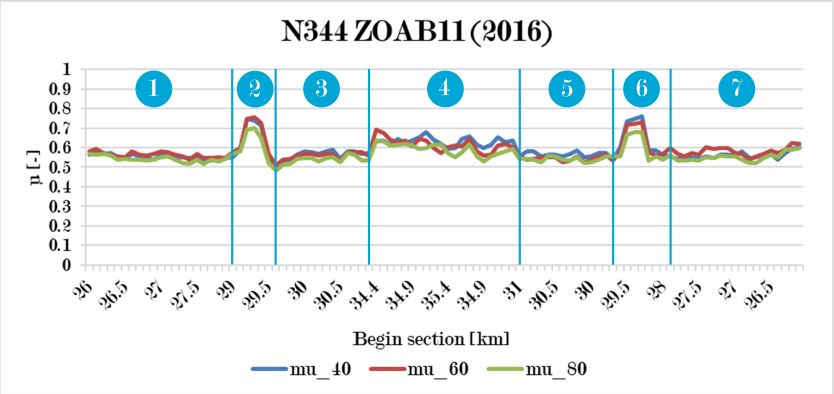

Figure 5.4: Example of a road visually divided into subsections. On the x-axis the 100 metre indication of the beginning of the section is shown, on the y-axis the measured skid resistance is given. For this road, 7 different values of μ_0 are estimated.

In total, 3 values for μ_0 ($\mu_{0,total,SPSS}$, $\mu_{0,road,SPSS}$, $\mu_{0,subsection,SPSS}$) were added to the dataset. These values were used in the multiple linear regression in step 2.

5.3.3. Step 2: multiple linear regression on dataset including μ_0

In the second step of this method, a multiple regression analysis was performed on:

$$ln\left(\frac{\mu_a}{\mu_0}\right) = D_1 \cdot V_a + D_2 \cdot \text{MPD} \cdot V_a \tag{5.11}$$

This can be rewritten into Equation (5.1b) by the following steps:

$$\mu_a = \mu_0 \cdot e^{D_1 \cdot V_a + D_2 \cdot \text{MPD} \cdot V_a} \tag{5.12a}$$

$$\mu_b = \mu_0 \cdot e^{D_1 \cdot V_b + D_2 \cdot \text{MPD} \cdot V_b} \tag{5.12b}$$

$$\frac{\mu_a}{\mu_b} = \frac{\mu_0 \cdot e^{D_1 \cdot V_a + D_2 \cdot \text{MPD} \cdot V_a}}{\mu_0 \cdot e^{D_1 \cdot V_b + D_2 \cdot \text{MPD} \cdot V_b}} \tag{5.12c}$$

$$\mu_a = \mu_b \cdot e^{D_1 \cdot (V_a - V_b) + D_2 \cdot \text{MPD} \cdot (V_a - V_b)} \tag{5.12d}$$

$$\mu_a = \mu_b \cdot e^{C_1 \cdot (V_b - V_a) + C_2 \cdot \text{MPD} \cdot (V_b - V_a)} \tag{5.12e}$$

$$\text{In which: } C_1 = -D_1, C_2 = -D_2$$

In the first step of this method, in total, 7 different speed intercepts were determined per 100 metre section. For these zero speed intercepts various multiple linear regressions were performed according to Equation (5.11):

- Functional approach:
  - $\mu_{0,total,100,solver}$
    - ◇ 1 regression based on 100% of the data
  - $\mu_{0,total,25,solver}$
    - ◇ 1 regression based on remaining 75% of the data
    - ◇ 1 regression based on 100% of the data
  - $\mu_{0,road,100,solver}$
    - ◇ 1 regression based on 100% of the data
  - $\mu_{0,road,25,solver}$

- ◇ 1 regression based on remaining 75% of the data
- ◇ 1 regression based on 100% of the data

- SPSS:

  Per speed intercept, one regression was performed on 100% of the data:

  - $\mu_{0,total,SPSS}$
  - $\mu_{0,subsection,SPSS}$
  - $\mu_{0,subsection,SPSS}$

5.3.4. Analysis of data

First of all, for a few combinations of variables the μ_0 was determined with help of SPSS for the total dataset. This gives insight in which variables had smaller standard errors on the dataset and predict speed intercepts that were feasible. With this method it was not possible to use predictive variables such that, when rewriting the obtained model as in Equation (5.12), a model with $1 - \frac{V_b}{V_a}$ would be obtained.

Table 5.4: Zero speed intercepts obtained for the total dataset by a regression in SPSS. The RMSE is given in the output of SPSS and is in the same unit of $ln(\mu_a)$.

Variables	μ_0	$\mathbf{R^2}$	**RMSE**
V, MPD·V	0.787	0.291	0.097
ln(V), MPD·V	0.620	0.299	0.097
MPD/RMS·V, MPD·V	0.742	0.234	0.101
MPD/RMS·V, ln(MPD)	0.713	0.110	0.109

Table 5.4 shows that the regression with ln(V) and MPD·V has the best R^2 and smallest standard error, but this regression gives a μ_0 which is much lower than the μ_0 for all other regressions. Therefore, the variables V and MPD·V are preferred. These variables give the second highest R^2 and have the same RMSE as the regression with variables ln(V) and MPD·V, and give a more feasible μ_0.

In total, 9 models are generated according to the zero speed intercept method. In all of these models the variables V_a and MPD·V_a are used as predictive variables. The regression coefficients and RMSE (according to Equation (5.12e), calculated in the datasheet with speed combinations) are shown in Table 5.5.

Table 5.5: Overview of regression constants and standard errors of the regressions performed with a zero speed intercept, with C_1 and C_2 as in Equation (5.12e). The RMSE is calculated in the datasheet with speed combinations and has the same unit as μ.

Regression	**Used μ_0**	$\mathbf{C_1}$	$\mathbf{C_2}$	**RMSE**
1	$\mu_{0,total,SPSS}$	0.00235	0.00120	0.040
2	$\mu_{0,road,SPSS}$	0.00573	-0.00338	0.034
3	$\mu_{0,subsection,SPSS}$	0.00580	-0.00337	0.033
4	$\mu_{0,total,100,solver}$	0.01143	0.00051	0.185
5	$\mu_{0,total,25,solver}$ (100% data used)	0.00740	0.00050	0.098
6	$\mu_{0,total,25,solver}$ (75% data used)	0.00804	0.00005	0.102
7	$\mu_{0,road,100,solver}$	0.00750	0.00050	0.100
8	$\mu_{0,road,25,solver}$(100% data used)	0.00757	0.00050	0.102
9	$\mu_{0,road,25,solver}$(75% data used)	0.00821	0.00005	0.105

The regression with the smallest RMSE is regression 3, in which the zero speed intercept is determined in SPSS for the roads divided in subsections.

The regressions performed with the zero speed intercept obtained with the functional approach give very high RMSE values. The solver function in Excel was very sensitive to the initial values given for

the unknown variables, and therefore the estimations of the speed intercepts are assumed not to be accurate. Furthermore, the signs of the coefficients for all regressions performed with the zero speed intercept obtained with the functional approach do not meet the expectations: both C_1 and C_2 are positive, indicating that a larger MPD increases the speed dependency whereas it is expected that a larger MPD decreases the speed dependency.

5.3.5. Conclusions of linear regression with zero speed intercept

Final model

The best obtained regression according to the method using a zero speed intercept is:

$$\mu_a = \mu_b \cdot e^{(0.005804 - 0.003373 \cdot \text{MPD}) \cdot (V_b - V_a)} \tag{5.13}$$

When applying this model in the datasheet with speed combinations, an RMSE of 0.033 is obtained.

Limitations of method

By estimating the μ_0, which is equal for every observation on the same 100 metre section, this method tried to avoid the loss of information that all observations of one 100 metre section are dependent on each other. However, this method has some drawbacks:

- First of all, the final regression is based on an estimated value of μ_0. The question is whether it is better to loose some valuable information, or to add some information which is estimated and therefore not 100% reliable.
- The zero speed intercepts are not estimated per 100 metre section, but per road or per subsection of a road. This makes the method less accurate, independent of the used method for estimating μ_0.
- Estimating the zero speed intercept in SPSS per subsection of a road gave the best final model. However, this speed intercept is influenced by the included predictive variables. Changing the model parameters would change the μ_0 and thus changing the final model.

Concluded can be that this method is difficult to implement, because it is challenging to make a good estimation of μ_0. In the above described procedure the zero speed intercept is too vulnerable to choices made in the regression process. If a functional approach would exist which predicts better values for μ_0, the models obtained by this regression could probably be improved.

5.4. Method 3: multilevel modelling

In this research, every 100 metre section has in most cases measurements at three different measuring speeds, and these three measurements are not independent of each other. For example, if the skid resistance at 40 km/h is 0.6, it is unlikely that the skid resistance at the same section at 60 km/h will be 0.2. Therefore, the observations are not independent and hierarchy of the data is present, and a multilevel analysis is performed. Multilevel models can implement a hierarchical structure and deal with dependent observations. An explanation of multilevel modelling is given in Section B.3.

5.4.1. Explanation of method

In this research, only random intercepts play a role and slopes are assumed to be equal. Figure 5.5 shows for every road the average measured skid resistances per measuring speed. This figure clearly shows that every line has a different level of skid resistance, and therefore a different intercept. Not all slopes are equal, since an influence of the texture is assumed, which affects the slope of the lines. If the influence of the texture is equal for all sections, this implies that no random slopes are present.

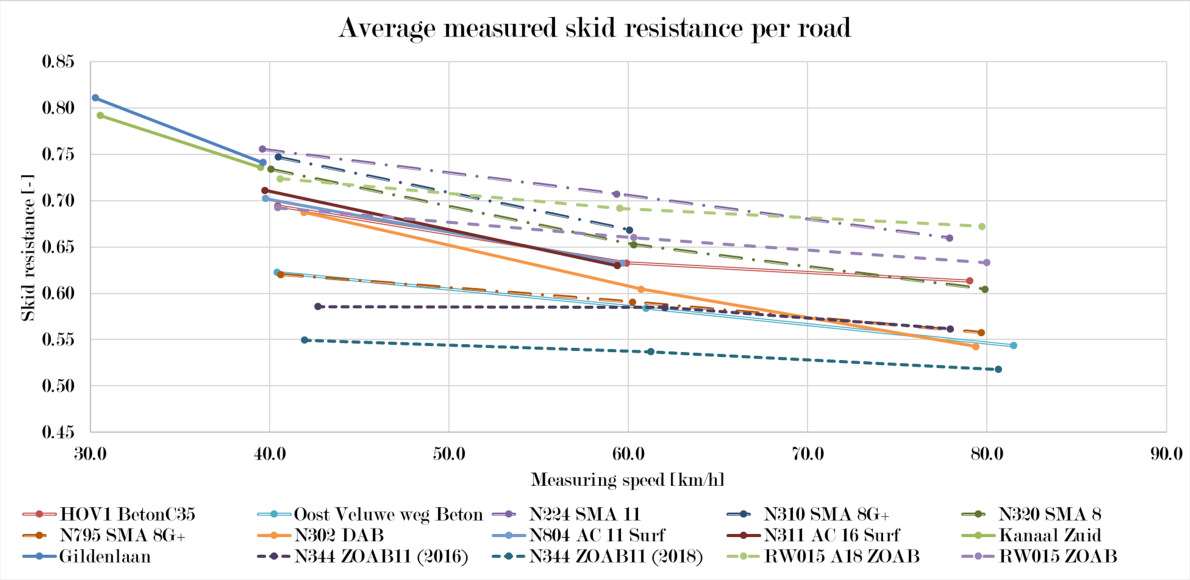

Figure 5.5: Overview of average measured skid resistances per road

The following sections explain the different hierarchical structures that are assumed, and clarify how to determine the correct number of levels.

Hierarchical structures for single, two, and three-level models

Figures 5.6 to 5.8 show the hierarchical structures for respectively a single-level model, a two-level model and a three-level model. The structures of the schemes can be explained as follows:

- In the single-level model, no hierarchy is assumed and the regression is a normal linear regression in which there are no random variables. Each measurement is considered separately from all other measurements.
- In the two-level model, the first level contains the individual measurements performed at certain measuring speeds and the second level contains the 100 metre sections to which the individual measurements belong.
- In the third-level model, it is assumed that the values of the measurements not only depend on the 100 metre sections, but also on the roads where the 100 metre section belongs to.

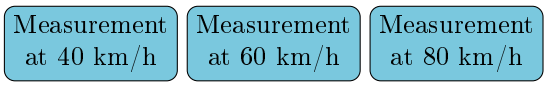

Figure 5.6: Hierarchical structure for a single-level model (which implies no hierarchy)

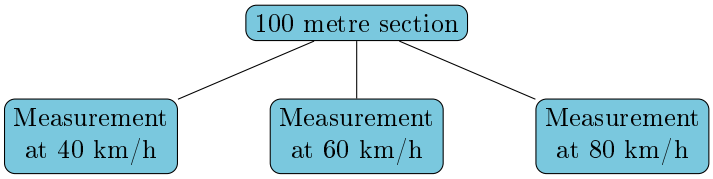

Figure 5.7: Hierarchical structure for a two-level model

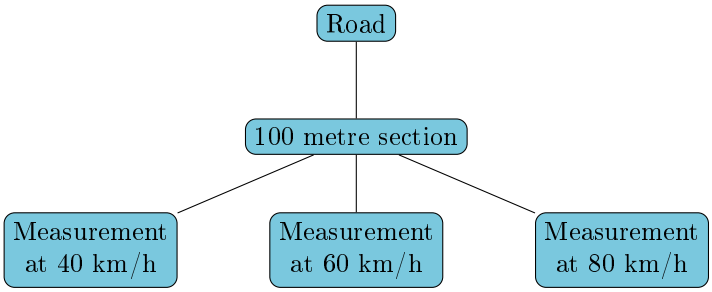

Figure 5.8: Hierarchical structure for a three-level model

The single-level model is formulated as follows:

$$ln(\mu_i) = C_0 + C_1 \cdot V_i + C_2 \cdot (\text{MPD}_i \cdot V_i) + \epsilon_i \tag{5.14}$$

Where:
- $ln(\mu_i)$ = Skid resistance of observation number i
- C_0 = Intercept of the overall model fitted to the data
- C_1 = Fixed slope for variable V_i
- V_i = Measuring speed V for observation i
- C_2 = Fixed slope for variable $V \cdot \text{MPD}_i \cdot V_i$
- MPD_i = MPD for observation i
- ϵ_i = Residual error term for observation i

Compared to the single-level, a random intercept is added to the two-level model for the 100 metre section on which a measurement is performed. Furthermore, an observation is not only indicated by the observation number i, but also by the 100 metre section j to which the observation belongs. The two-level is formulated as follows:

$$ln(\mu_{ij}) = (C_0 + U_j) + C_1 \cdot V_{ij} + C_2 \cdot (\text{MPD}_j \cdot V_{ij}) + \epsilon_{ij} \tag{5.15}$$

Where:
- $ln(\mu_{ij})$ = Skid resistance of observation number i, belonging to 100 metre section j
- C_0 = Intercept of the overall model fitted to the data
- U_j = Random intercept for 100 metre section j
- C_1 = Fixed slope for variable V_{ij}
- V_{ij} = Measuring speed V for observation i belonging to 100 metre section j
- C_2 = Fixed slope for variable $V \cdot \text{MPD}_j \cdot V_{ij}$
- MPD_j = MPD for 100 metre section j
- ϵ_{ij} = Residual error term for observation i within group j

The three-level model is an elaboration of the two-level model. Not only a random intercept for the 100 metre section appears, but also for the road where the measurement took place. An observation is now also indicated by the road k on which the measurement is performed. The model is formulated as follows:

$$ln(\mu_{ijk}) = (C_0 + T_k + U_{jk}) + C_1 \cdot V_{ijk} + C_2 \cdot (\text{MPD}_j \cdot V_{ijk}) + \epsilon_{ijk} \tag{5.16}$$

Where:
- $ln(\mu_{ijk})$ = Skid resistance of observation number i for 100 metre section j belonging to road k
- C_0 = Intercept of the overall model fitted to the data
- T_k = Random intercept for road k
- U_{jk} = Random intercept for 100 metre section j within road k
- C_1 = Fixed slope for variable V_{ijk}
- V_{ijk} = Measuring speed V for observation i belonging to 100 metre section j of road k
- C_2 = Fixed slope for variable $\text{MPD}_j \cdot V_{ijk}$
- MPD_j = MPD for 100 metre section j
- ϵ_{ijk} = Residual error term for observation i within 100 metre section j belonging to road k

In the equations above, the intercept values can be compared to the zero speed intercept from Section 5.3. The intercepts will be eliminated in the transformation from the regression model (Equations (5.14) to (5.16)) to the model in which the skid resistance can be converted between different measuring speeds (Equation (5.1b)), according to the same steps as in Equation (5.12). Therefore, the random intercepts are not generated as output. This process takes much time because there are many data points.

The hierarchical structure must be possible to be extracted from the data. Therefore, the datasheet for the multilevel model is as in Table 5.6.

Table 5.6: Structure of datasheet for regression method 3 - multilevel modelling

Unique code for 100 metre section	V_a	V_b	V_c	μ_a	μ_b	μ_c	**MPD**	**RMS**	**Road**	**... other information**
1	40	60	80	μ_{40}	μ_{60}	μ_{80}			X	
2	40	60	80	μ_{40}	μ_{60}	μ_{80}			X	
3	40	60	80	μ_{40}	μ_{60}	μ_{80}			Y	

The hierarchical structure can be extracted because each road has a unique indication (name) and every 100 metre section also has an unique code. Within one 100 metre section there are (a maximum of) three measurements, which are given a number (1/2/3) in SPSS. Therefore, the single-level, two-level and three-level models can be generated.

Determination of number of levels

For a multiple regression analysis the t-test is used to verify if a model significantly improved the R^2 compared to another model on the same dataset. In a multilevel analysis, no R^2 is given. For these regressions, the chi-square likelihood ratio test, which analyses the improvement of the -2 Log Likelihood (-2LL, see Section B.3.3), is used to verify whether a model makes a significant improvement compared to another model on the same dataset. For determining the optimal number of levels, it is analysed with help of the chi-square likelihood ratio test whether a two-level model makes a significant difference compared to a single-level model. Thereafter, if a two-level model makes a significant difference to a single-level model, it can be analysed whether a three-level model significantly improves the two-level model.

Table 5.7 shows the performed regressions in order to analyse the optimal hierarchy structure. During this analysis the variables V and MPD·V are used, because from regression method 1 (multiple linear regression) these appeared to be the best variables. Since in the first regression method the variables resulted in small differences to the standard errors of the obtained models only, the choice of predictive variables would presumably not make a significant difference in the determination of the optimal hierarchy structure.

Table 5.7: Performed regressions to analyse optimal hierarchy structure. The column 'Applied chi-square likelihood ratio test' gives the two regressions of which the -2LL is compared to verify whether the model is significantly improved by adding an additional level or predictive variable

Regression	**No. of levels**	**Predictive variables**	**Tested chi-square likelihood ratio test**
1	1	V	-
2	1	V, MPD·V	(-2LL(1))-(-2LL(2))
3	2	V	(-2LL(1))-(-2LL(3))
4	2	V, MPD·V	(-2LL(2))-(-2LL(4))
5	3	V	(-2LL(3))-(-2LL(5))
6	3	V, MPD·V	(-2LL(4))-(-2LL(6))

The hypothesis is that (for Equations (5.14) to (5.16)) C_1 will be a negative value, as a decline in skid resistance is assumed with an increasing speed, and that C_2 will be positive, because overall, a larger MPD is assumed to decrease the speed dependency of the skid resistance.

Determination of predictive variables

After the best hierarchical structure was determined, regressions with different predictive variables using this hierarchical structure were performed to analyse whether variations in the predictive variables could significantly improve the model.

In the output of a mixed model, no number such as a VIF is given to detect multicollinearity. Therefore, when combining variables, the VIFs of Table 5.2 were taken into account for choosing combinations of variables. The chi-square likelihood ratio test is only valid for comparing two models of which one model is an elaboration of the other model. Two models which are an elaboration of the same 'basis' model, can be compared to each other by comparing the chi-square likelihood ratio test with the same basis model. Therefore, some regressions with only one predictive variable were performed because this allows to compare two other models with each other. For example, for comparing a model with V and MPD·V to a model with $ln(V)$ and MPD·V as predictive variables, the chi-square likelihood ratio test must be performed with a model only containing MPD·V. The extended model with the best chi-square likelihood ratio test is then the model that fits better on the dataset.

Figure 5.9 shows the structure of the performed regressions with different variables. As one can see, by structuring the regressions in this way, it becomes clear that all models can be compared to each other, because indirectly, they all have a connection to a model with the same 'basis' model.

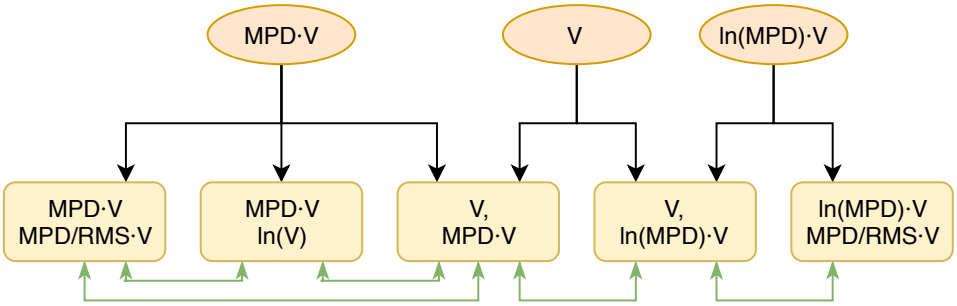

Figure 5.9: Structure of performed regressions to obtain comparable models. The orange ellipses are the basis models, the yellow rectangles are the extended models with an extra predictive variable. The green arrows indicate models of which the chi-square likelihood ratio test can be compared because of having the same basis model.

Table 5.8 shows the regressions performed to compare models with different predictive variables and the corresponding chi-square likelihood ratio test(s) which should be analysed. For some regressions, two χ^2_{Change} were tested, because the model could be an extension of two 'basic' models (ie. with one predictive variable less).

Table 5.8: Performed regressions to analyse the best combination of predictive variables. For the regression with V as predictive parameter, model 1/3/5 will be used, depending of the optimal hierarchy structure determined according to Table 5.7. The same holds for regressions 2/4/6.

Regression	**Predictive variables**	**Tested chi-square likelihood ratio test(s)**	
1/3/5	V	-	
2/4/6	V, MPD·V	(-2LL(5))-(-2LL(6))	(-2LL(8))-(-2LL(6))
7	V, ln(MPD)·V	(-2LL(5))-(-2LL(7))	(-2LL(11))-(-2LL(7))
8	MPD·V	-	
9	ln(V), MPD·V	(-2LL(8))-(-2LL(9))	
10	MPD·V, MPD/RMS·V	(-2LL(8))-(-2LL(10))	
11	ln(MPD)·V	-	
12	ln(MPD)·V, MPD/RMS·V	(-2LL(11))-(-2LL(12))	

5.4.2. Analysis of data

This section analyses the output of the regressions as described in Section 5.4.1. First, the optimal hierarchy structure for this dataset is determined after which regressions with different combinations of variables are analysed.

Optimal hierarchy structure

The outcomes of the regressions performed as in Table 5.7, in order to determine the best fitted hierarchy structure, are shown in Table 5.9. The used syntax (programming codes) in SPSS can be found in Section D.1.

Table 5.9: Output of regressions performed to analyse optimal hierarchical structure. C_1 is the regression coefficient for V and C_2 is the regression coefficient for MPD·V.

Regression	No. of levels	No. of parameters	-2LL	C_1	C_2	Chi-square likelihood ratio test	df_{change}
1	1	3	-2552.524	-0.00370	-	-	-
2	1	4	-2644.638	-0.00235	-0.00121	(1-2): 92.11	1
3*	2	6	-4186.464	-0.00325	-	(1-3): 1633.94	3
4*	2	7	-4235.063	-0.00439	0.00118	(2-4): 1590.43	3
5*	3	7	-4437.224	-0.00323	-	(3-5): 250.76	1
6	3	8	-4547.981	-0.00511	0.00195	(4-6): 312.91	1

* For these regressions the following warning was given: *'The final Hessian matrix is not positive definite although all convergence criteria are satisfied. The MIXED procedure continues despite this warning. Validity of subsequent result cannot be ascertained.'*. The exact cause of this warning is not known. Suggestions to solve this warning include changing the covariance structures or increase the number of step-halvings (IBM, 2016), but these proposed solutions did not change the warning.

For a df_{change} of 1, a χ^2_{Change} larger than 3.84 is significant and for a df_{change} of 3, the χ^2_{Change} should exceed 7.81 in order to be significant. This is true for all performed chi-square likelihood ratio tests.

First of all, by comparing regressions 1 and 2, a significant improvement of the model by adding MPD·V as a parameter is shown by the χ^2_{Change}. Furthermore, by comparing regressions 1-3-5 and 2-4-6, the improvement of the models by adding one or two levels to the hierarchical structure is shown. Therefore, the three-level model is chosen as the most optimal hierarchical structure. An additional chi-square likelihood test can be performed to see whether the addition of MPD·V also improves the three-level model by comparing the -2LL of regression 5 to the -2LL of regression 6:

$$\chi^2_{Change,(5,6)} = (-4437.224) - (-4547.981) = 110.757$$

With one extra predictive variable in regression 6 (compared to regression 5), the χ^2_{Change} is significant and thus adding the predictive variable MPD·V significantly improves the three-level model.

Best predictive variables

Table 5.10 shows some of the output of the regressions performed to determine the best combination of predictive variables, as given in Table 5.8. Section D.2 gives the syntax used for this analysis.

Table 5.10: Output of regressions performed to analyse best predictive variables. All regressions are performed with a three-level hierarchy.

Regression	Predictive variables	No. of parameters	-2LL	Chi-square likelihood ratio test(s)				df_{change}
5*	V	7	-4437.224		-		-	-
6	V, MPD·V	8	-4547.981	(5-6):	110.757	(8-6):	591.419	1
7	V, ln(MPD)·V	8	-4550.067	(5-7):	112.843	(11-7):	1103.207	1
8*	MPD·V	7	-3956.562		-		-	-
9	ln(V), MPD·V	8	-4526.403	(8-9):	569.841			1
10	MPD·V, MPD/RMS·V	8	-4477.220	(8-10):	520.658			1
11*	ln(MPD)·V	7	-3446.860		-		-	-
12	ln(MPD)·V, MPD/RMS·V	8	-4527.370	(11-12):	1080.510			1

* For these regressions the warning about the Hessian Matrix as given in Table 5.9 was given.

For a df_{change} of 1, the χ^2_{Change} is significant if the ratio is larger than 3.84. This holds for all performed tests.

First of all, the regressions which are an elaboration of the model with only V as predictive parameter are analysed. These are regressions 6 and 7, containing the additional variable MPD·V (regression 6) is and ln(MPD)·V (regression 7). The values of χ^2_{Change} for these regressions compared to the regression with only V differ very little from each other. Therefore, the 'simplest' variable is preferred, which is MPD·V.

Secondly, the models with MPD·V as basic model are analysed. By performing a regression solely on MPD·V (regression 8) and calculating the χ^2_{Change} for regressions with adding V, $ln(V)$, or $\frac{MPD}{RMS} \cdot V$, (respectively regressions 6, 9 and 10), it becomes clear that regression 6 fits best on the dataset, because of having the largest χ^2_{Change}.

Lastly, regressions with ln(MPD) as basic model are analysed. The elaborated regressions contain as variables V, and $\frac{MPD}{RMS} \cdot V$ (respectively regressions 7, and 12). The χ^2_{Change} of the regression with ln(MPD) and V is highest, and therefore this model fits better on the dataset than the model obtained with regression 12. However, it was already determined that the model with V and MPD·V fitted better on the dataset than the model with V and ln(MPD)·V.

Concluded can be that regression 7 fits best on the dataset, but because of the very small difference compared to regression 6, and because the variables of regression 6 are preferred above the variables of regression 7, the variables of regression 6 are chosen as the best variables for obtaining a model for the used dataset.

This gives the following model:

$$\mu_a = \mu_b \cdot e^{(0.00511 - 0.00195 \cdot \text{MPD}) \cdot (V_b - V_a)} \tag{5.17}$$

5.4.3. Separate regressions for MPD values larger or smaller than one millimetre

Besides the analysis described in Sections 5.4.1 and 5.4.2, one more analysis was performed. This analysis contains separate regressions for datapoints with an MPD larger than 1 mm and datapoints with an MPD smaller than 1 mm. As the frequency histogram of MPD in Figure C.4 shows, there are very few observations having an MPD of approximately 1 mm. However, there are two peaks in the frequency histogram of which one is around an MPD of 0.8 mm and the other peak is around an MPD of 1.3 mm. Therefore, separate regressions for observations having an MPD< 1 mm and having an MPD> 1 mm were performed to see whether this improves the standard error of the total dataset.

Hierarchy structure and predictive variables

First of all, regressions with V and MPD·V were performed to identify whether also for these regressions a three-level analysis would be the most optimal hierarchy structure. Table 5.11 shows an overview of the performed regressions. These are similar to the regressions performed on the total dataset for verifying the optimal hierarchy structure, and therefore only the table with output is given.

Table 5.11: Output of regressions performed to analyse optimal hierarchical structure for separate regressions for observations with an MPD smaller or larger than 1 mm.

Regression	No. of levels	predictive variables	No. of parameters	Chi-square likelihood ratio test	MPD<1 mm		MPD>1 mm	
					-2LL	χ^2_{Change}	-2LL	χ^2_{Change}
1	1	V	3		-1714.541		-961.991	
2	1	V, MPD·V	4	(-2LL(1))-(-2LL(2))	-1715.015	0.474	-1142.534	180.543
3	2	V	6	(-2LL(1))-(-2LL(3))	-2631.963	917.422	-1863.199	901.208
4	2	V, MPD·V	7	(-2LL(2))-(-2LL(4))	-2641.714	926.699	-1863.232	720.698
5	3	V	7	(-2LL(3))-(-2LL(5))	-2741.959	109.996	-2130.388	267.189
6	3	V, MPD·V	8	(-2LL(4))-(-2LL(6))	-2770.884	129.170	-2139.521	276.289

There is one χ^2_{Change} which is not significant and this is for the chi-square likelihood test between regression 1 and 2 for an MPD< 1 mm. However, a two-level model improves the one-level model, and the three-level model improves the one-level model for regressions with the same parameters. By

performing a chi-square likelihood ratio test for regression 5 and 6, it is observed that for the three-level model adding MPD·V does improve the model, contrary to for the single-level model.

Table 5.12 shows several regressions to analyse which variables fits best on the dataset as predictive variables.

Table 5.12: Output of regressions performed to analyse best predictive variables for separate regressions for observations having an MPD smaller or larger than 1 mm. All regressions are performed with a three-level hierarchy.

Regression	**predictive variables**	**No. of parameters**	**Chi-square likelihood ratio test**	**MPD<1 mm**		**MPD>1 mm**	
				-2LL	χ^2_{Change}	**-2LL**	χ^2_{Change}
5	V	7		-2741.959		-2130.388	
6	V, MPD·V	8	(-2LL(5))-(-2LL(6))	-2770.884	28.925	-2139.521	9.133
			(-2LL(8))-(-2LL(6))		338.522		57.071
7	V, ln(MPD)	8	(-2LL(5))-(-2LL(7))	-2782.866	40.907	-2141.891	11.503
8	MPD·V	7		-2432.362		-2082.450	
9	$ln(V)$, MPD·V	8	(-2LL(8))-(-2LL(9))	-2793.944	361.582	-2109.061	26.611

For observations with an MPD< 1 mm, the regression with $ln(V)$ and MPD·V fits best on the dataset. For observations with MPD> 1 mm, the regression with V and ln(MPD) fits best on the dataset.

Standard error of the estimates

In total, two values of the total RMSE are calculated: one for regressions with V and MPD·V as predictive variables, and one for regressions with the best predictive variables for each dataset. The variables V and MPD·V fit best on the total dataset and with this regression the improvement of estimating the regression coefficients separately for MPD< 1 mm and MPD> 1 mm can be seen. This gives the following models:

- For MPD< 1 mm, the following equations are used to determine the RMSE:

$$\mu_a = \mu_b \cdot e^{(0.00562 - 0.00196 \cdot \text{MPD}) \cdot (V_b - V_a)} \tag{5.18a}$$

$$\mu_a = \mu_b \cdot e^{-0.280051 \cdot ln\left(\frac{V_a}{V_b}\right) - 0.00103754 \cdot \text{MPD} \cdot (V_b - V_a)} \tag{5.18b}$$

- For MPD> 1 mm, the following equations are used to determine the RMSE:

$$\mu_a = \mu_b \cdot e^{(0.00313 - 0.00094 \cdot \text{MPD}) \cdot (V_b - V_a)} \tag{5.19a}$$

$$\mu_a = \mu_b \cdot e^{(0.00227 - 0.00142 \cdot ln(\text{MPD})) \cdot (V_b - V_a)} \tag{5.19b}$$

Table 5.13 shows the RMSE values for the different models.

Table 5.13: RMSE values on total dataset for combinations of separate models for observations with MPD values smaller or larger than 1 mm.

Used model		**RMSE MPD<1**	**RSME MPD>1**	**RMSE total**
MPD<1	**MPD>1**			
Equation (5.17)	Equation (5.17)	0.0366	0.0236	0.0319
Equation (5.18a)	Equation (5.19a)	0.0368	0.0211	0.0312
Equation (5.18b)	Equation (5.19b)	0.0348	0.0209	0.0298

The RMSE for observations with an MPD< 1 mm is always larger than the RMSE for observations with an MPD> 1 mm. For an MPD< 1 mm, the RMSE is always larger than 0.03 whereas for an MPD> 1 mm the RMSE is always smaller than 0.03. Furthermore, it can be seen that the differences in RMSE are very small. Equation (5.17) is the equation with $V_b - V_a$ and MPD·$(V_b - V_a)$ determined for the whole dataset, whereas Equation (5.18a) and Equation (5.19a) are regressions with the same predictive variables but determined separately for observations with MPD< 1 mm and MPD> 1 mm.

The difference in the final RMSE is only 0.0007. When using the best fitted models —with different predictive variables per model— for observations with MPD> 1 mm and MPD< 1 mm (Equations (5.18b) and (5.19b)), an improvement of the 0.0021 is found. However, with this RMSE, for both models different predictive variables are used.

Visualisation of the models

Figures 5.10a and 5.10b show a visualisation of Equations (5.18) and (5.19).

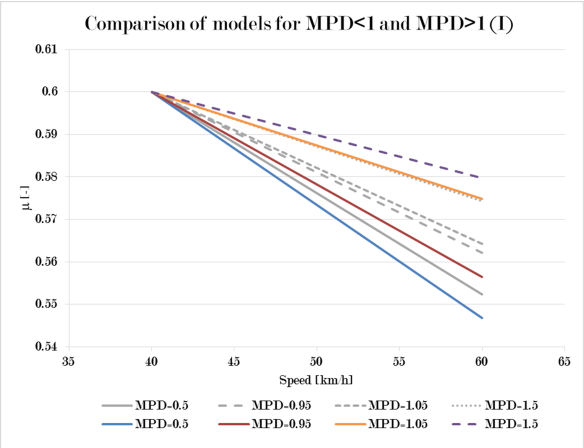

(a) For both ranges of MPD, the models with V and MPD·V as predictive variables are used, these models are shown in Equations (5.18a) and (5.19a).

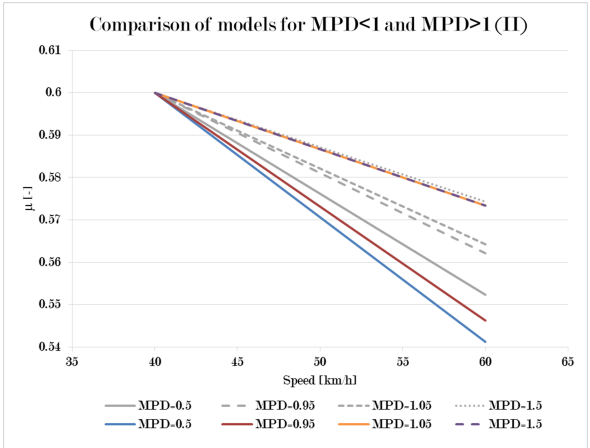

(b) For both ranges of MPD, the best predictive model is used. Thus, for MPD< 1 mm Equation (5.18b) is used, and for MPD> 1 mm Equation (5.19b) is used.

Figure 5.10: Comparison of models for MPD< 1 mm and MPD> 1 mm, the grey lines indicate Equation (5.17), which is equal for all values of MPD. A conversion of the skid resistance between 40 and 60 km/h is calculated, based on a skid resistance of 0.6 at 40 km/h.

In Figure 5.10a, the regression for MPD values smaller than 1 mm gives a larger dependency of skid resistance with speed than the overall model. For MDP values larger than 1 mm this is opposite: here, the overall model gives a larger dependency of skid resistance with speed. gives a larger dependency of skid resistance with speed

In Figure 5.10b, for MPD values smaller than 1 mm, this effect increases. Equation (5.18b) gives even a larger dependency of skid resistance with speed than Equation (5.18a).

Therefore, the overall model of Equation (5.17) might over-estimate the skid resistance for increasing measuring speeds for road sections with an MPD smaller than 1 mm. For MPD values larger than 1 mm, the overall model might under-estimate the skid resistance for increasing vehicle speeds. With converting the skid resistance to a lower measuring speed, this effect is opposite.

Furthermore, for both models, a difference can be observed between the predicted dependency of skid resistance with speed for observations with an MPD smaller or larger than 1 mm. For an MPD of 0.95 or 1.05 mm, a different prediction of the skid resistance at 60 km/h is made, despite the small difference in texture. This 'jump' is of course undesirable.

Conclusions

With making separate models for observations having an MPD smaller or larger than 1 mm, a small improvement of the RMSE can be obtained. When using the same predictive variables as in the best obtained model for the total dataset, an improvement of 0.0007 is made. By using different predictive variables for both regressions, an improvement of the RMSE of 0.0021 is reached.

For two reasons, using the best obtained models per MPD range is not preferred:

1. For both regressions, different predictive variables are used. These are 'randomly' selected, because they generate the lowest RMSE. However, it cannot be explained why different predictive variables should be used, and it is preferred to use equal predictive variables.

2. For observations with MPD values marginally above or below 1 mm, a very different skid resistance adjustment is calculated. This is an undesired effect of performing separate regression analyses.

Consequently, the models obtained by performing separate regressions depending on the MPD values are not considered in the further analyses.

5.4.4. Conclusions of multilevel modelling

Final model

The best obtained model with the hierarchical model is (equal to Equation (5.17)):

$$\mu_a = \mu_b \cdot e^{(0.00511 - 0.00195 \cdot \text{MPD}) \cdot (V_b - V_a)} \tag{5.20}$$

When applying this model in the datasheet with speed combinations, an RMSE of 0.0319 is obtained.

Hierarchical structure

The dataset fits best on a three-level model with the following hierarchical structure as in Figure 5.11.

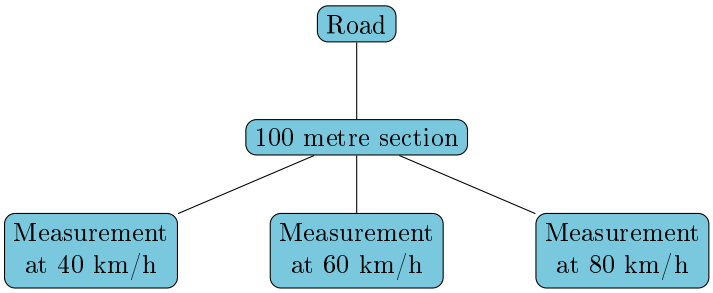

Figure 5.11: Hierarchical structure for a three-level model

The first level include the individual measurements performed at different measuring speeds, the second level are the 100 metre sections and the third level are the different roads to which the 100 metre sections belong.

Predictive variables

From comparing models with different predictive variables it was concluded that two three-level models fitted best to the dataset, namely the models with as predictive variables:

- V, MPD$\cdot V$
- V, ln(MPD)$\cdot V$

The chi-square likelihood ratio test of the second regression was slightly higher than of the first regression. But, because the difference was so small, the first regression is chosen as the preferred regression because of the more simple predictive variable (MPD$\cdot V$ is preferred above ln(MPD)$\cdot V$).

5.5. Comparison of different methods

Three regression methods are performed to obtain a speed conversion model for the skid resistance measured with the SKM. The obtained models per regression method are:

- Method 1:

  $$\mu_a = \mu_b \cdot e^{(0.00560 - 0.00263 \cdot \text{MPD}) \cdot (V_b - V_a)}$$

  RMSE: 0.032

- Method 2:

  $$\mu_a = \mu_b \cdot e^{(0.00580 - 0.00337 \cdot \text{MPD}) \cdot (V_b - V_a)}$$

  RMSE: 0.033

- Method 3:

$$\mu_a = \mu_b \cdot e^{(0.00511 - 0.00195 \cdot \text{MPD}) \cdot (V_b - V_a)}$$

  RMSE: 0.032

The values of the RMSE are calculated based on the datasheet of speed combinations, such that the regressions can be compared to each other.

Figure 5.12 shows a plot in which all three models are shown. A skid resistance of 0.6 at 40 km/h is converted into a skid resistance at 60 km/h. Three different macro textures are included: 0.5, 1.0 and 1.5. Table 5.14 shows the numerical values of the calculated values of the skid resistance at 60 km/h.

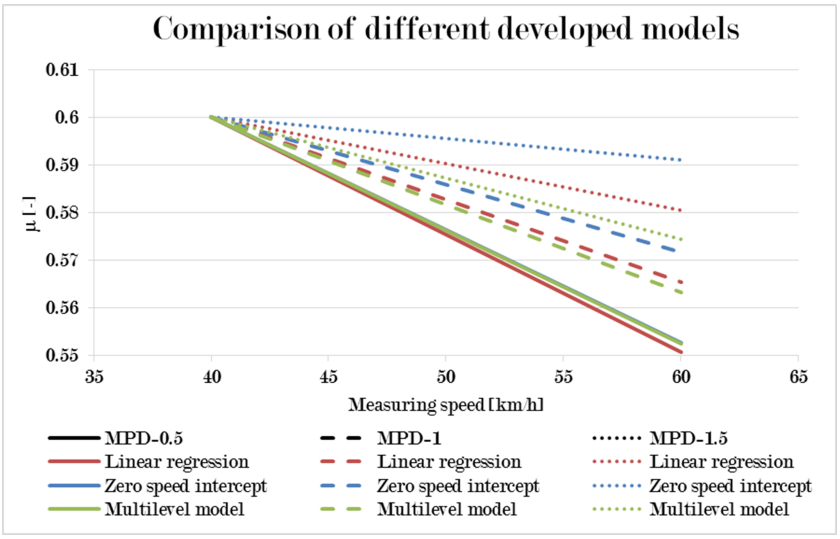

Figure 5.12: Comparison of final models obtained with the three regression methods

Table 5.14: Comparison of final models obtained with the three regression methods. μ_a at 60 km/h is calculated based on $\mu_b = 0.6$ at a speed of 40 km/h. μ_a is shown per model for an MPD of 0.5, 1 and 1.5 mm.

MPD	μ_a		
	Linear regression	**Zero speed intercept**	**Multilevel model**
0.5	0.551	0.553	0.552
1	0.565	0.572	0.563
1.5	0.581	0.591	0.574

As one can see, for an MPD of 0.5 mm, the model results barely depart from each other. The skid resistance obtained with the zero speed intercept model cannot be seen in the plot, because it is almost equal to the skid resistance obtained with the multilevel model. The larger the MPD, the more the models diverge. The multilevel model shows the smallest influence of the MPD, whereas the model obtained with the zero speed intercept shows the largest influence of the MPD.

Figure 5.13 shows the predicted values of the skid resistance for the first and third regression methods. Because the model obtained with the zero speed intercept diverges much from the other two obtained models, this model is not shown.

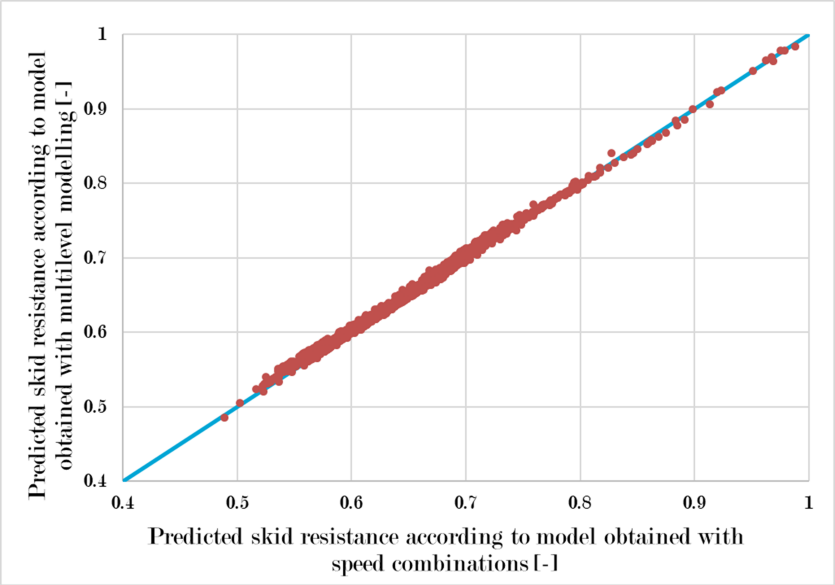

Figure 5.13: Plot with on the x-axis the predicted skid resistance according to regression method 3 and on the y-axis the predicted skid resistances according to regression method 1.

As Figure 5.13 shows, the dots show a very small spread around the line $y = x$. This indicates that both models predicts very identical values of the skid resistance.

As already mentioned, with regression method 1 (multiple linear regression), the problem of dependent observations arises. This makes the data inappropriate for performing a multiple linear regression.

For the second method, which makes use of the zero speed intercept, estimating the zero speed intercept according to a functional approach results in poor values of the RMSE. Estimating the zero speed intercept in SPSS gives better results, but this makes the intercept value dependent on the chosen predicted variables. Furthermore, it is not possible to estimate a zero speed intercept per 100 metre section, but only for larger sections.

Regression method 3, the multilevel analysis, deals with both problems from regression methods 1 and 2. For this method, observations can be dependent, and because of the random intercept values, every 100 metre section is given another random intercept. These intercepts are not given in the output, but during the transformation of the obtained regression to the speed conversion model, the intercept values are eliminated. Because the data fulfils the criteria for obtaining a model according to a multilevel analysis, this model is considered to be the most reliable model.

5.6. Conclusions

During the model analysis, three methods were used:

1. multiple linear regression on speed combinations,
2. linear regression with zero speed intercept, and
3. multilevel modelling.

With the first method, the problem of dependency between observations arose. This was tried to avoid in the second method with help of a zero speed intercept, however, it appeared to be difficult to give a good estimation of the zero speed intercept. The last method is the best regression method for this dataset, because it can deal with the dependent observations and the hierarchy present in the data. The model obtained with the multilevel modelling is given in Equation (5.20) and is as follows:

$$\mu_a = \mu_b \cdot e^{(0.00511 - 0.00195 \cdot \mathrm{MPD}) \cdot (V_b - V_a)}$$

The standard error obtained with this model, calculated on the dataset with speed combinations, is 0.032.

6

Verification of model

This chapter gives a verification of the model obtained in Chapter 5. This model is the model developed by the three-level hierarchical regression, and is given in Equation (5.20). The model is as follows:

$$\mu_a = \mu_b \cdot e^{(0.00511 - 0.00195 \cdot \text{MPD}) \cdot (V_b - V_a)}$$

The model verification consist of several parts. Firstly, Section 6.1 gives the standard error of the estimate. In Section 6.2 the model is applied on new data, namely 25% of the data which is not used for the model generation and on a small dataset consisting of curved sections. Section 6.3 extrapolates the model to 20 and 100 km/h to verify whether expected values are predicted at these measuring speeds. Section 6.4 gives some visualisations of the residuals and Section 6.6 compares several previously developed speed conversion models to Equation (5.20). Finally, Section 6.7 gives conclusions of the model verification.

6.1. Standard error of the estimate

The RMSE of this model, when applied on the datasheet with speed combinations, is 0.032. This RMSE is for all data, thus conversions from 30 to 40, 60 to 40, 80 to 60 and 80 to 40 are included. To obtain a better indication of how large or small this RMSE is, the RMSE is calculated separately over the following speed conversions:

- 30 to 40 km/h: 0.035
- 60 to 40 km/h: 0.031
- 80 to 60 km/h: 0.022

The average standard error is larger for lower measuring speeds. This could be expected because the skid resistance is assumed to change more at lower measuring speeds than at higher measuring speeds, thus the error of estimates will also be higher at lower measuring speeds.

6.2. Model applied on new data

Besides the standard error of the used data, the standard error of new data is analysed, for which two different datasets are used. Firstly, the model is applied on 25% of the dataset which was not used for the model generation. Thereafter, the model is applied on a small dataset consisting of measurements performed on curved sections.

6.2.1. Remaining 25% of data

All regressions as described in this chapter are performed on 75% of all available data. Therefore, the model is applied on the remaining 25% of the data. If the RMSE of the model on this part of the data is much larger than on the fitted data, it can indicate that the model is overfitted to the used dataset.

The RMSE for the remaining 25% is 0.034, which is very similar to the RMSE of the data on which the model is fitted. The RMSE's per speed interval are:

- 30 to 40 km/h: 0.044
- 60 to 40 km/h: 0.035
- 80 to 60 km/h: 0.022

The values above slightly higher than the standard errors of the model on the data which is used for the regression. Since the model is based on 75% of the data, the standard error for this 75% is expected to be smaller than the standard error for the non-used 25% of the data.

6.2.2. Curved sections

Some new measurements were performed on bends to verify whether the developed model can also be used for curved sections. These measurements are obtained on the intersection Beekbergen, near Apeldoorn, which includes both curves to the left and to the right. The curve to the right has a radius of approximately 82 metres and is measured at 45 and 55 km/h, whereas the curve to the left has a radius of approximately 105 metres and is measured at 45 and 60 km/h. In total, only 13 100 metre sections were measured.

When applying the model on these 13 100 metre sections, the standard errors are as follows:

- From 45 km/h converted to 55/60 km/h: 0.0094
- From 55/60 km/h converted to 45 km/h: 0.0090

The average difference between the skid resistance measured at these measuring speeds is 0.029.

The standard errors for the curved sections are smaller than the standard errors of the model applied on the used dataset. Furthermore, for most sections, the speed dependency is under estimated. For few sections the speed dependency is over estimated, but no clear difference between left or right curved sections was found. This could indicate that the model can also be applied on curved sections. However, only few 100 metre sections are included and it is recommended to include more measurements performed on curved sections before drawing a conclusion.

6.3. Extrapolation of model

The model is obtained with data measured at 40, 60 and 80 km/h, and some of the data is measured at 30 km/h. The skid resistances at 20 and 100 km/h are calculated to see whether the model acts as expected for these speed ranges. Because an exponential model is used, it should be prevented that for small measuring speeds the skid resistance will exceed one, or that for larger measuring speeds the skid resistance approaches zero.

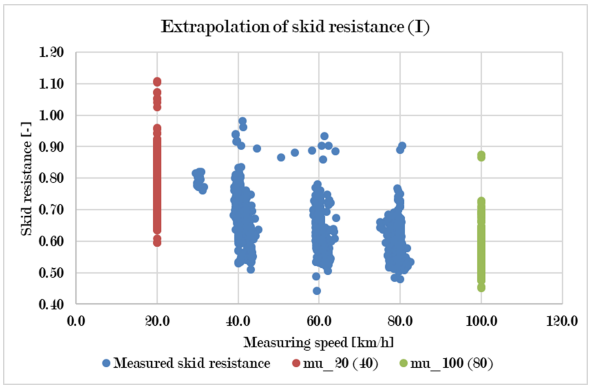

(a) Skid resistance at 20 km/h predicted with measurements at 40 km/h, skid resistance at 100 km/h predicted with measurements at 80 km/h

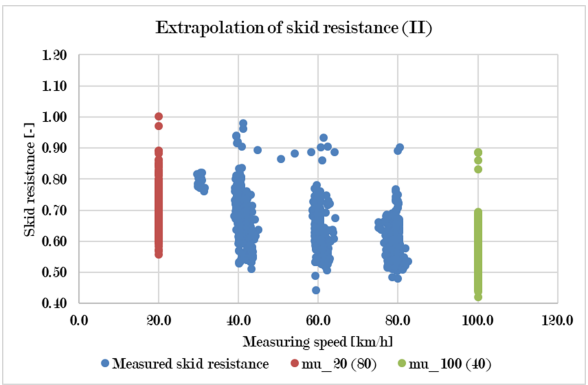

(b) Skid resistance at 20 km/h predicted with measurements at 80 km/h, skid resistance at 100 km/h predicted with measurements at 40 km/h

Figure 6.1: Plot showing the measured values for the skid resistance at 30, 40, 60 and 80 km/h and the extrapolated values of the skid resistances at 20 and 100 km/h.

Figure 6.1 shows the extrapolated values for 20 and 100 km/h. In Figure 6.1a the skid resistance at 20 km/h is calculated based on the measurements performed at 40 km/h and the skid resistance at 100 km/h is calculated based on the measurements performed at 80 km/h. In Figure 6.1b the opposite is shown: the skid resistance at 20 km/h is calculated based on measurements at 80 km/h and the skid resistance at 100 km/h is calculated based on measurements at 40 km/h. It is unlikely that the model will be used for conversing skid resistance over large speed differences as in Figure 6.1b, but in this plot it is analysed what the influence of such a large speed difference can be.

As Figure 6.1a shows, the ranges for 20 km/h are very large and even exceed 1, which is not possible for measured values of skid resistance. However, at 40 km/h some of the measured values are very high and these measurements pushes skid resistances above one at 20 km/h. Figure 6.1b shows only one value that exceeds a skid resistance of one. Overall, the extrapolation does not show unlikely large increases in skid resistance when approaching 20 km/h or unlikely large decreases when approaching 100 km/h.

6.4. Residuals

In this section, the residuals of the model are analysed. One must realise that the 'real' residuals of the model cannot be calculated. These should be calculated from the datasheet that is used for the mixed model, but then also the random intercepts should be known. Furthermore, the interest of this research is to convert skid resistance measurements to values of skid resistance at another measuring speed. Therefore, the residuals of the model calculated for the datasheet with speed combinations are analysed.

Figure 6.2a shows a plot with on the x-axis the measured value of the skid resistance and on the y-axis the residuals of the predicted values of the skid resistance. According to the theory of a linear regression, the residuals must be normally distributed. In a scatterplot, no clear pattern should be visible, because if a clear pattern can be seen, the residuals are not normally distributed. Furthermore, Figure 6.2b shows a frequency histogram of the residuals. This histogram shows a distribution which is roughly normal.

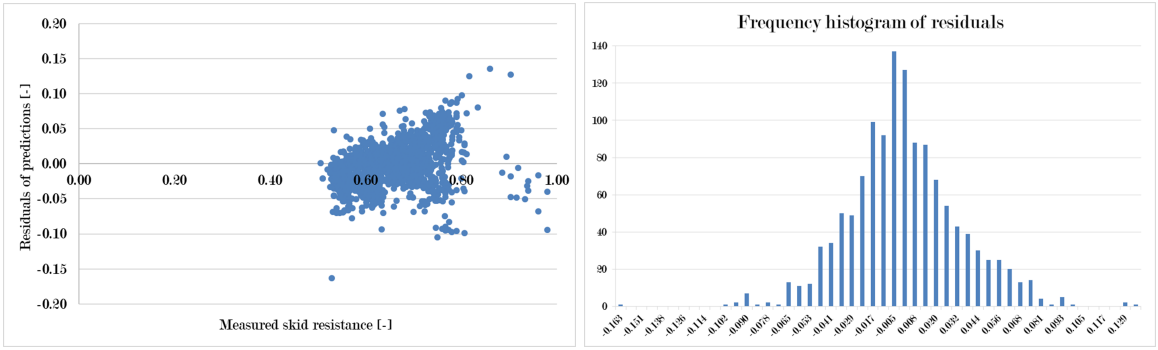

(a) Plot showing on the x-axis the measured values for the skid resistance μ_a and on the y-axis the residuals (μ_{measured}-$\mu_{\text{predicted}}$), calculated for μ_a=40 or 60 and μ_b=60 or 80

(b) Histogram of residuals for the model applied on the datasheet with speed combinations

Figure 6.2: Plots of measured skid resistances with the predicted skid resistances for several reference speeds

Figure 6.3 shows a plot of the measured skid resistance on the x-axis, and the predicted skid resistance on the y-axis. Ideally, all datapoints would be plotted on the line $y = x$.

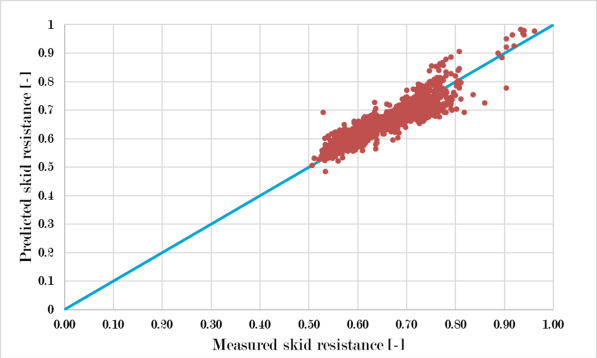

Figure 6.3: Plot of measured skid resistance with predicted skid resistance for all data points

Figure 6.4 show the same plot of Figure 6.3, but separated into four plots for four different speed combinations.

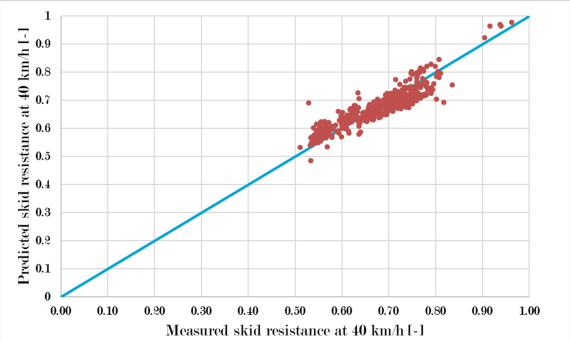

(a) Skid resistance at 40 km/h, predicted with measurements at 60 km/h

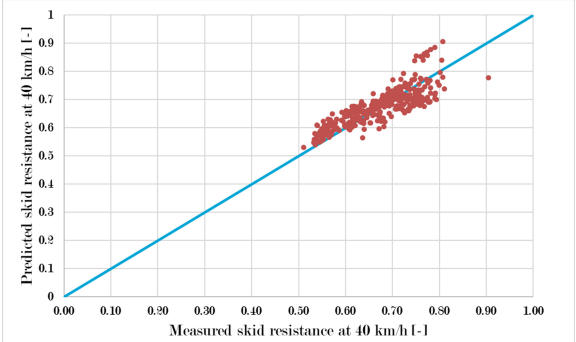

(b) Skid resistance at 40 km/h, predicted with measurements at 80 km/h

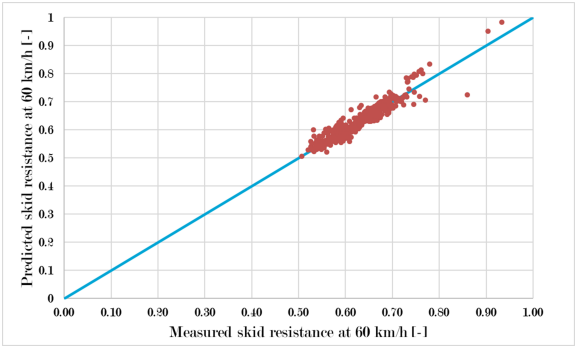

(c) Skid resistance at 60 km/h, predicted with measurements at 80 km/h

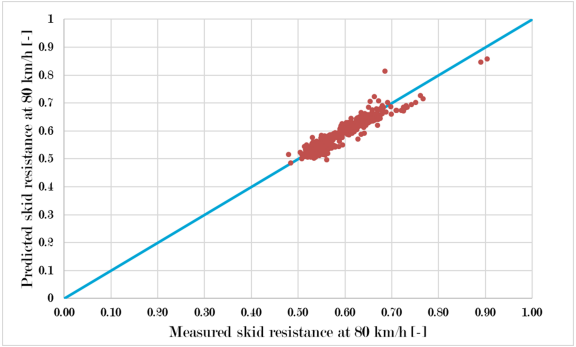

(d) Skid resistance at 80 km/h, predicted with measurements at 60 km/h

Figure 6.4: Plots of measured skid resistances with the predicted skid resistances for several reference speeds

Figure 6.4b shows a wider spread of the dots around $y = x$ than the other figures of Figure 6.4. This is as expected, because Figure 6.4b converts the skid resistance over 40 km/h, whereas to other figures show a conversion of 20 km/h. Therefore, more scatter is expected in Figure 6.4b. Furthermore, no large differences between the scatterplots are observed.

Figure 6.5 also shows a similar plot as Figure 6.3, but now separated into one plot containing datapoints with an MPD$<$ 1 mm, whereas the other plot contains datapoints of an MPD$>$ 1 mm.

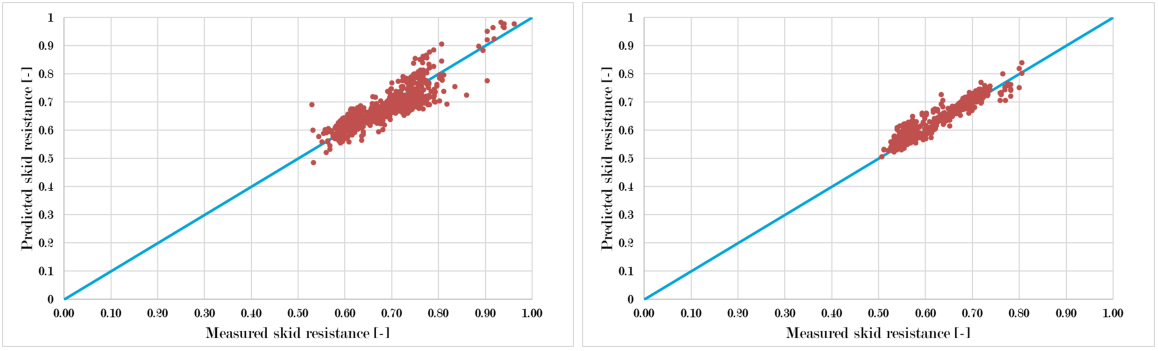

(a) Plot of measured skid resistance with predicted skid resistance for datapoints with MPD< 1 mm

(b) Plot of measured skid resistance with predicted skid resistance for datapoints with MPD> 1 mm

Figure 6.5: Plot of measured skid resistance with predicted skid resistance, separated into datapoints with an MPD< 1 mm and an MPD> 1 mm

Figure 6.5a shows a wider spread of the dots around $y = x$ than Figure 6.5b. Because for observations with an MPD smaller than 1 mm the speed dependency is larger, a wider spread of the dots can be expected.

6.5. Sensitivity analysis of macrotexture

The best fitting model has MPD and speed difference as the principal predictive input parameters. The MPD cannot always be measured accurately especially not when a test is performed on a rainy day or on a wet pavement surface. Laser measurements conducted on these conditions may lead to wrong estimates of MPD. For this reason a computational analysis was performed to see how sensitive the developed model is for wrong input of MPD. For a few examples, values of 0.5 times MPD and 1.5 times MPD were substituted for the actual value of MPD.

Furthermore, the model is compared to a multilevel (three-hierarchical) model in which only the speed difference $V_b - V_a$ is used as a predictive parameter. This model is given by regression 5 of Table 5.9 and is as follows:

$$\mu_a = \mu_b \cdot e^{0.00323 \cdot (V_b - V_a)} \tag{6.1}$$

Four random 100 metre sections with different MPD values were selected from the database. In Figure 6.6, for each of the four 100 metre sections, five different plots of the skid resistance are shown:

- measured values;
- skid resistance at 60 km/h converted to 40 km/h and 80 km/h, according to Equation (5.20);
- skid resistance at 60 km/h converted to 40 km/h and 80 km/h, according to Equation (5.20), but now with 0.5· MPD instead of the measured MPD;
- skid resistance at 60 km/h converted to 40 km/h and 80 km/h, according to Equation (5.20), but now with 1.5· MPD instead of the measured MPD; and
- skid resistance at 60 km/h converted to 40 km/h and 80 km/h, according to Equation (6.1).

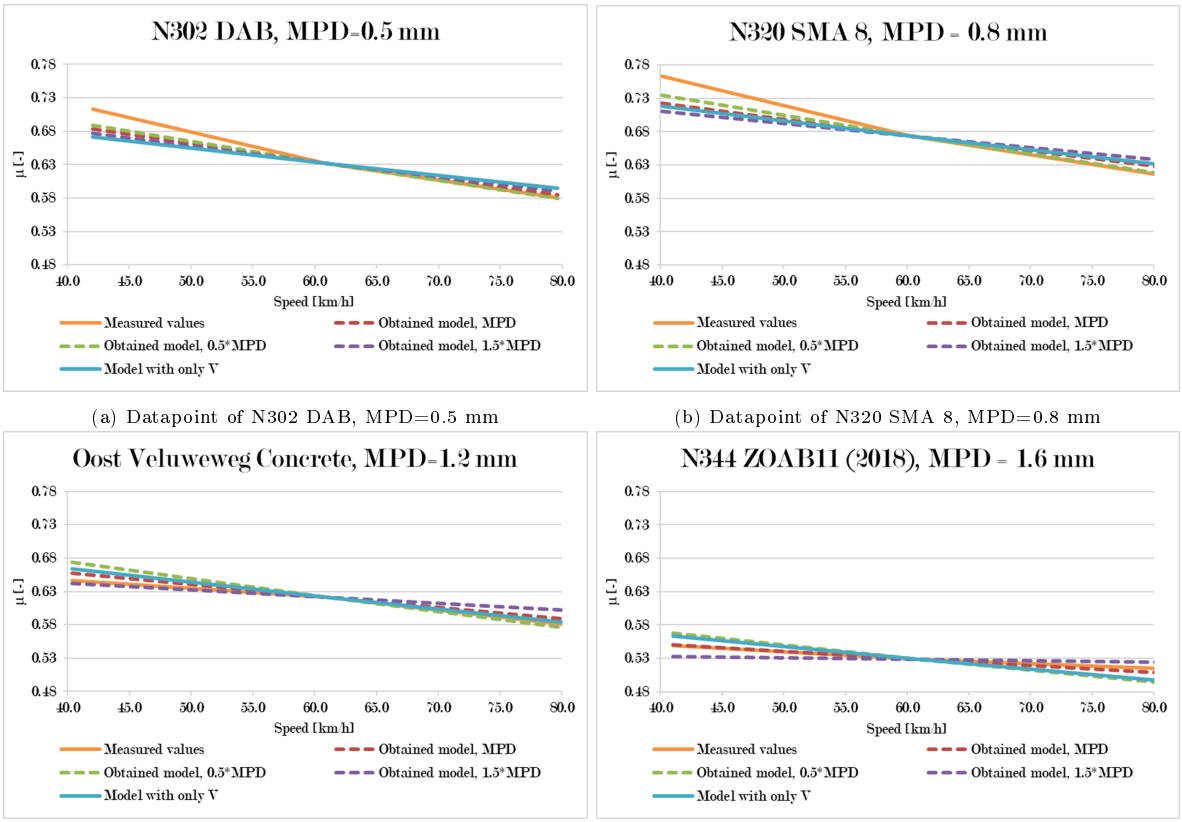

(a) Datapoint of N302 DAB, MPD=0.5 mm

(b) Datapoint of N320 SMA 8, MPD=0.8 mm

(c) Datapoint of Oostveluweweg Concrete, MPD=1.2 mm

(d) Datapoint of N344 ZOAB11, MPD=1.6 mm

Figure 6.6: Visualisation of texture influence on model. 4 random datapoints are selected for which the skid resistance at 40 and 80 km/h are calculated, the skid resistance at 60 km/h is taken as reference point. In the obtained model, the measured MPD, the measured 0.5·MPD and the measured 1.5·MPD are entered.

Figures 6.7a to 6.7d show per converted value of the skid resistance the difference with the measured value of the skid resistance. At 60 km/h, this difference is zero because 60 km/h was taken as the reference speed. Furthermore, a positive value indicates that the measured skid resistance was larger than the converted skid resistance.

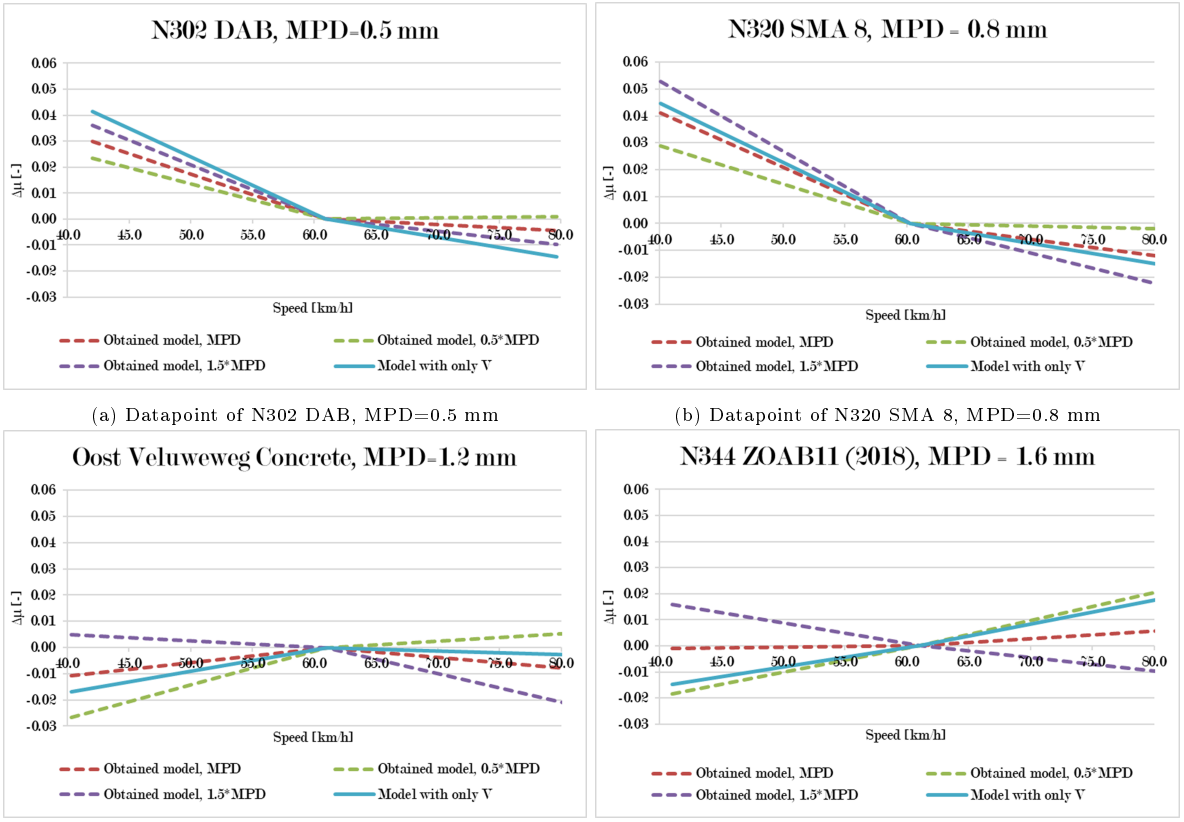

(a) Datapoint of N302 DAB, MPD=0.5 mm

(b) Datapoint of N320 SMA 8, MPD=0.8 mm

(c) Datapoint of Oostveluweweg Concrete, MPD=1.2 mm

(d) Datapoint of N344 ZOAB11, MPD=1.6 mm

Figure 6.7: Visualisation of texture influence on model. 4 random datapoints are selected for which the skid resistance at 40 and 80 km/h are calculated, the skid resistance at 60 km/h is taken as reference point. In Equation (5.20), the measured MPD, the measured MPD·0.5 and the measured MPD·1.5 are entered. The figures show the measured skid resistances minus the converted skid resistances.

From the figures above, several observations and conclusions can be made. First of all, the conversions to a skid resistance of 40 km/h according to Equation (5.20) are more accurate for the datapoints with larger MPD values (1.2 mm, 1.8 mm) than for the datapoints with smaller MPD values (0.5 mm, 0.8 mm). Furthermore, for the datapoints with smaller MPD values the speed dependency according to Equation (5.20) is underestimated, whereas for the larger MPD values, the speed dependency is overestimated.

For the datapoints with smaller MPD values, the conversions with 0.5·MPD and 1.5·MPD have, logically, small differences compared to the conversion with the measured MPD. These differences are also small compared to the error of the estimate made in that conversion. For the datapoints with larger MPD values, the differences for conversions with 0.5·MPD and 1.5·MPD compared to the error of the estimates are larger. As Figures 6.7c and 6.7d show, the error of the estimate can become twice as large.

For all four datapoints, Equation (5.20) gives a better conversion than Equation (6.1), the model with only the speed difference as a predictive variable. However, for the datapoints with smaller MPD values, the differences between the conversion of Equation (6.1) and the conversions of Equation (5.20) with incorrect values of the MPD are small compared to the total increase or decrease in skid resistance. For the datapoints with larger MPD values, Equation (5.20) gives a better conversion of the skid resistance than when 0.5·MPD or 1.5·MPD is used in Equation (5.20). Therefore, when MPD values are unknown, it is advised to use Equation (6.1) instead of Equation (5.20).

6.6. Comparison of developed model with previous developed models

This section compares the model that is developed in this research, i.e. Equation (5.20), with several previously developed speed conversion models as described in Chapter 4. Not all models can be compared, because for some models the exact numbers were not known. The comparison is divided into two sections, namely Section 6.6.1, that compares Equation (5.20) to previously developed models for the RWS Skid Resistance Tester, and Section 6.6.2, that compares Equation (5.20) to previously developed models for the SKM or SCRIM.

6.6.1. Conversion models for the RWS Skid Resistance Tester

The following comparisons are analysed:

- Equation (5.20) with Koac•WMD (Equation (4.7)): conversion model for RWS Skid Resistance Tester measurements, including MPD and positive/negative textures. Possible to convert between several measuring speeds.
- Equation (5.20) with Koac •NPC (Equation (4.13)): conversion model for RWS Skid Resistance Tester measurements, including MPD. Possible to convert a measurement at a speed between 20 to 50 km/h to a skid resistance at 50 km/h.
- Equation (6.1) with Koac•NPC (Equation (4.14)): conversion model for RWS Skid Resistance Tester measurements, with only the speed difference as a predictive variable. Possible to convert a measurement at a speed between 20 to 50 km/h to a skid resistance at 50 km/h.

Because the conversion models of Koac•NPC can only convert to a skid resistance at a measuring speed of 50 km/h, a measured skid resistance of 0.6 at 40 km/h is chosen as basis of this comparison, and this is converted to a skid resistance at 50 km/h.

Figures 6.8a and 6.8b show the differences between the predicted skid resistances according to Equation (5.20) and according to the model as given in the legend. A positive number indicdates that Equation (5.20) predicts a larger value of the skid resistance at 50 km/h, and thus a smaller speed dependency of the skid resistance.

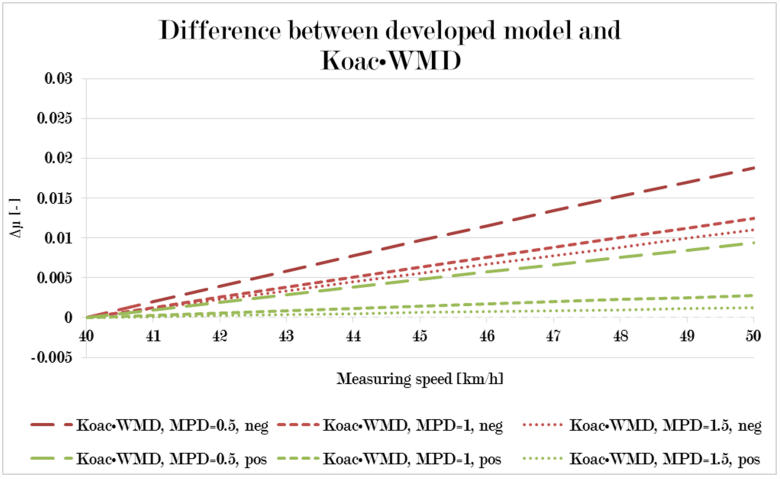

(a) Differences of skid resistance predicted with Equation (5.20) and with the speed conversion model developed by Koac•WMD (Equation (4.7)). The Koac•WMD model is applied for both a positive [pos] and a negative [neg] texture.

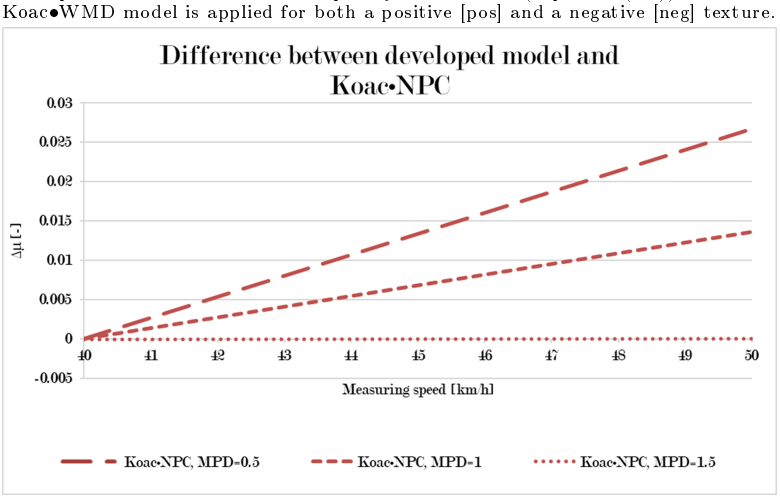

(b) Differences of skid resistance predicted with Equation (5.20) and with the speed conversion model developed by Koac•NPC (Equation (4.13)).

Figure 6.8: Comparison of several previously developed speed conversion models with the model obtained in this research (Equation (5.20)). A skid resistance of 0.6 at 40 km/h is converted to a skid resistance at 50 km/h for different values of MPD. The difference between the predicted skid resistance with Equation (5.20) and the corresponding model is shown. A positive value indicates that Equation (5.20) predicts a larger value of the skid resistance and thus a smaller speed dependency.

Figure 6.8a compares the model developed by Koac•WMD (Equation (4.7)) to Equation (5.20). The model developed by Koac•WMD is developed for measurements performed with the RWS Skid Resistance Tester (which measures the LFC), thus these measurements could have a different speed dependency. It can be seen that for positive textures, the conversions for an MPD of 1 mm and 1.5 mm are quite similar, whereas for an MPD of 0.5 mm there is a larger difference. Koac•WMD gives a larger speed dependency than Equation (5.20). For negative textures, the model developed by Koac•WMD converts to a much lower skid resistance than Equation (5.20). This is remarkable, because approximately 90% of the data used in this research contains values of MPD/RMS$<$ 1.58, indicating a negative texture according to Equation (4.7).

Figure 6.8b compares the model developed by Koac•NPC (Equation (4.13)) with Equation (5.20). The model developed by Koac•NPC is developed for measurements performed with the RWS Skid Resistance Tester. As the figure shows, the models are equal for an MPD of 1.5 mm. However, the smaller the MPD, the larger the difference.

Besides Equation (4.13), Koac•NPC also developed a speed conversion model with only the speed difference as a predictive variable, given in Equation (4.14). No visualisation of this model is given,

because the only coefficient is the coefficient of the speed difference. From observing these coefficients, it was concluded that Equation (4.14) applies a much larger speed dependency than Equation (6.1). Thus, for both Equations (4.13) and (4.14), Koac•NPC predicts a larger speed dependency than the models developed in this research. This holds also for the comparison with the model developed by Koac•WMD.

The models developed by Koac•NPC and Koac•WMD were developed on LFC-data with a 86% retained wheel, whereas the model developed in this research is based on SFC-data with a yaw angle of 20°. This difference in test set-up generates different hysteresis and adhesion, which might have their effect on the speed dependency of skid resistance. The difference of the influence of MPD could also indicate that different levels of values of MPD were used in the regression analyses that generated in turn different relationships.

6.6.2. Conversion models for the SKM or SCRIM

This section compares Equation (5.20) to previously developed conversion models based on the SKM or SCRIM. The following comparisons are analysed:

- Equation (5.20) with SCRIM (Equation (4.15)): conversion model for SCRIM, no texture included. Possible to convert a measurement performed between 25 and 85 km/h to a skid resistance at 50 km/h.
- Equation (5.20) with TP Griff-StB (SKM) (Equation (4.16)): conversion model for SKM, no texture included. Possible to convert at most over 10 km/h.
- Equation (5.20) with BASt (Equation (4.18)): conversion model for SKM, MPD included. Extension of TP Griff-StB (SKM) model, therefore probably possible to convert at most over 10 km/h.

Because the conversion models from the TP Griff-StB (SKM) and BASt cannot exceed a speed difference of 10 km/h, a measured skid resistance of 0.6 at 40 km/h is chosen as basis of this comparison, and this is converted to a skid resistance at 50 km/h.

Figure 6.9 show the differences between the predicted skid resistances according to Equation (5.20) and according to the model as given in the legend. A positive number means that Equation (5.20) predicts a larger value of the skid resistance at 50 km/h, and thus a smaller speed dependency of the skid resistance.

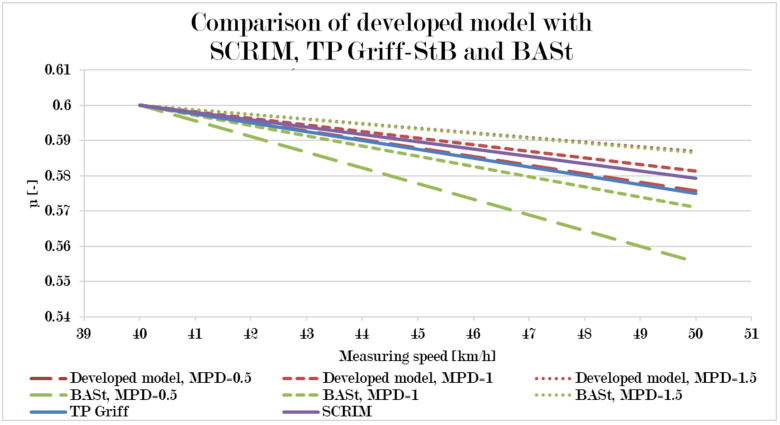

Figure 6.9: Comparison of several previously developed speed conversion models for the SKM or SCRIM with the model obtained in this research (Equation (5.20)). A skid resistance of 0.6 at 40 km/h is converted to a skid resistance at 50 km/h for different values of MPD. The difference between the predicted skid resistance with Equation (5.20) and the corresponding model is shown. A positive value indicates that Equation (5.20) predicts a larger value of the skid resistance and thus a smaller speed dependency.

Figure 6.9 shows the comparison for models developed for the skid resistance measured with the SKM or SCRIM, which both measure the SFC. The conversion of TP Griff-StB, which does not include a texture measurement, is almost similar to the conversion of Equation (5.20) for an MPD of 0.5 mm.

This can be clarified by the fact that in Germany much more dense pavements are used than in the Netherlands, which indicate often lower values of MPD. The conversion of the SCRIM lies between the conversion of Equation (5.20) for an MPD of 0.5 mm and an MPD of 1 mm. Finally, the model of BASt, which is an extension of TP Griff-StB including MPD measurements, shows a much wider variation of converted values than Equation (5.20). The texture has a larger influence in the model developed by BASt than in Equation (5.20). Especially for the smaller textures there is a large difference in the conversion of the skid resistance. No obvious reason could be found for this discrepancy.

6.7. Conclusions

This chapter performed some test to verify the model developed in Chapter 5. This section summarises the conclusions from this verification.

The standard error of the model applied on the dataset with speed combinations is 0.032. When applying the model on the 25% of the data not used for the model generation, a standard error of 0.034 was found. This is slightly higher than the standard error of the model applied on the 75% of the data which is used for the model generation. The residuals of the model are normally distributed and a larger variation is found for observations having an MPD$<$ 1 mm than for observations having an MPD$>$ 1 mm.

Besides the model with predictive parameters $V_b - V_a$ and MPD$\cdot(V_b - V_a)$, also a three-level model with only $V_b - V_a$ as predictive parameter was developed. Based on sensitivity analyses, with Equation (5.20) using 0.5 and 1.5 times the measured MPD values, it was concluded that if no MPD is known or it is unsure whether the MPD measurements are reliable, it is advised to use the model with only $V_b - V_a$ as predictive parameter instead of Equation (5.20).

A comparison between previously developed speed conversion models and the model developed in this research was performed. A skid resistance of 0.6 at 40 km/h was converted to a skid resistance at 50 km/h according to several models. It was observed that the models developed for the RWS Skid Resistance Tester have a larger speed dependency for equal values of MPD. For an MPD of 1.5 mm, the models are approximately equal. Furthermore, the model is compared to other models developed for SWF measurements. Compared to the model of TP Griff-StB (SKM), which does not include a texture measurement, an MPD of 0.5 mm gave approximately an equal conversion of skid resistance. This can be clarified by the fact that in Germany more dense pavements are used, and an MPD of 0.5 mm is a more standard MPD value. The model used for the SCRIM does also not include a texture measurement. The converted value of the SCRIM is in between the converted values for an MPD of 0.5 and 1 mm according to the model developed in this research. Lastly, the extended model of the TP Griff-StB (SKM), developed by BASt, has a larger influence of texture than the model developed in this research. No clarification for this larger influence is known.

7

Conclusions and recommendations

In this research, efforts have been made to search for an answer to the following question:

How can the correlation between the SKM measured skid resistance at different speeds be described, taking into account the macrotexture of the road surface?

In this chapter the conclusions and recommendations of the research programme are described. Section 7.1 contains the conclusions, followed by the recommendations in Section 7.2.

7.1. Conclusions

Literature study

A comprehensive literature study was conducted on the theoretical background and speed dependency of skid resistance, and several previously developed speed conversion models were analysed. In general, a decline in skid resistance can be observed with increasing vehicle speeds. In previously developed speed conversion models, often an exponential relationship between the speed difference and the change in skid resistance is assumed, whereas in fewer models a linear relationship is assumed.

Predictive variables frequently used are the speed difference and the MPD. Furthermore, the MPD/RMS is also used once in a model. This parameter can indicate if a texture is positive or negative.

Measurements performed on curved sections or new pavement layers and measurements performed at low measuring speeds were classified as sections that could give difficulties or a different speed dependency of the skid resistance.

The available dataset consisted practically completely of data measured at straight road sections and sections with a large horizontal radius. The lack of data from sections with sharp horizontal radii hampered development of a speed dependency model specific for these sections. Since the developed model applies to a large range of skid resistance values and consists of a relative adjustment factor, the model is considered to be appropriate for curved sections as well.

Furthermore, no reliable data on ages of the road sections were available. Also in this case, the developed model may be used with confidence on all ages of wearing courses.

Model generation

Three regression methods were performed to generate the speed conversion model for the skid resistance measurements over speed with the macrotexture incorporated. The methods were as follows:

- multiple linear regression on speed combinations,
- linear regression with zero speed intercept, and
- multilevel modelling.

From the multiple linear regression on speed combinations, it can be concluded that an exponential relationship fits better to the used dataset than the linear relationship. However, the multiple linear regression is not considered as an appropriate method to generate the speed conversion model. This was concluded because of the dependency of observations and the interdependency information which is lost by separating the data of each road section into multiple records with various speed combinations.

The linear regression with zero speed intercept tried to prevent the information loss by estimating an zero speed intercept for every 100 metre section. With help of the excel solver, a functional approach was used to estimate the zero speed intercept. However, the outcomes of this estimation depended much on the initial values given to the solver, making the results not robust. The zero speed intercept was also estimated with help of SPSS, but with this method, the intercepts depended on the chosen predictive variables. Furthermore, it was not possible to determine a zero speed intercept for every 100 metre section separately, but only per road, or per road divided into several subsections. Therefore, the linear regression with zero speed intercept is also not considered to be an appropriate method for generating the speed conversion model.

Multilevel modelling manages dependent observations and hierarchical structures of a dataset. Therefore, this method appeared to be the most appropriate method for the model generation in this research. The three-level structure came forward as the most optimal hierarchical structure. This structure is as follows:

- level 1: individual measurements (performed at a certain measuring speed), which all belong to a specific 100 metre section;
- level 2: 100 metre sections, which all belong to a specific road; and
- level 3: different roads on which the measurements were performed.

The models having the best fit contained the predictive variables V and MPD$\cdot V$, and V and ln(MPD)$\cdot V$. The accuracy of the two models were almost equal. Preference was given to the first model, because no transformations are needed in this model.

Final model

The obtained model is as follows:

$$\mu_a = \mu_b \cdot e^{(0.00511 - 0.00195 \cdot \mathrm{MPD}) \cdot (V_b - V_a)} \tag{7.1}$$

Limitations of the usage of this model are given by the used data:

- The model was derived for skid resistance values ranging from 0.44 to 0.98.
- The data used in the model includes measurements performed at 40, 60 and 80 km/h, and few measurements performed at 30 km/h. Therefore, the model should ideally only be used for converting the skid resistance between these speed ranges.
- All data is obtained with SKM measurements, a device measuring the SFC with help of a measuring wheel mounted at the right-hand side of the vehicle with a 20° yaw angle anticlockwise. Therefore, the obtained model should only be used for measurements performed with an equal SKM, or with an SKM with the measuring wheel mounted at the left-hand side at a clockwise yaw angle.
- The dataset included measurements on sections with an MPD varying between 0.21 and 1.80 mm. However, the frequency histogram of the MPD values shows that there is a lack of MPD values around 0.6 and 1 mm. Therefore, the model might be less reliable for road sections having these MPD values.

Verification of model

From previously developed models, no approach was found for determining how reliable an obtained model is. Therefore, in this research, a model verification was performed. In this verification, several aspects of the model were verified and tested.

The final model has a standard error over various speed combinations of 0.032. When applying the model to other data than used in the development phase, the standard error is 0.034. This is only a very small increase, and therefore it can be concluded that the model was not over-fitted on the dataset. Furthermore, the model is applied to a small dataset (13 sections of 100 metres) consisting of measurements performed on curved sections. The standard error of the model on this dataset was 0.0094, which is much smaller than the standard error of the model applied to the training data. Although this standard error is obtained with a small dataset, it could indicate that the model can also be applied to curved sections.

The data used in the model includes measurements performed at 40, 60 and 80 km/h, and few measurements performed at 30 km/h. However, an extrapolation of the observations to 20 and 100 km/h, did not give outstanding values of the skid resistance.

Besides the model with predictive parameters $V_b - V_a$ and MPD$\cdot(V_b - V_a)$, also a three-level model with only $V_b - V_a$ as predictive parameter was developed. This model is as follows:

$$\mu_a = \mu_b \cdot e^{0.00323 \cdot (V_b - V_a)} \tag{7.2}$$

Based on sensitivity analyses, performed by applying Equation (7.1) to datapoints with artificial uncertainties (50% of mean value) of the MPD, the conclusion can be drawn that if no MPD is known or it is unsure whether the MPD measurements are reliable, it is advised to use Equation (7.2) instead of Equation (7.1).

A comparison between previously developed models and the model generated in this report was performed. A skid resistance of 0.6 at 40 km/h was converted to a skid resistance at 50 km/h, with MPD values of 0.5, 1.0 and 1.5 mm. In conclusion can be stated that the models developed for the RWS Skid Resistance Tester often implied a larger speed dependency. These models are based on LFC data with a 86% retained wheel, whereas the model developed in this research is based on SFC data with a yaw angle of 20°. This difference in test set-up generates a different skid resistance, which might influence the speed dependency of the skid resistance. Furthermore, the current applied speed conversion, given by the TP Griff-StB (SKM) gave an equal conversion for the conversion model developed in this research when an MPD of 0.5 mm was used. This can be clarified by the fact that the arterial road network in Germany consists mainly of dense asphalt wearing courses, and that therefore an MPD of 0.5 mm is a more or less standard MPD value. When comparing Equation (7.1) to the model developed by BASt, the latter had a larger influence on the texture than the model developed in this research. No clarification for this larger influence is known.

7.2. Recommendations

This section provides recommendations for further research on the topic discussed in this thesis. A distinction is made between recommendations based on the theoretical background of the research and recommendations for the used data and performed regression analysis.

7.2.1. Theoretical background

This section contains recommendations relating to the theoretical background of the research.

Effect of increased vehicle speed

Increasing the vehicle speed changes the measured value of the skid resistance. From measurements can concluded that the skid resistance generally declines with an increasing speed. However, it is not known due to which phenomenon the skid resistance decreases (see Section 2.4.4). If better understanding of this phenomenon would be obtained, it might become possible to make better choices on for example which variables to use in the regression.

Applied temperature correction

For this research, the temperature correction as used in the TP Griff-StB (SKM) was applied to adjust the skid resistance measurements for temperature variations. However, from the literature study it became clear that the influence of temperature is an actual topic of research. Therefore, when further analyses on the speed conversion model will be performed, it is recommended to stay up to date of

the temperature correction models. If more accurate models are developed, it is advised to apply these models to the data instead of the correction used in the TP Griff-StB (SKM).

7.2.2. Data

This section contains recommendations with respect to the obtained data.

Registration of data

For the future performed measurements it is recommended to accurately register the mixture type and age of the pavement during measurements. With this information a better data analysis can be performed.

SKM measurements at low speeds

In this study, measurements performed at a measuring speed of 30 km/h or higher were used, and only few of these measurements were performed at 30 km/h. This indicates that no conclusions could be drawn about the speed dependency at very low measuring speeds (20-40 km/h) for measuring on roundabouts, where the SKM cannot measure with high measuring speeds. Therefore, it is recommended to perform research to the speed dependency at low measuring speeds. More data of measurements performed at low measuring speeds could be obtained and included in the multilevel modelling.

Measurements performed on curved sections

In the model verification, only few measurements performed on curves were used to verify the applicability of the model on curved sections. In total, 13 100 metre sections consisting of curved road sections were obtained. These datapoints showed a small standard error when applying the model, but because only a small number of datapoints is involved, it is recommended that in future research more measurements on curved sections need to be performed and analysed to verify whether curved sections will have a different speed dependency than straight sections.

MPD values

The MPD values of the measured data show two peaks in the frequency histogram, around 0.8 and 1.2 mm. There are almost no datapoints having an MPD around 1 mm, and also there are less datapoints with small MPD values around 0.6 mm. It is recommended to extend the database with measurements performed at sections with these MPD values.

Roads with DGD

Unfortunately, all measurements performed at pavements with a DGD layer were performed under wet circumstances. Therefore, no macrotexture measurements of these roads were available. It is recommended to extend the database with measurements performed on roads with DGD. In Figure 7.1 the course of measured skid resistance over speed is shown for pavements which were measured under wet circumstances, and which were therefore not included in the regression analysis. Three of these roads were DGD roads. As one can see, the N304 DGAD 2 and N338 2ZOAB show a higher decline in skid resistance at higher speeds, and the road N304 DGAD shows a very small difference in the decline between 40 an 60, and 60 and 80 km/h.

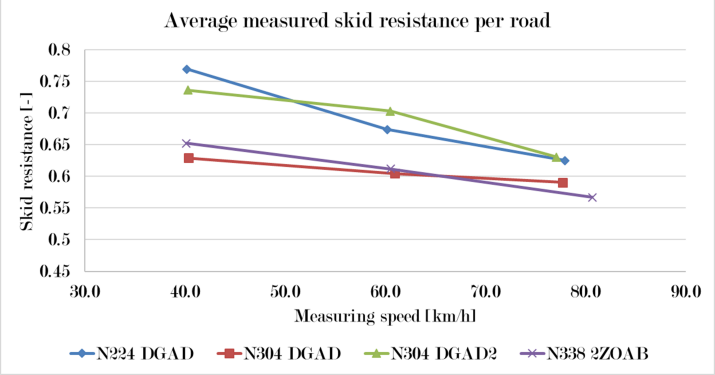

Figure 7.1: Average measured skid resistance per road from measurements which were performed under wet circumstances. These observations are therefore not included in the regression analysis.

If the database is not extended with measurements on DGD roads, the developed model should not be applied to these road types.

Age of road surfaces

For the obtained data, the year of the pavement construction was sometimes given, but this does not give certainty about possible maintenance services or whether parts of the pavements were renewed. On new pavements, different relations for the speed dependency could be applicable. Therefore, it is recommended for future research to invest more time in analysing whether the pavements are older than one year and eliminate measurements performed on renewed pavements from the dataset.

7.2.3. Regression analysis

Three methods were used for performing the regression analysis and it became clear that the multilevel modelling is the best regression method for the purpose of this research. This section gives recommendations on further research relating the regression analysis.

Averaged observations

For the first two regression methods (the multiple linear regression and the zero speed intercept method), measurements per measuring speed for the same section were averaged. However, a multilevel model can deal with repeated measurements. Due to time restrictions and difficulties to compare models obtained from different datasets, the multilevel model was also obtained based on the averaged measurements. Because it was concluded that the multilevel modelling is the best method for this research topic, in the future, datasets without averaged measurements should be used. Also, the difference in obtained models with averaged or repeated data can be analysed.

Outlier analysis

Although SPSS selected outliers and highly influential points, no observations were excluded from the analysis, because it was not known why observations were marked as outliers or highly influential points. For future research it is recommended to obtain more knowledge of the dataset to be able to perform a more useful outlier analysis. For example, photographs of the measurements could be inspected and/or the roads could be visited.

Hierarchical structure for multilevel model

For the hierarchical structure of the three-level model, the second level is defined as the separate 100 metre sections and the third level is defined as the different roads on which measurements were performed. The latter is chosen because on roads of the same type and wearing course, comparable values of the skid resistance are expected. However, it can be tried to define what 'road' means, such as: type of mixture, age or traffic intensity. For example, some roads will exists of multiple mixture types and if this would be accurately registered during measurements, a better hierarchical structure could possible be defined.

Zero speed intercept

In this research, attempts were made to estimate the zero speed intercept with help of a functional approach. This appeared to be difficult which made the method inappropriate for the purpose of this research. However, if a functional approach would be found to properly estimate the zero speed intercept, the regression method using this zero speed intercept could be improved.

Physical requirements

The developed model does not fulfil the physical requirements of skid resistance. For a small speed, the skid resistance can exceed a value of 1, something which is not possible in reality. Therefore, further research could be performed on changing the form of the model such that it fulfils the physical requirements, which is that the converted skid resistance will always be between 0 and 1.

Repeatability analysis

A short repeatability analysis in this research was performed. However, because measurements were only performed twice, this analysis could be improved by including more repeated measurements. By comparing the repeatability of SKM measurements to the RMSE of the obtained models, a better understanding of the impact of this RMSE could be obtained.

Bibliography

Al-Assi, M. and Kassem, E. (2017). Evaluation of adhesion and hysteresis friction of rubber-pavement system. *Applied Sciences*, 7(10):1029. https://doi.org/10.3390/app7101029.

Anupam, K. (2012). *Numerical simulation of vehicle hydroplaning and skid resistance on grooved pavement*. PhD thesis, National University of Singapore. http://scholarbank.nus.edu.sg/handle/10635/30696.

Anupam, K., Srirangam, S. K., Scarpas, A., and Kasbergen, C. (2013). Influence of Temperature on Tire-Pavement Friction. *Journal of Transportation Research Board*, 2369:114–124. https://doi.org/10.3141/2369-13.

Anupam, K., Srirangam, S. K., Scarpas, A., Kasbergen, C., and Kane, M. (2014). Study of Cornering Maneuvers of Pneumatic Tires on Asphalt Pavement Surfaces Using Finite Element Method. *Transportation Research Record*, 2457:129–139. https://doi.org/10.3141/2457-14.

Arbeitsgruppe Infrastrukturmanagement (2007). TP Griff-StB (SKM). *FGSV Verlag*. Technische Prüfvorschriften für Griffigkeitsmessungen im Straßenbau.

Army and Air Force (1988). Standard Practice for Pavement Recycling. Technical Report 5-822-10, Air Force Manual AFM 88-6, Chapter 6, Departments of the Army and Air Force, Washington, D.C.

ASTM E1960-98 (2015). *Standard Practice for Calculating International Friction Index of a Pavement Surface*. ASTM International, West Conshohocken, PA.

Bazlamit, S. M. and Farhad Reza, P. E. (2005). Changes in Asphalt Pavement Friction Components and Adjustment of Skid Number for Temperature. *Journal of Transportation Engineering*, 131:470–476. https://doi.org/10.1061/(ASCE)0733-947X(2005)131:6(470).

Bürckert, M., Gauterin, F., and Unrau, H. (2012). Untersucuch des Einflusses der Grobtextur auf Messergebnisse mit dem SKM-Messverfahren. Technical Report S78, Die Bundesanstalt für Straßenwesen (BASt).

Chu, L. J. and Fwa, T. F. (2017). A functional approach for determining skid resistance threshold state of porous pavement. *International Journal of Pavement engineering*, 20(4):481–489. https://doi.org/10.1080/10298436.2017.1309195.

Day, A. (2014). *Braking of road vehicles*. Elsevier Inc., Oxford.

de Vocht, A. (2009). *Basishandboek SPSS 17*. Bijleveld Press, Utrecht.

Derksen, G. B. (2017). Statistical analyses skid resistance swf versus raw. Technical Report R10041, TNO.

Descornet, G., Schmidt, B., Boulet, M., Gothié, M., Do, M., Fafié, J., Alonso, M., Roe, P., Forest, R., and Viner, H. (2006). Harmonization of European Routine and research Measuring Equipment for Skid Resistance. Technical Report 2006/01, FEHRL.

Fenghua, J. (2013). *Modelling skid resistance of rolling tires on textured pavement surfaces*. PhD thesis, National University of Singapore. Retrieved from: http://scholarbank.nus.edu.sg/handle/10635/48327.

Field, A. (2005). *Discovering Statistics using SPSS*. SAGE publications, London, second edition.

Field, A. (2009). *Discovering Statistics using IBM SPSS*. SAGE publications, London, third edition.

Field, A. (2013). *Discovering Statistics using IBM SPSS*. SAGE publications, London, fourth edition.

Flintsch, G., McGhee, K., de León Izeppi, E., and Najafi, S. (2012). *The Little Book of Tire Pavement Friction*. Pavement Surface Properties Consortium.

Fuentes, L. G. (2009). *Investigation of the Factors Influencing Skid Resistance and the International Friction Index*. PhD thesis, University of South Florida, department of Civil and Environmental Engineering. Retrieved from: http://scholarcommons.usf.edu/etd/3920.

Fwa, T. (2017). Skid resistance determination for pavement management and wet-weather road safety. *International Journal of Transportation Science and Technology*, 6(3):217–227. http://dx.doi.org/10.1016/j.ijtst.2017.08.001.

Gandhi, R. (2018). Improving the Performance of a Neural Network. https://towardsdatascience.com/how-to-increase-the-accuracy-of-a-neural-network-9f5d1c6f407d, accessed on: 08-11-2018.

Groenendijk, J. (2011). Verkenning deklaag- en snelheid-onafhankelijk meten en verwerken van stroefheid op het hoofdwegennet. Technical Report e110360601, Koac•NPC.

Groenendijk, J. (2015). Influence on traffic safety of water film thickness on pavements - a literature survey. Technical Report e150332001, Koac•NPC.

Groenendijk, J. (2018). Influence of temperature and season on wet skid resistance of pavements. Technical Report e180117101, Kiwa KOAC.

Hair Jr., J. F., Black, W. C., Babin, B. J., and Anderson, R. E. (2014). *Multivariate Data Analysis*. Pearson New International Edition, seventh edition.

Hall, J. W., Smith, K., Titus-Glover, L., Wambold, J. C., Yager, T. J., and Rado, Z. (2009). *Guide for Pavement Friction*. The National Academies Press, Washington, DC. https://www.nap.edu/catalog/23038/guide-for-pavement-friction.

Harrison, X. A., Donaldson, L., Correa-Cano, M. E., Evans, J., Fisher, D., Goodwin, C. E. D., RObinson, B. S., Hodgson, D. J., and Inger, R. (2018). A brief introduction to mixed effects modelling and multi-model inference in ecology. *PeerJ*, 6(e4794). https://peerj.com/articles/4794/, accessed on: 26-02-2019.

Henry, J., Wambold, J., Antle, C. E., and Rado, Z. (1995). International Experiment to Compare and Harmonize Skid Resistance and Texture Measurements. Technical Report 01.04.TEN, PIARC.

Henry, J. J. (2000). Evaluation of Pavement Friction Characteristics - A Synthesis of Highway Practice. Technical Report NCHRP synthesis 291, National Cooperative Highway Research Program, Washington, D.C.

Highways England (2015). *Design manual for roads and bridges*. The Stationery Offic, part of Williams Lea. HD28/15, volume 7, section 3, part 1.

Hosking, J. and Woodford, G. (1976a). Measurement of skidding resistance, part II: Factors affecting the slipperiness of a road surface. Technical Report 738, Transport and Road Research Laboratory, Crowthorne, Berkshire.

Hosking, J. and Woodford, G. (1976b). Measurement of skidding resistance, part III: Factors affecting SCRIM measurements. Technical Report 739, Transport and Road Research Laboratory, Crowthorne, Berkshire.

IBM (2016). Final Hessian matrix not positive definite or failure to converge warning. https://www-01.ibm.com/support/docview.wss?uid=swg21480810, accessed on: 26-02-2019.

IBM (2018). Collinearity diagnostics. https://www.ibm.com/support/knowledgecenter/en/SSLVMB_23.0.0/spss/tutorials/reg_cars_collin_01.html. Accessed on: 19-01-2019.

Kahane, L. H. (2001). *Regression Basics*. Sage Publications, Thousand Oaks, California.

Karadimitriou, S. M. and Marshall, E. (2018). Outliers, Durbin-Watson and interactions for regression in SPSS. *Statstµtor*. https://www.sheffield.ac.uk/polopoly_fs/1.531431!/file/MASHRegression_Further_SPSS.pdf, accessed on: 08-11-2018.

Kiwa KOAC (2015). Stroefheid raw 86% vertraagd wiel.

Kiwa KOAC (2016). Technisch infoblad stroefheidsmetingen swf-methode.

Kogbara, R. B., Masad, E., Kassem, E., Scarpas, A., and Anupam, K. (2016). A state-of-the-art review of parameters influencing measurement and modeling of skid resistance of asphalt pavements. *Construction and Building Materials*, 114:602–617. https://doi.org/10.1016/j.conbuildmat.2016.04.002.

Laerd statistics (2018). Multiple Regression Analysis using SPSS Statistics. https://statistics.laerd.com/spss-tutorials/multiple-regression-using-spss-statistics.php. Accessed on: 26-10-2018.

Leandri, P. and Losa, M. (2015). Peak friction prediction model based on surface texture characteristics. *Transportation Research Board*, 2525(1):91–99. https://doi.org/10.3141/2525-10.

Leu, M. and Henry, J. (1978). Prediction of skid resistance as a function of speed from pavement texture measurements. *Transportation Research Board*, 666:7–13.

Lubis, A. S., Muis, Z. A., and Gultom, E. M. (2018). The effect of contaminant on skid resistance of pavement surface. *IOP Conference Series: Earth and Environmental Science*, 126:012040. https://doi.org/10.1088/1755-1315/126/1/012040.

Mataei, B., Zakeri, H., Zahedi, M., and Nejad, F. (2016). Pavement Friction and Skid Resistance Measurement Methods: A Literature Review. *Open Journal of Civil Engineering*, 6(4):537–565. http://dx.doi.org/10.4236/ojce.2016.64046.

McDonald, J. H. (2014). *Handbook of Biological Statistics*. Sparky House Publishing, Baltimore, Maryland, third edition. http://www.biostathandbook.com/independence.html, Accessed on: 19-01-2019.

McGhee, K. and Flintsch, G. W. (2003). High-speed texture measurement of pavements. Technical Report VTRC 03-R9, Virginia Center for Transportation Innovation and Research, Charlottesville.

Michelin (2001). *Grip on road surfaces*. Société de Technologie Michelin, Clermont-Ferrand. Retrieved from: http://www.dimnp.unipi.it/guiggiani-m/Michelin_Tire_Grip.pdf.

Minitab (2017). Test for autocorrelation by using the Durbin-Watson statistic. https://support.minitab.com/en-us/minitab/18/help-and-how-to/modeling-statistics/regression/supporting-topics/model-assumptions/test-for-autocorrelation-by-using-the-durbin-watson-statistic/. Accessed on: 02-11-2018.

Molin, E. (2018a). Lecture slides tb234b - lecture 1: Regressieanalyse & toetsen.

Molin, E. (2018b). Lecture slides tb234b - lecture 2: Multiple regressie I - intro.

NEDARC (2016). Statistical Terms Dictionary. http://www.nedarc.org/statisticalHelp/statisticalTermsDictionary.html. Accessed on: 30-10-2018.

NEN (2004). *ISO 13473-2:2002 Characterization of pavement texture by use of surface profiles — Part 2: Terminology and basic requirements related to pavement texture profile analysis*. Nederlands Normalisatie Instituut. Delft.

O'Flaherty, C. A. (2002). *Highways - The Location, Design, Construction & Maintenance of Pavements*. Butterworth-Heinemann, fourth edition.

Optimizely (2018). Optimization Glossary. https://www.optimizely.com/optimization-glossary/statistical-significance/. Accessed on: 30-10-2018.

Pennsylvania State University (2018). 4.6 - Normal Probability Plot of Residuals. https://onlinecourses.science.psu.edu/stat501/node/281/, accessed on: 08-11-2018.

Pythagoras & That (2014). Scatter Graphs. http://www.pythagorasandthat.co.uk/scatter-graphs. Accessed on: 26-10-2018.

ReStore (2011a). 3.14 Model Diagnostics and Checking your Assumptions. http://www.restore.ac.uk/srme/www/fac/soc/wie/research-new/srme/modules/mod3/14/index.html. Accessed on: 02-11-2018.

ReStore (2011b). Using Statistical Regression Methods in Education Research - Glossary. http://www.restore.ac.uk/srme/www/fac/soc/wie/research-new/srme/index.html. Accessed on: 02-11-2018.

Rijkswaterstaat (2017). Stroefheidsmetingen. https://www.rijkswaterstaat.nl/zakelijk/werken-aan-infrastructuur/bouwrichtlijnen-infrastructuur/autosnelwegen/stroefheidsmetingen.aspx. Accessed on: 06-09-2018.

Roe, P. G., Parry, A. R., and Vinier, H. E. (1998). High and low speed skidding resistance: the influence of texture depth. Technical Report 367, Transport Research Laboratory, Crowthorne, Berkshire.

Sahhaf, S. A. and Rahimi, S. (2014). Investigation of laser systems used in pavement management systems (pms). Technical report, ALLEN institute for Artificial Intelligence.

Scharnigg, K., Stöckert, U., Pinkofsky, L., Bennis, T., van Ooijen, W., Vos, E., and Nugteren, H. (2016). Cooperation in the field of skid resistance between Germany and the Netherlands. *Eurasphalt & Eurobitume*. dx.doi.org/10.14311/EE.2016.143.

Srirangam, S. K. (2015). *Numerical simulation of tire-pavement interaction*. PhD thesis, Delft University of Technology. https://doi.org/10.4233/uuid:ccf73339-112f-4fff-b846-a828a6120a3d.

Stat Trek (2018). Transformations of Variables. https://stattrek.com/regression/linear-transformation.aspx. Accessed on: 01-11-2018.

Statistics How To (2016). RMSE: Root Mean Square Error. https://www.statisticshowto.datasciencecentral.com/rmse/, accessed on: 08-02-2019.

Statistics Solutions (2018a). Homoscedasticity. https://www.statisticssolutions.com/homoscedasticity/. Accessed on: 19-01-2019.

Statistics Solutions (2018b). Multicollinearity. https://www.statisticssolutions.com/multicollinearity/. Accessed on: 19-01-2019.

Statistics Solutions (2018c). Testing Assumptions of Linear Regression in SPSS. https://www.statisticssolutions.com/testing-assumptions-of-linear-regression-in-spss/. Accessed on: 02-11-2018.

Statistiek, S. P. (2018). SPSS Kolmogorov-Smirnov Test for Normality. https://www.spss-tutorials.com/spss-kolmogorov-smirnov-test-for-normality/#kolmogorov-smirnov-normality-test-what-is-it. Accessed on: 19-01-2019.

StatTrek (2018). Statistics dictionary. https://stattrek.com/statistics/dictionary.aspx?definition=coefficient_of_determination. Accessed on: 18-10-2018.

Steele, F. (2008). Module 5: Introduction to Multilevel Modelling Concepts. Technical report, Centre for Multilevel Modelling, University of Bristol.

Tang, T., Anupam, K., Kasbergen, C., and Scarpas, A. (2017). Study of Influence of Operating Parameters on Braking Distance. *Transportation Research Record*, 2641:139–148. https://doi.org/10.3141/2641-16.

Texas Education Agency (2018). 12.4 Testing the Significance of the Correlation Coefficient. https://www.texasgateway.org/resource/124-testing-significance-correlation-coefficient-optional. Accessed on: 30-10-2018.

UCLA (2018). What is the difference between categorical, ordinal and interval variables? https://stats.idre.ucla.edu/other/mult-pkg/whatstat/what-is-the-difference-between-categorical-ordinal-and-interval-variables/. UCLA: Statistical Consulting Group. Accessed on: 30-10-2018.

van Es, G. W. H., van Leest, A. J., Fafié, J., van der Vegte, R., van Dijk, H., and van Gurp, C. A. P. M. (2004). Correlation of self-wetting friction-measuring devices. In *FAA Worldwide Airport Technology Transfer Conference*.

van Gurp, C. (2005). Harmonisation of test results of runway surface friction assessment surveys. In *1st International European Airport Pavement Workshop. CROW, Schiphol*.

Vos, E. (2008). *Normstelling natte stroefheid van rijkswegen : herijking stroefheidniveau en uitbreiding met een meetsnelheid van 70 km/u*. RWS/DVS. Version 1.2.

Vos, E., Bennis, T., Bouman, F., Kuijper, P., Voskuilen, J., and Groenendijk, J. (2017). *Skid resistance on national roads*. Rijkswaterstaat.

Vos, E. and Groenendijk, J. (2009). Report on analysis and findings of previous skid resistance harmonisation research projects. Technical Report FP7-217920, FEHRL Tyrosafe.

Vroomans, E. (2016). Eerste ervaringen SWF. Power-point presentation.

Wennink, P. (2000). Toetsen van het huidige snelheidsafhankelijke stroefheidsmodel aan de hand van metingen op de proefvakken te Sperenberg. Technical Report e99121, KOAC •WMD.

Wilson, D. J. (2006). *An Analysis of the Seasonal and Short-Term Variation of Road Pavement Skid Resistance*. PhD thesis, The University of Auckland, Department of Civil and Environmental Engineering. http://hdl.handle.net/2292/1432.

A

Original speed conversion models

This appendix gives an overview of the original speed conversion models discussed in Chapter 4. In Chapter 4 multiple symbols have been changed in order to make it more uniform. This appendix gives the formulas with the symbols used in the sources. No explanation of the symbols is given because the meaning is the same as in the formulas of Chapter 4, nor they are included in the nomenclature of this research.

A.1. SCRIM conversion (1976)

In the direction of trafficking:

$$SFC = 0.015 \cdot PSV + 0.028 \cdot TD - 0.0027 \cdot K - 0.286 \tag{A.1a}$$

In the opposite direction of trafficking:

$$SFC = 0.014 \cdot PSV + 0.026 \cdot TD - 0.0025 \cdot K - 0.200 \tag{A.1b}$$

A.2. Penn State Model (1978)

$$\mathrm{SN} = \mathrm{SN}_0 \cdot e^{-\frac{\mathrm{PSNG}}{100} \cdot V} \tag{A.2}$$

A.3. Rado Model

$$\mu(S) = \mu_{peak} \cdot e^{-\left[\frac{ln(S/S_{peak})}{C}\right]} \tag{A.3}$$

A.4. PIARC Model (1992)

$$\mathrm{FR60} = \mathrm{FRS} \cdot e^{\frac{S-60}{S_p}} \tag{A.4}$$

A.5. KOAC•WMD (1999)

$$f_v = f_x \cdot e^{((p+q \cdot ln(MPD)+r) \cdot (v-x))} \tag{A.5}$$

A.6. ESDU (2003)

For the ESDU model the original formula is given.

A.7. FEHRL Hermes project (2006)

$$\mathrm{EFI} = B \cdot F_{30} \tag{A.6a}$$

$$F_{30} = F \cdot e^{\frac{S-30}{S_0}} \tag{A.6b}$$

$$S_0 = a \cdot \mathrm{MPD}^b \tag{A.6c}$$

A.8. E. Vos (2008)

$$\text{For open asphalt: } STR70 = \frac{42}{45} \cdot STR50 \ (= 0.993 \cdot STR50) \tag{A.7a}$$

$$\text{For dense asphalt: } STR70 = \frac{39}{44} \cdot STR50 \ (= 0.886 \cdot STR50) \tag{A.7b}$$

A.9. Koac•NPC (2009)

$$\mu_{50} = \mu \cdot e^{(V-A)\cdot(B-C\cdot MPD)} \tag{A.8}$$

$$\mu_{50} = \mu \cdot e^{B\cdot(V-A)} \tag{A.9}$$

A.10. SCRIM Model

$$\mathrm{SR}(50) = \mathrm{SR}_s \cdot \frac{-0.0152 \cdot s^2 + 4.77 \cdot s + 799}{1000} \tag{A.10}$$

A.11. TP-Griff-StB (2007)

$$m_v = m + \frac{V_{\text{ist}} - V_{\text{soll}}}{20} \cdot 0.05 \tag{A.11}$$

A.12. BASt (2012)

$$m_v = m + \frac{V_{ist} - V_{sol}}{20} \cdot (0.120 - 0.062) \frac{1}{mm} \cdot MPD \tag{A.12}$$

B

Introduction to regression analyses using SPSS

In order to obtain a conversion model for the skid resistance at different speeds, a regression analysis in SPSS will be executed. This appendix firstly explains some statistical theory related to regression analyses in Section B.1. After that, the concept of multiple linear regressions is explained (Section B.2). Section B.3 explains what multilevel models are.

B.1. Statistical theory related to regression analyses

This section describes some of the statistical theory related to regression analyses. Several aspects are explained, but the details of calculations are omitted. SPSS performs calculations and plots graphs and therefore it is not needed to perform calculations by hand, but understanding of how to interpret the output of SPSS is important.

B.1.1. Pearson's correlation coefficient r

The Pearson's correlation coefficient r gives information about the linear relationship between two variables. It is a number in between -1 and 1. If the correlation coefficient is -1, this means there is a perfect negative linear relationship. All the data points can be exactly plotted on one straight, declining, line. If the correlation coefficient is $+1$, this means there is a perfect positive linear relationship. All data points can now exactly be plotted on one straight increasing line. If the correlation coefficient is 0, this means there is no linear relationship between the two variables. The higher $|r|$ the stronger the relationship (de Vocht, 2009).

B.1.2. Coefficient of determination R^2

The coefficient of determination measures the proportion of the variance and is defined as the square of the correlation coefficient r. Often, for a regression with one variable the coefficient of determination is denoted as r^2, whereas for a linear regression with multiple predictive variables the coefficient of determination is denoted as R^2. The coefficient of determination tells you what percentage of the behaviour of the predicted variable y is explained by the predictive variable x (Kahane, 2001), or, in case of a multiple regression analysis, by the predictive variables $x_1, ..., x_n$. For a strong relationship must account: $|R| \geq 0.8$ and thus $R^2 \geq 0.64$ (de Vocht, 2009).

B.1.3. Adjusted coefficient of determination

The adjusted R^2 is a modified measure of the coefficient of determination that takes into account the number of independent, predictive variables included in the regression analysis. Adding more predictive variables will always cause the coefficient of determination to rise whilst the adjusted coefficient of determination may also fall if the added variables have little extra explanatory power. Therefore, this statistic is useful when comparing models with different predictive variables (Hair Jr. et al., 2014).

B.1.4. Statistical significance

Statistical significance is the likelihood that the difference in conversion rates between a given variation and the regression line is not due to random chance. Thus, the result of an experiment is said to have statistical significance if it is not likely caused by chance for a given statistical significant level (Optimizely, 2018). Not only the correlation coefficient r, but also the sample size n determines if a regression is statistically significant (Texas Education Agency, 2018).

Often 95% is chosen as a significance level, which means that you can be 95% sure that the results are real and not an error caused by randomness. If the result is not statistical significant, the result is only valid for the sample data and cannot be generalised. To determine whether we accept a certain regression coefficient or not, first we define the null-hypothesis: there is no significant relation between two variables.

The three requirements to test if a regression coefficient is statistically significant are (Molin, 2018b):

- an (absolute) t-value > 1.96,
- a p-value $< \alpha$, and
- the 95% confidence interval does not contain the value 0.

We only reject the null-hypothesis if the 3 requirements are met, hence there *is* a significant relation between two variables. If a regression coefficient is not statistically significant, one should not reject the null-hypothesis, and therefore not use the calculated regression coefficient and set the value of the coefficient to 0.

t-value

The t-value tells you how many times larger the regression coefficient is compared to the standard deviation of the regression coefficient. In general, we say that for samples larger than 120, if $|t| > 1.96$, the coefficient is statistical significant (Molin, 2018a). If the sample size is smaller than 120, one should use a t-table to determine the limiting values.

p-value

The p-value is used in hypothesis testing to verify whether a hypothesis must be rejected or not (Kahane, 2001). If we test if there is a regression coefficient for a certain variable in a regression, and the p-value of this regression coefficient is smaller than a chosen level of significance (often 5%), then we must reject the null hypothesis of not having a regression coefficient and accept the regression coefficient. If the p-value is larger than the chosen level of significance, we accept the null hypothesis.

95% confidence interval

All values within the 95% confidence interval are possible regression coefficients for which the difference with the estimated regression coefficient is not statistically significant. SPSS gives for calculated coefficients, such as a in $y = a \cdot +b$, a 95% confidence interval. If a is 3 and the lower and upper boundaries of the 95% confidence intervals are 2.75 and 3.25, this means that in 95% of the samples (or data points) a value of a between 2.75 and 3.25 will give the right predicted parameter. All values between 2.75 and 3.25 are possible regression coefficients for which the difference with the regression coefficient is not statistically significant (Molin, 2018b).

If 0 is a number within the 95% confidence interval, the regression coefficient does not significantly differ from 0, hence we do not use the regression coefficient.

B.1.5. RMSE

The root mean square error (RMSE) indicates the absolute fit of the model to the data. The smaller the RMSE, the closer the observed data points are to the predicted values of the model. The RMSE is defined as the square root of the variance of the residuals and the unit matches the unit of the predicted variable.

The RMSE is calculated as follows (Statistics How To, 2016):

$$RMSE = \sqrt{\frac{\sum_1^n (\mu_{pred,i} - \mu_{measured,i})^2}{n}} \tag{B.1}$$

When comparing several regressions, the values of the RMSE can be compared as long as the predicted variable is in the same unit.

B.2. Multiple linear regression

A multiple linear regression model demands a linear correlation between all predictive variables and the variable which must be predicted. An example of a linear function is:

$$f(x_1, x_2, \dots, x_n) = A_0 + A_1 \cdot x_1 + A_2 \cdot x_2 + \dots + A_n \cdot x_n \tag{B.2}$$

All predictive variables $(x_1, \dots, x_n)$ have a linear relationship with the predicted variable through $A_1, \dots, A_n$ and A_0 is the intercept.

When there is only one predictive variable x_1 it is called a linear regression analysis, whereas having multiple predictive variables, it is called a multiple linear regression analysis. Thus, if only the speed difference would be considered as an influencing parameter, a linear regression analysis should be performed. If besides the speed difference, also the MPD as a predictive parameter is considered, a multiple regression analysis should be performed. The goal of this research is to develop a conversion model with speed and texture as input parameters, thus the section about linear regressions will focus on multiple linear regressions.

B.2.1. Assumptions

There are several assumptions which must be met for performing a multiple linear regression. These are (Laerd statistics, 2018):

- There must be a **linear relationship** between the dependent and independent variables.
- The dependent variable should be measured at a **continuous level**. This means, the variable can take any value. Height is an example of a continuous variable whilst gender, which can only be male or female, is not. In this research, the reference skid resistance is an example of a continuous variable.
- The independent, predictive, variables should be measured at **continuous or categorical level**. A categorical variable (or nominal variable) has several categories which do not have an order (UCLA, 2018). Gender or hair colours are examples of categorical variables. Hair colour can be brown, blond, black, etc. But one colour is not better than the other, and thus it does not have an order. In this research, positive or negative macrotexture is a categorical variable, whilst measuring speed and measured skid resistance are continuous variables.
- The data must not show **multicollinearity**. This occurs when two or more predictive variables are highly correlated with each other. Multicollinearity can be a problem because if two variables are highly correlated they might be predictors for the same phenomena.
- There should be **no significant outliers** or **highly influential points**. These can disturb the regression. If outliers or highly influential points are present, these must be omitted from the data.
- You should have **independence of observations**. This means that the occurrence of one observation, does not provide information about the occurrence of the subsequent observation (NEDARC, 2016). Often, when time is one of the measurement variables, there is no independence of observations (McDonald, 2014). If the occurrence of one observation does provide information of the occurrence of another observation, we say that the autocorrelation is present. An example of autocorrelation is that the pavement temperature on day 1 influences the pavement temperature on day 2.
- The data needs to show **homoscedasticity**. This implies that the error term of the predicted dependent variable is the same across all values of the independent variables (Statistics Solutions, 2018a).

Furthermore, after a regression has been performed, one must check whether the residuals (errors) of the regression line are approximately **normally distributed**. This is needed in order to determine the statistical significance explained in Section B.1.4.

Thus, before starting performing a linear regression analysis, one must check whether the data set fulfils the assumptions above. The next section will explain how these assumptions can be examined.

B.2.2. Examine assumptions

This paragraph explains how to examine the assumptions which must be fulfilled by the data set before performing a linear regression analysis.

Linear relationship

Analysing whether a predictive parameter has a linear relationship with the predicted parameter can easily be done with help of a scatterplot. A scatterplot visualises the relationship between two variables by plotting the values obtained for two different variables. One variable is plotted on the y-axis and one on the x-axis. The scatterplots of Figure B.1 show how a scatterplot could indicate a linear relationship.

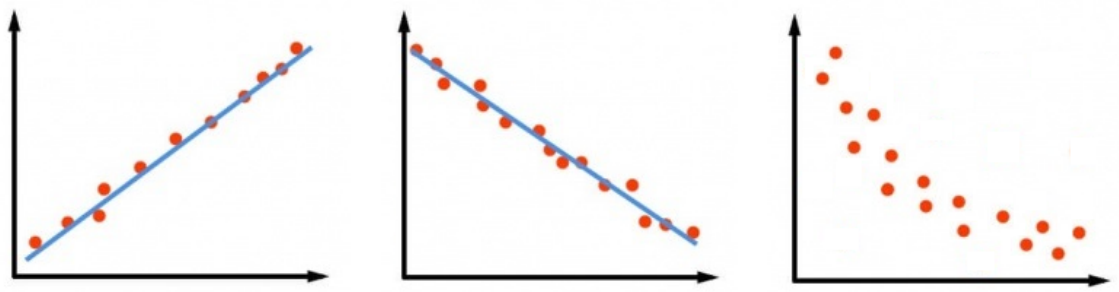

(a) Positive correlation (b) Negative correlation (c) Nonlinear correlation

Figure B.1: Scatterplots showing linearity of data, (adapted from Pythagoras & That, 2014)

When a straight line can be drawn through the data, a linear relationship exists. This can be positive or negative correlated. For a positive correlation (Figure B.1a), a formula for this data will be in the form of $y = ax + b$, with a a positive number. For a negative correlation (Figure B.1b), the formula for this data will be in the form of $y = -ax + b$, thus, the constant value before x is now negative. If no straight line can be drawn through the data set, there is no linear relationship, as for example shown by Figure B.1c.

Besides the scatterplot, the Pearson's correlation coefficient r gives information about the linearity between two variables. In a scatterplot, a higher $|r|$ means that the data points lie closer to the regression line, whereas a smaller $|r|$ corresponds to data points that deviate more from the regression line. Thus, if we would compare the correlation coefficients from Figures B.2a and B.2c with the correlation coefficients from Figures B.2b and B.2d, the first ones would be closer to 1 than the second ones.

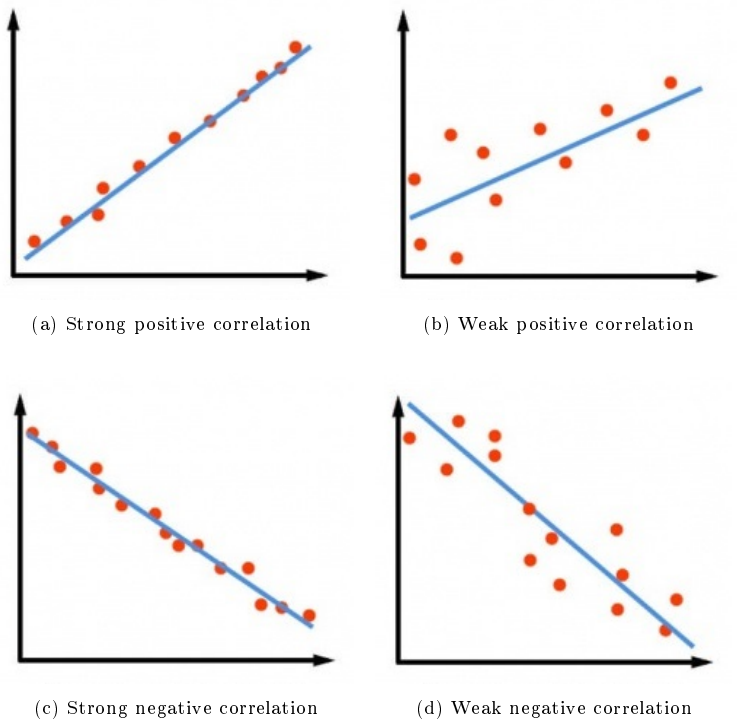

(a) Strong positive correlation (b) Weak positive correlation

(c) Strong negative correlation (d) Weak negative correlation

Figure B.2: Different scatterplots showing a strong or weak correlation (adapted from Pythagoras & That, 2014)

For a linear relationship the correlation between two variables is significant. If the correlation coefficient between two variables is not significant, there is no linear relationship (Texas Education Agency, 2018). Often a significance level of 5% is chosen, which means that for a p-value smaller than 0.05 the correlation coefficient is significant (Texas Education Agency, 2018)

If a scatterplot or the correlation coefficient does not show a linear relationship, one can apply a transformation to the variables to make their relation linear. Table B.1 gives some examples of transformations (Stat Trek, 2018).

Table B.1: Examples of transformations

Method	**Transform**	**Regression equation**	**Predicted value ($\hat{y}$)**
Standard linear regression	None	$y = b_0 + b_1 \cdot x$	$\hat{y} = b_0 + b_1 \cdot x$
Exponential model	$log(y)$	$log(y) = b_0 + b_1 \cdot x$	$\hat{y} = 10^{b_0 + b_1 \cdot x}$
	$ln(y)$	$ln(y) = b_0 + b_1 \cdot x$	$\hat{y} = e^{b_0 + b_1 \cdot x}$
Quadratic model	$\sqrt{y}$	$\sqrt{y} = b_0 + b_1 \cdot x$	$\hat{y} = (b_0 + b_1 \cdot x)^2$
Reciprocal model	$1/y$	$\frac{1}{y} = b_0 + b_1 \cdot x$	$\hat{y} = \frac{1}{b_0 + b_1 \cdot x}$
Logarithmic model	$log(x)$	$y = b_0 + b_1 \cdot log(x)$	$\hat{y} = b_0 + b_1 \cdot log(x)$
Power model	$log(y)$	$log(y) = b_0 + b_1 \cdot log(x)$	$\hat{y} = 10^{b_0 + b_1 \cdot log(x)}$

If also with transforming variables no linear relationship can be obtained, a nonlinear regression must be performed.

Multicollinearity

A correlation coefficient between two predictive variables higher than 0.8 might indicate multicollinearity(ReStore, 2011a). Multicollinearity can be identified analysing Variance Inflation Factor (VIF) (Laerd statistics, 2018) and the collinearity diagnostics table (IBM, 2018). In the output of a linear regression, values for the VIF are given. These are an indicator of the effect that the other independent variables have on the standard error of a regression coefficient (Hair Jr. et al., 2014). Often, a VIF of 10 is used

as the cut-off limit. For a VIF above 10,there is cause for concern (Myers (1990) and Bowerman & O'Connell (1990), as cited in Field (2005)). Also, the eigenvalues of the collinearity diagnostics table can be analysed. Eigenvalues close to zero indicate multicollinearity and thus small changes in the data values may lead to large changes in the estimates of the coefficients (IBM, 2018).

If multicollinearity is present, the confidence intervals of the regression coefficients can become very wide and the standard errors are likely to be high. It becomes difficult to reject the null hypothesis and accept the regression coefficients (Statistics Solutions, 2018b).

When multicollinearity is present, for example between two predictive variables x_1 and x_2, one could either remove one of the two variables —if very high correlated— or define a new variable that is composed of the two correlated variables, namely $x_3 = x_1 \cdot x_2$ (ReStore, 2011b). When including this variable in the regression analysis performed with the Stepwise method, SPSS includes the new variable and makes it possible to verify with the partial F value if the added variable has a significant contribution.

Outliers and highly influential points

Outliers can, among others, be identified with help of a scatterplot. Figure B.3 gives an example of a scatterplot where an outlier can be identified very clearly.

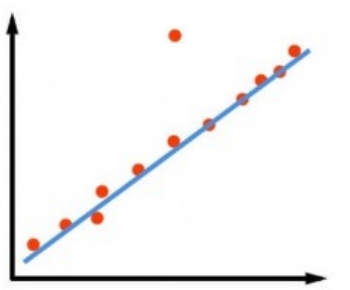

Figure B.3: Scatterplot showing a outlier

Besides using a scatter plot, SPSS has a function called *Casewise Diagnostics*. When collecting casewise diagnostics, SPSS tells you which cases have residuals that are three (or a chosen multiplication) or more standard deviations away from the mean residual(ReStore, 2011a). These cases have the largest errors and thus could be outliers. After analysing these points, one could decide to exclude these points from the analysis and perform the regression analysis one more time without these points.

Also, the Cook's distance and the Centered Leverage Value of data points can be calculated during a regression. The Cook's distance gives information of data points which have a very large influence on the regression parameters. Cases where the Cook's distance is larger than 1 may cause a disturbed regression (ReStore, 2011a). Karadimitriou and Marshall (2018) propose comparing the Cook's distance for each observation with 4/n where n is the number of observations used in the regression. Observations with a Cook's distance higher than 4/n might be a problem. Furthermore, cases with a high leverage might pull the regression line towards it (Karadimitriou and Marshall, 2018). Leverage values of $\frac{3 \cdot (k+1)}{n}$, where k are the number of predictive variables, indicate high leverage for an observation.

Independence of observations

In this research no time element is present, but still the observations might be dependent. Because multiple measurements on one 100 metre section are performed, these measurements are not fully independent.

Independence of observations can be tested with the Durbin Watson statistic. The Durbin Watson statistics measures whether there is autocorrelation or not. If this is the case, a regression can underestimate the standard error of the coefficients. The predictive variable can now seem significant whilst it is not (Minitab, 2017). The Durbin Watson statistic is a number between 0 and 4 and Karadimitriou and Marshall (2018) state that for a value between 1.5 and 2.5 the variables are not autocorrelated.

Homoscedasticity

When performing a linear regression with one predictive variable, homoscedasticity can sometimes be discovered with a scatterplot. As Figure B.4 shows, the variance of the data changes along the horizontal axis. For larger values on the horizontal axis, the values on the vertical axis vary much more than for smaller values on the horizontal axis.

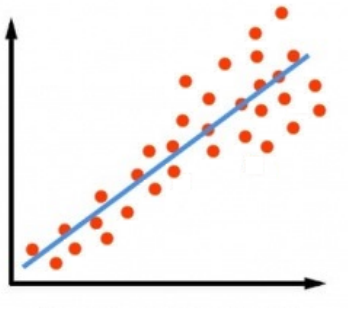

Figure B.4: Scatterplot showing no homoscedasticity

However, the scatterplot with the data points is not always clear enough to see whether the data set shows homoscedasticity or not. Also, when having multiple predictive variables, one cannot plot one scatterplot to see the variance of the data. With help of SPSS it is also possible to check for homoscedasticity in another way, namely by plotting a scatterplot which plots the standardised predicted values (ZPRED) on the x-axis and the standardised residuals on the y-axis (ZRESID) (ReStore, 2011a), as is shown in Figure B.5.

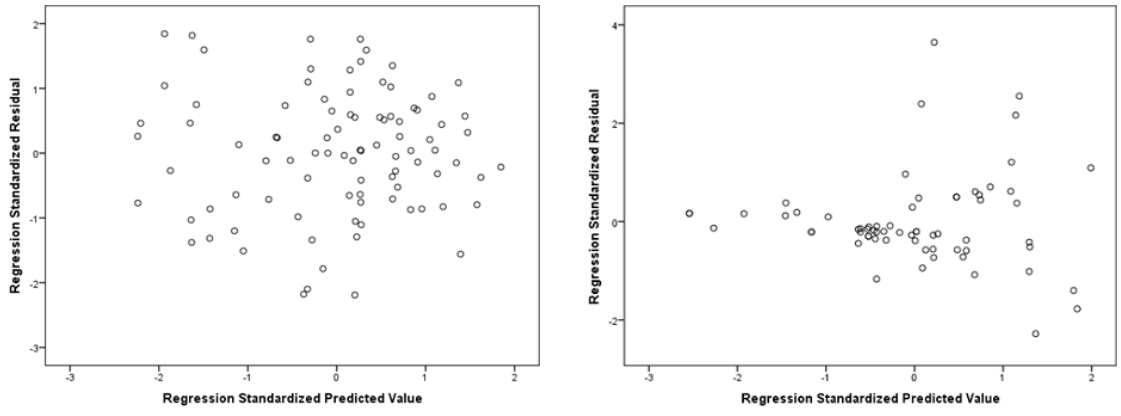

(a) Scatterplot of residuals showing homoscedasticity (b) Scatterplot of residuals not showing homoscedasticity

Figure B.5: Scatterplots of residuals (Statistics Solutions, 2018c)

In Figure B.5a the residuals are equally distributed above and below the x-axis, which implies homoscedasticity of the data. In Figure B.5b this is not the situation, and thus this data does not show homoscedasticity (Statistics Solutions, 2018c).

Normally distributed residuals

A histogram of the residuals can be plotted to see whether the residuals are normally distributed, see Figure B.6a. This histogram is not always very clear and therefore a P-P plot should be checked, see Figure B.6b. If this graph shows a straight line, the residuals are normally distributed (ReStore, 2011b).

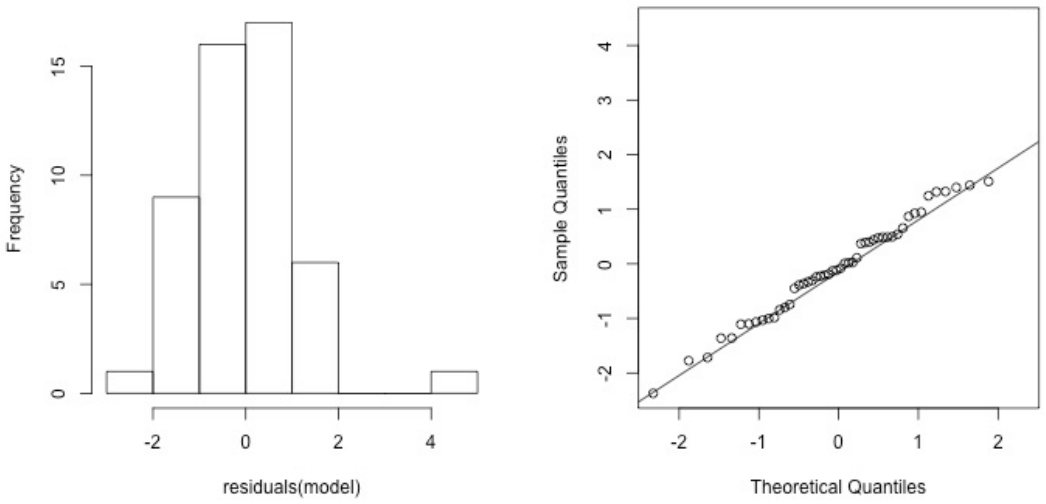

(a) Example of a histogram of residuals (b) Example of a p-plot

Figure B.6: Examples of histogram and p-plot to check whether the residuals are normally distributed (Pennsylvania State University, 2018)

Also, the Kolmogorov-Smirnov value can be calculated to verify whether there is a normal distribution. If the p-value for the Kolmogorov-Smirnov normality test is larger than 0.05, a normal distribution for the tested variable can be assumed (Statistiek, 2018).

B.2.3. Choosing the right variables

When performing a multiple regression analysis, one can use as many predictive variables as wanted. However, adding more variables does not always improve the model. When using too many variables the danger of over-fitting exists: the regression is fitted too exactly to a particular set of data and cannot be generalised.

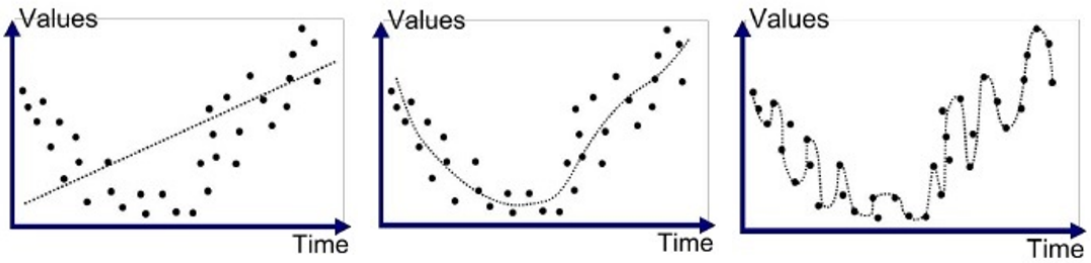

(a) Underfitted (b) Good fit (c) Overfitted

Figure B.7: Illustrations of model fittings (Gandhi, 2018)

To prevent over-fitting, one must analyse which variables to use. Performing a regression according to the Stepwise method can help to search for the best combination of predictive variables.

Stepwise

Stepwise is a regression method that searches for the best combination of coefficients. The process starts with a regression with one variable, the variable with the highest correlation coefficient. The second variable that is added, is the variable that explains the largest statistically significant portion of the unexplained (error) variance remaining from the first regression equation (Hair Jr. et al., 2014). Therefore, the second added predictive variable does not have to be the variable with the second largest correlation coefficient. New regressions are made every time with one more predictive variable, until

all variables are used or until adding a new variable does not add a statistical significant change to the model.

Partial F value

The adjusted R^2 can be used to analyse if an added variable makes sense. If the adjusted R^2 increases much by adding a new variable, it makes sense. However, if the adjusted R^2 does not increase much, it might be better to not include the variable in the model. This can be verified with the partial F test. A significant (<0.05) F-change means that the added variable in this step significantly improves the regression and thus should be included. If the addition of the variable is not significant, then one should eliminate the variable (Hair Jr. et al., 2014). SPSS calculates and displays the R^2 and partial F tests for the performed regressions.

B.2.4. Dummy variables

Usually, the predictive variables in SPSS are numbers which can take any value. However, it is possible to use a dichotomous variable, which is a variable with two possible categories that is coded with a 1 or 0. Because in this research there is a possibility that the 'positive or negative macro texture' will be used as a predictive variable in the model, one should understand how to implement a dichotomous variable.

A dichotomous variable which is used in a regression analysis is called a *dummy variable*. The first step of using a dummy variable is defining the possible outcomes of the variable as 0 or 1. For example, a negative macrotexture corresponds to 0 whereas a positive macrotexture corresponds to 1. The dummy variable is used to indicate of the presence or absence of a certain effect that influences the outcome of the regression analysis (de Vocht, 2009). The outcome of the dummy variable which is set to 0 is the reference category, and in the regression analysis the influence of the presence of 'group' 1 on the predicted variable is compared to the influence of the reference category on the predicted variable. Thus, an extra regression coefficient is generated which will only be used if the dummy variable has the value 1.

B.2.5. SPSS output multiple linear regression

When performing a multiple linear regression, SPSS gives various output tables. This sections gives an overview of the data generated in SPSS and discusses how to interpret this output. For every table, the amount of rows corresponds (in case of the stepwise method) to the number of performed regression. Thus, the first row contains one regression variable, whereas row n contains n regression variables. This section discusses the basic output generated by SPSS. One should be aware that much more output can be generated. For the tables an example regression is performed, which has no meaning for this research, but is solely used to explain the output of the regression analysis.

Variables Entered/Removed

This table gives, when using the stepwise method, an overview of the variables that are added to every new regression. Another method which you can use is backward, which starts with all possible variables and removes one variable per new regression. If this method would be used, this table shows which variables are removed every new regression.

Variables Entered/Removed[a]

Model	Variables Entered	Variables Removed	Method
1	var_2	.	Stepwise
2	var_5	.	Stepwise
3	var_4	.	Stepwise

Figure B.8: Linear regression output SPSS: table 'Variables Entered/Removed'

Figure B.8 shows that the first regression only uses var_2 as input, whereas the third regression uses var_2, var_5 and var_ 4 as input.

Model summary

This table gives an overview of the statistics of all models generated during the regression analysis. The r, R^2, adjusted R^2, standard error of the estimate and partial F values are given. This table can thus be used to compare the outcome of the different models. The best model has the highest R^2 and adjusted R^2, and the smallest standard error.

Model Summary

Model	R	R Square	Adjusted R Square	Std. Error of the Estimate	Change Statistics				
					R Square Change	F Change	df1	df2	Sig. F Change
1	,497[a]	,247	,232	20,362	,247	15,767	1	48	,000
2	,614[b]	,377	,351	18,719	,130	9,796	1	47	,003
3	,680[c]	,462	,427	17,587	,085	7,248	1	46	,010

Figure B.9: Linear regression output SPSS: table 'Model summary'

From Figure B.9 it becomes clear that the third regression has the highest R^2 and adjusted R^2 and the lowest standard error of estimate. Furthermore, the addition of var_4 significantly improves the model because the Sig. F Change value is smaller than 0.05. Thus, the third model is the best model from three obtained models. Adding another variable would not change the model significantly, thus SPSS stops the stepwise regression.

ANOVA

ANOVA stands for Analysis of Variance and with this table one can test if the whole model is significant (de Vocht, 2009). It reports how well the regression equation fits the data and hence how well it predicts the dependent variable (Laerd statistics, 2018). First, the significance of the F-test should be smaller than 0.05 for having a significant model. Furthermore, the sum of squares for the regression and residuals are given.

The sum of squares regression gives the sum of the squared differences between the mean and predicted values of the predicted variable for all observations. It gives an impression of the amount of improvement in explanation of the predicted, dependent variable by the independent variable(s) (Hair Jr. et al., 2014). Therefore, the larger this value, the better. The sum of squared residuals is the sum of squared differences in prediction errors (residuals) from all observations. It is used to denote the variance in the predicted variable not accounted for by the regression model (Hair Jr. et al., 2014). Therefore, this value should be as small as possible.

ANOVA[a]

Model		Sum of Squares	df	Mean Square	F	Sig.
1	Regression	6537,379	1	6537,379	15,767	,000[b]
	Residual	19901,501	48	414,615		
	Total	26438,880	49			
2	Regression	9969,814	2	4984,907	14,226	,000[c]
	Residual	16469,066	47	350,406		
	Total	26438,880	49			
3	Regression	12211,599	3	4070,533	13,161	,000[d]
	Residual	14227,281	46	309,289		
	Total	26438,880	49			

Figure B.10: Linear regression output SPSS: table 'ANOVA'

All three models have a significant F-test. And considering the sum of squares, the third model gives the best regression model.

Coefficients

From the table Coefficients the model can be obtained. The unstandardised coefficients for the different predictive variables are given, thus if $y = b_1 \cdot var_1 + b_2 \cdot var_2 + b_3 \cdot var_3$, the values obtained for b_1, b_2 and b_3 are given in the table. Also the significance of the variables are given, which should all be smaller than 0.05. In the last columns the table gives the 95.0% confidence intervals for B.

Coefficients[a]

Model		Unstandardized Coefficients		Standardized Coefficients	t	Sig.	95,0% Confidence Interval for B	
		B	Std. Error	Beta			Lower Bound	Upper Bound
1	(Constant)	40,913	7,099		5,763	,000	26,639	55,187
	var_2	,489	,123	,497	3,971	,000	,242	,737
2	(Constant)	21,113	9,089		2,323	,025	2,827	39,398
	var_2	,444	,114	,451	3,890	,000	,214	,674
	var_5	,406	,130	,363	3,130	,003	,145	,667
3	(Constant)	10,959	9,335		1,174	,246	-7,833	29,750
	var_2	,408	,108	,415	3,778	,000	,191	,626
	var_5	,364	,123	,326	2,964	,005	,117	,612
	var_4	,337	,125	,296	2,692	,010	,085	,588

Figure B.11: Linear regression output SPSS: table 'Coefficients'

In Figure B.11, the model would thus be:

$$y = 10.959 + 0.408 \cdot var\_2 + 0.364 \cdot var\_5 + 0.337 \cdot var_4 \tag{B.3}$$

The standardised coefficients can be used to analyse the independent influence of each variable, because the units are standardised. This can be usable when, for example, one variable is expressed as euros whereas the other variable is expressed as age. Furthermore, in the column 'Sig.' one can see that all variables are statistically significant and that 0 does not belong to one of the 95% confidence intervals, hence, we should not omit one of the variables from our model.

Excluded variables

In the table Excluded Variables (Figure B.12) the variables are shown which are *not* included in every model. The partial correlation coefficients of these variables are calculated. The variable with the highest partial correlation coefficient is added to the consecutive regression (as explained in the paragraph 'Stepwise' of Section B.2.3).

Excluded Variables[a]

Model		Beta In	t	Sig.	Partial Correlation	Collinearity Statistics Tolerance
1	var_1	,320[b]	2,526	,015	,346	,881
	var_3	,293[b]	2,362	,022	,326	,931
	var_4	,338[b]	2,864	,006	,385	,981
	var_5	,363[b]	3,130	,003	,415	,984
	var_6	-,270[b]	-2,248	,029	-,312	1,000
2	var_1	,248[c]	2,037	,047	,288	,839
	var_3	,236[c]	2,014	,050	,285	,904
	var_4	,296[c]	2,692	,010	,369	,965
	var_6	-,160[c]	-1,301	,200	-,188	,866
3	var_1	,145[d]	1,132	,263	,166	,709
	var_3	,142[d]	1,159	,252	,170	,778
	var_6	-,155[d]	-1,344	,186	-,196	,866

Figure B.12: Linear regression output SPSS: table 'Excluded variables'

As can be seen in Figure B.12, in the first regression variables 1 and 3 to 6 are excluded from the model. Var_5 has the highest partial correlation coefficient, thus in the second regression, var_5 is added to the used variables.

B.3. Multilevel models

A multilevel model is a linear model that deals with a hierarchical structure in a dataset. Often this is explained with examples from biological sciences, such as individuals nested within geographical areas (Steele, 2008). We expect individuals from the same geographical area to be more equivalent than two individuals from different areas, and therefore a hierarchical structure in the data is present. The lowest level of observation in the hierarchy, which are the individuals, is called the first and the groups, which are the geographical areas, is the second level (Steele, 2008). Even third or higher levels can be modelled. A multilevel linear model takes into account the hierarchy of a dataset and the independence of the data within one group, in contrary to a multiple linear regression which assumes that all observations are independent.

B.3.1. Fixed and random effects

In multilevel models a difference is made between fixed coefficients and random coefficients. Fixed coefficients are equal for every individual observation, independent of the cluster it belongs to. Random effects are, in contrary, different per cluster, thus per level 2 variable. One can make a difference between a random intercept and random slope model: for a random intercept model, the intercept value differs per group, and for a random slope model the slopes are different per group. Figure B.13 gives a visualisation of a dataset with random intercepts (Figure B.13a) and of a dataset with both random intercepts and random slopes (Figure B.13b).

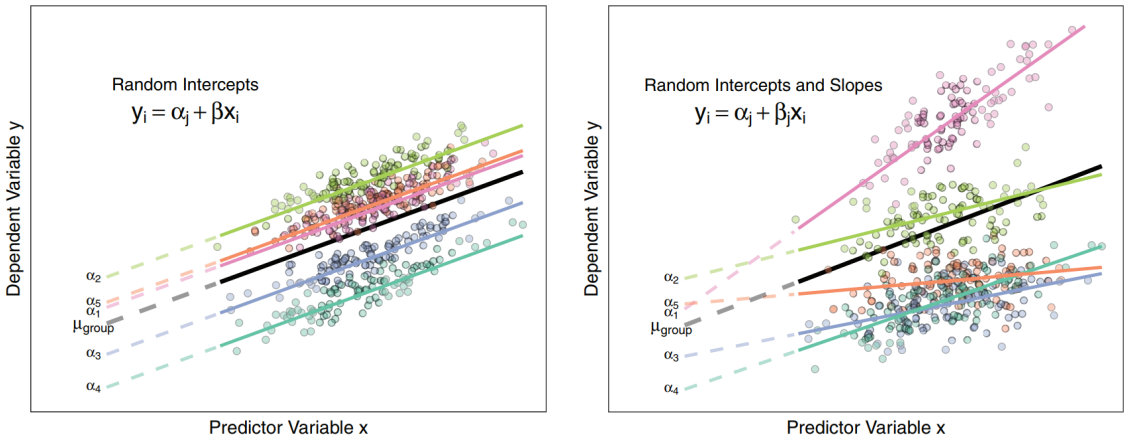

(a) Model containing random intercepts for group ID's (coloured lines, α_1 to α_5). The slope is fixed and therefore the regression lines are parallel.

(b) Model containing both random intercepts and random slopes per group ID.

Figure B.13: Differences between Random Intercept vs Random Slope Models (Harrison et al., 2018)

The multilevel model with 2 levels can be represented as follows (Field, 2013):

$$Y_{ij} = (b_0 + u_{0j}) + (b_1 + u_{1j})X_{ij} + \epsilon_{ij} \tag{B.4}$$

Where:

Y_{ij}	=	Observed value i belonging to group j
b_0	=	Fixed intercept of overall model fitted to the data
u_{0j}	=	Random intercept for group j
b_1	=	Fixed fixed slope for overall model for predictive variable X
u_{1j}	=	Random slope for variable X_{ij}, for group j
X_{ij}	=	Predictive variable
ϵ_{ij}	=	Error term

B.3.2. Regression methods

Two different regression methods can be used while performing a multilevel analysis. These are the maximum-likelihood estimation (ML) or restricted maximum likelihood estimation (REML). Field (2013) suggests that the ML produces more accurate estimates of the fixed effects, whereas the REML produces more accurate estimates of the random variances. Often, the results obtained with an REML or ML only make a small difference to the estimated regression coefficients.

B.3.3. Analysing a multilevel model

The output generated from a multilevel model does not give a R^2 or standard error of the estimate, as is given in the output of a multiple linear regression. Instead, the -2 Log Likelihood (-2LL) is given, which is called the deviance. The Log Likelihood function gives an indication of how well the data fits a certain model. The higher the log likelihood, the larger the possibility that the model fits the dataset. The log likelihood function can be either positive or negative. If the log likelihood is positive, it follows that the -2LL must be as negative possible, because then the log likelihood will be largest. If the log likelihood is negative, the -2LL closest to 0 represents the best model.

To compare two models the chi-square likelihood ratio test is used (Field, 2013):

$$\chi_{Change}{}^2 = (-2LL_{old}) - (-2LL_{new}) \tag{B.5a}$$

$$df_{Change} = \kappa_{old} - \kappa_{new} \tag{B.5b}$$

Where: κ = number of parameters in the respective model

With help of Table B.2 one can determine if the ${\chi_{Change}}^2$, in combination with the change in number of parameters, is significant, which indicates a significant improvement to the model.

Table B.2: Critical values of chi-square distribution (Field, 2009)

	p			p	
df	0.05	0.01	df	0.05	0.01
1	3.84	6.63	25	37.65	44.31
2	5.99	9.21	26	38.89	45.64
3	7.81	11.34	27	40.11	46.96
4	9.49	13.28	28	41.34	48.28
5	11.07	15.09	29	42.56	49.59
6	12.59	16.81	30	43.77	50.89
7	14.07	18.48	35	49.80	57.34
8	15.51	20.09	40	55.76	63.69
9	16.92	21.67	45	61.66	69.96
10	18.31	23.21	50	67.50	76.15
11	19.68	24.72	60	79.08	88.38
12	21.03	26.22	70	90.53	100.43
13	22.36	27.69	80	101.88	112.33
14	23.68	29.14	90	113.15	124.12
15	25.00	30.58	100	124.34	135.81
16	26.30	32.00	200	233.99	249.45
17	27.59	33.41	300	341.40	359.91
18	28.87	34.81	400	447.63	468.72
19	30.14	36.19	500	553.13	576.49
20	31.41	37.57	600	658.09	683.52
21	32.67	38.93	700	762.66	789.97
22	33.92	40.29	800	866.91	895.98
23	35.17	41.64	900	970.90	1001.63
24	36.42	42.98	1000	1074.68	1106.97

Two restrictions limit the use of the chi-square distribution (Field, 2013):

1. the full maximum-likelihood estimation should be used (and not the restricted maximum likelihood), and
2. the new model contains all of the effects of the older model.

Restriction one deals with a difference in regression methods and says that the chi-square test only works for the ML method. Furthermore, for comparing two models, the second model should be an elaboration of the first model. If the first model contains variable X_{ij}, the second model cannot only contain variable Y_{ij} but should also contain X_{ij}.

C

Available data

This appendix describes the data that is used in this study and how this data is prepared for the analysis. Different datasets from different projects are provided which are described in Section C.1. After that, a general procedure of the data preparation is given in Section C.2. Section C.3 visualises the data by different plots of the data and finally, Section C.4 gives a short repeatability analysis of the data.

C.1. Obtained data

C.1.1. Measurements performed by Kiwa-KOAC for RWS

In an early stage of this research, a dataset was obtained consisting of measurements performed in the past (2016 - 2018) by Kiwa-KOAC for RWS. For several reasons, some of the measurements needed to be repeated. If these repeated measurements were performed at another measuring speed than the first measurement, a data point could be obtained consisting of two measurements speeds and two corresponding values for the skid resistance.

Only 75 datapoints consisting of two measurements at different measuring speeds were obtained from this dataset. These measurements were performed on different days and the average time in between two measurements was 50 days. The measurements were therefore affected by temperature and seasonal variations. Furthermore, neither the pavement types nor the construction years of the pavements were known. Therefore, it was decided to exclude this dataset from the further analysis.

C.1.2. Measurements performed for SKM and RWS Skid Resistance Tester comparison

In 2016, a study was performed in which the correlation was analysed between SKM and RWS SKid Resistance Tester measurements at different speeds, types of road sections and types of pavements. Aveco de Bondt and Kiwa-KOAC both provided a dataset for this analysis. These datasets consisted of both RWS Skid Resistance Meter and SKM measurements at different measuring speeds on different sections. The measurements performed with the SKM are used in this research. The dataset of Aveco de Bondt is called 'Dataset A' and the dataset of Kiwa-KOAC is called 'Dataset B', corresponding to the reports of the study for which these measurements are performed. The sections below give a description of the two datasets.

Dataset A: measurements performed by Aveco de Bondt

Table C.1 gives an overview of the dataset measured by Aveco de Bondt with the SKM. Measurements were performed at three measuring speeds, namely 40, 60 and 80 km/h. The type and texture of the pavements vary.

Table C.1: Overview of dataset A, measured by Aveco de Bondt

Road	No. of usable 100m sections	Type	Construction year	Measuring speeds	MPD			Avg. MPD/RMS	Conditions	Measuring date
					min	max	avg.			
N795	79	SMA 8G+	2014	40-60-80	0.72	0.91	0.84	1.15	Dry	15-9-2016
N320	121	SMA 8	2010/2015	40-60-80	0.68	0.98	0.83	1.22	Dry	19-9-2016
HOV1	79	Concrete C35/45	2000/2013/2015	40-60(-80[1])	0.19	0.98	0.41	1.57	Dry	22-9-2016
N224	30	SMA 11 type 2	2004	40-60-80	0.67	1.08	0.94	1.26	Dry	27-9-2016
N311	40	AC 16 Surf	1994	40-60	0.52	0.95	0.69	1.72	Dry	27-9-2016
N804	10	AC 11 Surf	2007	40-60	0.55	0.90	0.71	1.65	Dry	27-9-2016
RW015 (A18)	56+24[2]	ZOAB 16	?	40-60-80	0.40	1.54	1.22	1.26	Dry	15-8-2016
N310	40	SMA 8G+	2015/2016	40-60	0.33	0.99	0.79	1.27	Dry	15-9-2016

[1] 52 sections are not measured at 80 km/h
[2] 56 sections with texture measurement and 24 sections without texture measurement

Dataset B: measurements performed by Kiwa-KOAC

Table C.2 gives an overview of the dataset measured by Kiwa-KOAC for the research about the correlation between the SKM and RWS Skid Resistance Tester. The measurements shown below are all performed with the SKM. Kiwa-KOAC measured a variety of pavement types. Unfortunately, several measurements have been performed on wet surfaces which makes the texture measurements unreliable.

Table C.2: Overview of dataset B, measured by Kiwa-KOAC

Road	No. of usable 100m sections	Type	Construction year	Measuring speeds	MPD			Avg. MPD/RMS	Conditions	Measuring date
					min	max	avg.			
N304	40	DGD	2009	40-60-80	0.77	1.00	0.88	0.65	Dry	2-8-2016
N344	20 + 80[1]	ZOAB 8+ ZOAB 11	2011	40-60-80	0.71	1.73	1.32	0.95	Dry	2-8-2016
N304	40	DGD	2009	40-60-80	0.80	1.50	1.00	0.90	Wet	3-8-2016
N224	81	DGD	2008	40-60-80	0.51	1.25	0.93	0.61	Wet	3-8-2016
N338	40	2-ZOAB	2006	40-60-80	0.71	1.25	0.86	0.71	Drying	3-8-2016
RW015 (A18)	70 + 10[2]	ZOAB + DAB	?	40-60-80	0.45	1.32	1.13	1.24	Dry	15-8-2016

[1] 20 sections with ZOAB 8, 80 sections with ZOAB 11
[2] 70 sections with ZOAB, 10 sections with DAB

C.1.3. New measured data

Besides the provided data described above, another round of measurements with the SKM was performed by Kiwa-KOAC. This data is described in Table C.3. Additional to the measurements performed at 40, 60 and 80 km/h, this dataset also contains a few measurements performed at 30 km/h.

Table C.3: Overview of new measured data

Road	No. of usable 100m sections	Type	Construction year	Measuring speeds	MPD			Avg. MPD/RMS	Conditions	Measuring date
					min	max	avg.			
N302	20	DAB	?	40-60-80	0.3	0.6	0.47	1.26	Dry	7-11-2018
Oostveluweweg	8	Concrete	?	40-60-80	0.9	1.2	0.99	1.41	Dry	7-11-2018
N344	20	ZOAB11	?	40-60-80	1.6	1.8	1.64	1.09	Dry	7-11-2018
Gildenlaan	12	Dense	?	30-40	0.5	0.7	0.52	1.37	Dry	18-12-2018
Kanaal Zuid	12	Dense	?	30-40	0.5	0.6	0.53	1.33	Dry	18-12-2018

C.2. Preparation of data

Before the data can be analysed, the data needs to be prepared. This preparation phase consists of several steps. First, for every road an overview sheet was made. All these overview sheets have the same structure, as is explained in Section C.2.1. Thereafter, for every regression method (see Chapter 5) a separate datasheet was compiled. This description is given in Section C.2.2.

C.2.1. Overview sheets per road

1. The datasets were separated into multiple excel files. Each excel file contained information of one road, for which multiple measurements were conducted. All measurements were separated into separate sheets. In most situations, measurements were performed at 40, 60 and 80 km/h and twice per measuring speed. Therefore, this leads to 6 sheets per road: 40-1, 40-2, 60-1, 60-2, 80-1 and 80-2 (or in some situations, one of the measuring speeds is missing or different).

2. In the data the *raw skid resistance* and the *skid resistance* is given. The *raw skid resistance* is the skid resistance measured with the SKM, and corrections for temperature and speed were applied to obtain the *skid resistance*. Equations (4.16) and (4.17) were used to calculate the corrected skid resistance from the raw (measured) skid resistance. For this study, the skid resistance was only

corrected for temperature variations and not for speed variations. Therefore, either the corrected skid resistance minus the applied speed correction according to Equation (4.16) was taken, or the raw skid resistance plus the temperature correction as in Equation (4.17).

3. Per measuring speed, measurements for the same section are averaged. This means, the average speed and the average skid resistance, corrected for temperature variations, are calculated.
4. Per excel file, a single overview sheet was prepared consisting of several columns:
   - Unique, characterisation code for every 100 metre section (consisting of road name, start and end hectometre indication).
   - Average measuring speeds for (mostly) 40, 60 and 80 km/h and for some sections 30 km/h.
   - Average skid resistance values —corrected for temperature variations— at 40, 60 and 80 km/h.
   - MPD of the first measurement for the corresponding section[1] For some measurements, prior to the skid resistance measurements a texture measurement was performed. A separate sheet called 'Texture' was setup and the texture measurements were read from this sheet.
   - RMS.
   - MPD divided by RMS.
   - Type of pavement, given in measurement data. These were:
     - ZOAB: ZOAB, ZOAB-2 (double layered ZOAB), ZOAB 8, ZOAB 11
     - SMA: SMA 11 type 2, SMA 8G+, SMA 8
     - Concrete: concrete C35/45, concrete
     - Dense asphalt: DAB, dense
     - DGD
     - AC 16 Surf
     - AC 11 Surf
   - Excel file (in a later stadium the overview sheets were to be extracted and compiled into one excel file, this column facilitates easy retrieval of the original data). Excel files were named after the roads on which the measurements were performed. Each excel file containes data of one road.
   - Pavement category: from the measurements various pavement types were measured. From some pavements categories, for example ZOAB, multiple types were measured, such as double layered ZOAB, ZOAB 8 and ZOAB 16. This column divides the pavement types in bigger groups which contain several pavement types, namely:
     - ZOAB: ZOAB 8, ZOAB 11, ZOAB 16, double layered ZOAB, ZOAB (without further indications)
     - SMA: SMA 8G+, SMA 8, SMA 11 type 2
     - Concrete: concrete C35/45, concrete (without further indications)
     - Dense: DAB, AC 16 surf, AC 11 Surf, dense (without further indications)
     - DGD: no further indications

   During the analysis the different pavement types could easily be selected to perform analyses on separate pavement types.

[1] After the first measurement, the road surface is wet from the water layer, which makes later texture measurement unreliable. Therefore, the first texture measurement was taken in the analysis.

- Weather conditions: some measurements were performed under wet conditions, and therefore the texture measurements of these measurements were not reliable. This column states if the pavement was wet, dry or drying. Only the dry pavements were used in the analysis.
- The difference in skid resistance per km/h of vehicle speed between 40 and 60, and 60 and 80 km/h. In this case a linear relationship was assumed. This difference was used as quality control. If this difference would be much lower or higher on a road section than average, the dataset on that road section might be invalid.
- Column for comments measurements.

If for certain measurements no skid resistance or MPD value was obtained, these cells were set to -9999. In SPSS, -9999 will be set as a missing value. SPSS will ignore rows during regressions in which data that is needed are set as a missing value.

Multiple excel files are obtained of which the first sheet contains the measurement data of that road. All files were equally structured such that the data could easily be collected into one overview datasheet.

C.2.2. Combining data into one datasheet

The excel files with measurements data per road were combined into one excel file containing all datapoints needed in the analysis. Different datasheet were compiled. The structure of these datasheets depended on the regression method (see Chapter 5). Furthermore, for these excel files, the data from Section C.1.1 were not used. This data was measured under different weather circumstances and thus temperature differences might have caused deviating measurement values. Therefore this data was first omitted.

Datasheet for regression method 1: multiple linear regression

The first regression method is described in Section 5.2. An observation must consist of two measurements performed on the same section, thus the data must be split into several combinations of skid resistance measurements with corresponding measurement speeds.

The excel file has the following content:

- characterising code for every 100m section
- V_a: corresponds to 40 or 60 km/h
- V_b: corresponds to 60 or 80 km/h (and for one section to 30 km/h)

  If one section is measured at 40, 60 and 80 km/h, 3 data points will be made per section. These are combinations of 40 and 60, 60 and 80 and 40 and 80 km/h.
- μ_a: skid resistance at V_a
- μ_b: skid resistance at V_b
- MPD
- RMS
- MPD/RMS
- comments
- type of pavement according to measurement
- excel file containing original data
- pavement category
- weather conditions
- measuring speeds: number of which the first two digits contain V_a and the last two digits V_b, each rounded to the nearest ten. For example, if V_a is 39.8 and V_b is 61.5, this cell will contain the value 4060. This number can be used to include or exclude certain data points during the analysis.

Next to this content, few columns were added with calculated variables which could be predictive variables for the model. These are:

- $V_b - V_a$
- MPD_{dry}: only shows the MPD when the pavement was dry during measurements. Otherwise, the MPD is set to -9999. This variable is used for calculating the other variables containing MPD below.
- MPD$\cdot(V_b - V_a)$
- $ln(\text{MPD}) \cdot (V_b - V_a)$
- $\frac{\text{MPD}}{\text{RMS}} \cdot (V_b - V_a)$
- $\frac{\text{MPD}}{\text{RMS}} \cdot (V_b - V_a)$ as a dummy variable:
  - $(V_b - V_a)$ if $\frac{\text{MPD}}{\text{RMS}} > 1.58$
  - 0 if $\frac{\text{MPD}}{\text{RMS}} < 1.58$
- 1-$\frac{V_b}{V_a}$
- MPD$\cdot(1 - \frac{V_b}{V_a})$
- $\frac{\text{MPD}}{\text{RMS}} \cdot (1 - \frac{V_b}{V_a})$
- $ln(\text{MPD}) \cdot (1 - \frac{V_b}{V_a})$

The number of individual data points (consisting of a measurement with measuring speed code 4030, 4060 and 4080) are:

- ZOAB: 922 (of which 192 under wet conditions)
- DGD: 480 (all under wet conditions)
- SMA: 723
- Dense: 161, and
- Concrete: 161.

In total, the dataset consisted of 2420 data points. 1748 of these datapoints contained measurements performed under dry conditions.

Datasheet for regression method 2: linear regression with zero speed intercept

The regression method which used the zero speed intercept is described in Section 5.3. For this method, a datasheet was needed consisting of one measurement per observation. Therefore, instead of V_a, V_b, μ_a and μ_b, this datasheet contained only V_a and a corresponding μ_a. Furthermore, some columns were added with calculated variables which could be predictive variables. These are:

- MPD$\cdot V_a$
- $ln(\text{MPD}) \cdot V_a$
- $\frac{\text{MPD}}{\text{RMS}} \cdot V_a$
- $\frac{\text{MPD}}{\text{RMS}} \cdot V_a$ as a dummy variable:
  - V_a, if $\frac{\text{MPD}}{\text{RMS}} > 1.58$

    0, if $\frac{\text{MPD}}{\text{RMS}} < 1.58$

The amount of observations (consisting of one measurement) are:

- ZOAB: 641 (of which 133 under wet conditions)
- DGD: 480 (all under wet conditions)

- SMA: 774
- Dense: 236
- Concrete: 198

In total, this dataset contains 2012 observations.

Datasheet for regression method 3: multilevel modelling

The third regression method is called the multilevel analysis. For this method, all data consisting of one 100 metre section were listed in one observation. This means that, compared to the datasheet of method 1, instead of two measurements all measurements are given in one observation. If only two measurements are performed for a section, then the third measurement speed and skid resistance are set to -9999, which will be seen as a missing value in SPSS. Furthermore, no new variables were calculated, because this computation would be catered for by SPSS.

The amount of observations (consisting of one 100 metre section with multiple measurements) are:

- ZOAB: 309 (of which 64 under wet conditions)
- DGD: 160 (all under wet conditions)
- SMA: 282
- Dense: 104
- Concrete: 87

C.2.3. Selection of data points for regression

The regression analysis was performed on approximately 75% of the data as described in the previous sections. The remaining 25% of the data were to used to test the model. Therefore, 75% of the data were randomly selected. In the datasheet for the third regression method, an observation coincides with one 100 metre section. In this datasheet, per road, 75% of the 100 metre sections were randomly selected. In the datasheets for regression method 1 and 2, this selection was adopted.

C.3. Visualisation of data

This section visualises the data as described in the previous section. Only the observations that could be used for the regression are included. This means that no pavements with DGD are included, because all data from DGD pavements were performed under wet conditions, which makes the macrotexture measurements unreliable. Also, other observations without macrotexture measurements were not taken into account. Furthermore, this analysis is based on 100% of the data, and not on the selected 75%.

Figure C.1 shows the distribution of the average measured skid resistances at the average measuring speeds. A declining trend in skid resistance with increasing measuring speed is visible. Furthermore, the slope of the two roads with measurements performed at 30 km/h and 40 km/h is steeper than the slopes of the roads with higher measuring speeds. This agrees with the assumption that at low speeds, the skid resistance declines more per km/h than at high speeds.

Furthermore, the figure shows that not for all roads a decreasing trend of the slope can be observed. For example, RW015 A18 ZOAB shows a steeper slope for the decline from 60 to 80 km/h than for the decline in skid resistance from 40 to 60 km/h.

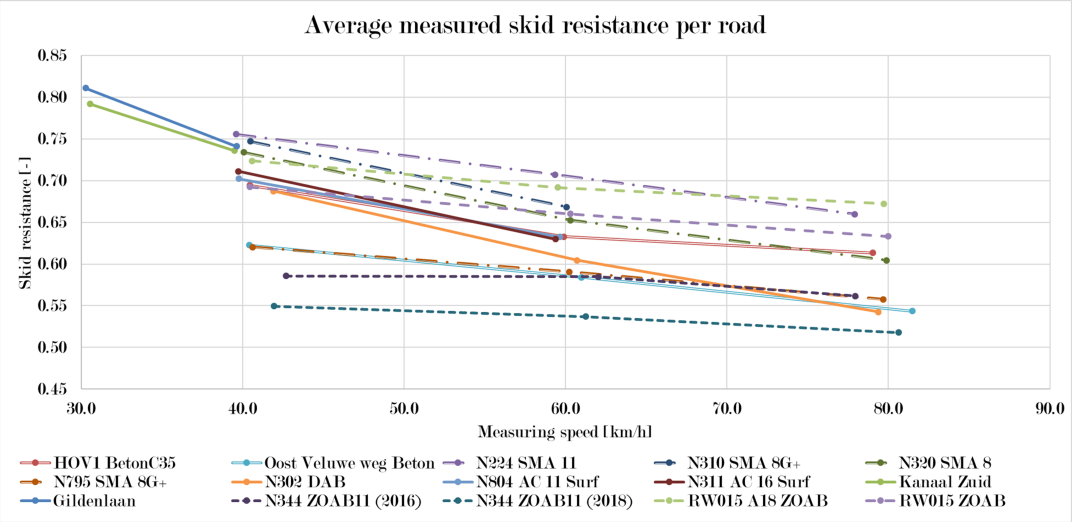

Figure C.1: Overview of average skid resistances per road

Figure C.2 shows a scatterplot of all measurements. Some concrete sections have a very high skid resistance. Furthermore, the skid resistance generally ranges from 0.45 to 0.85. Also, the larger the measuring speed is, the less the values of the measured skid resistances vary.

Figure C.3 shows all measurements performed at 40 km/h, with on the x-axis the MPD. There is no clear distribution between the height of the skid resistance and the MPD.

Figure C.2: Plot of measured skid resistances at different measuring speeds

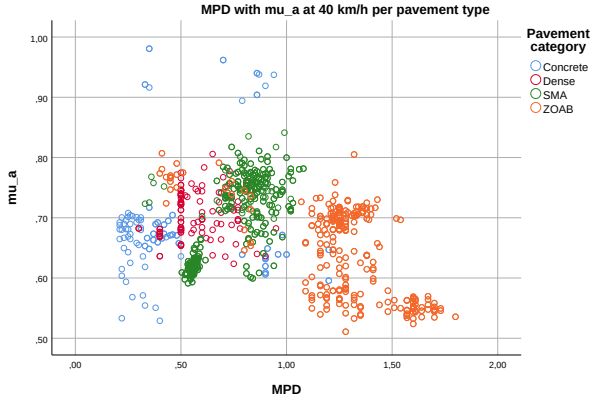

Figure C.3: Plot with on the x-axis the MPD and on the y-axis the skid resistance measured at 40 km/h

Figure C.4 shows a histogram of the measured MPD values, with a distinction between different pavement types.

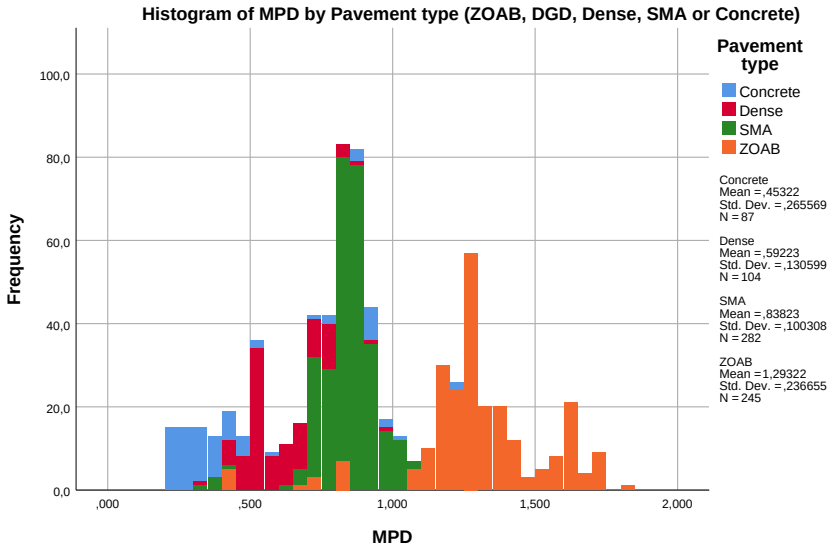

Figure C.4: Histogram of MPD divided over different pavement types

A clear separation between MPD sizes and pavement types is visible. As expected, ZOAB contains pavements with the largest MPD values, followed by pavements with SMA. Furthermore, the distribution is far from a normal distribution, but the data could be separated into measurements containing an MPD<1 and measurements containing an MPD>1.

Figures C.5a to C.5d show for different speed combinations the measured skid resistances.

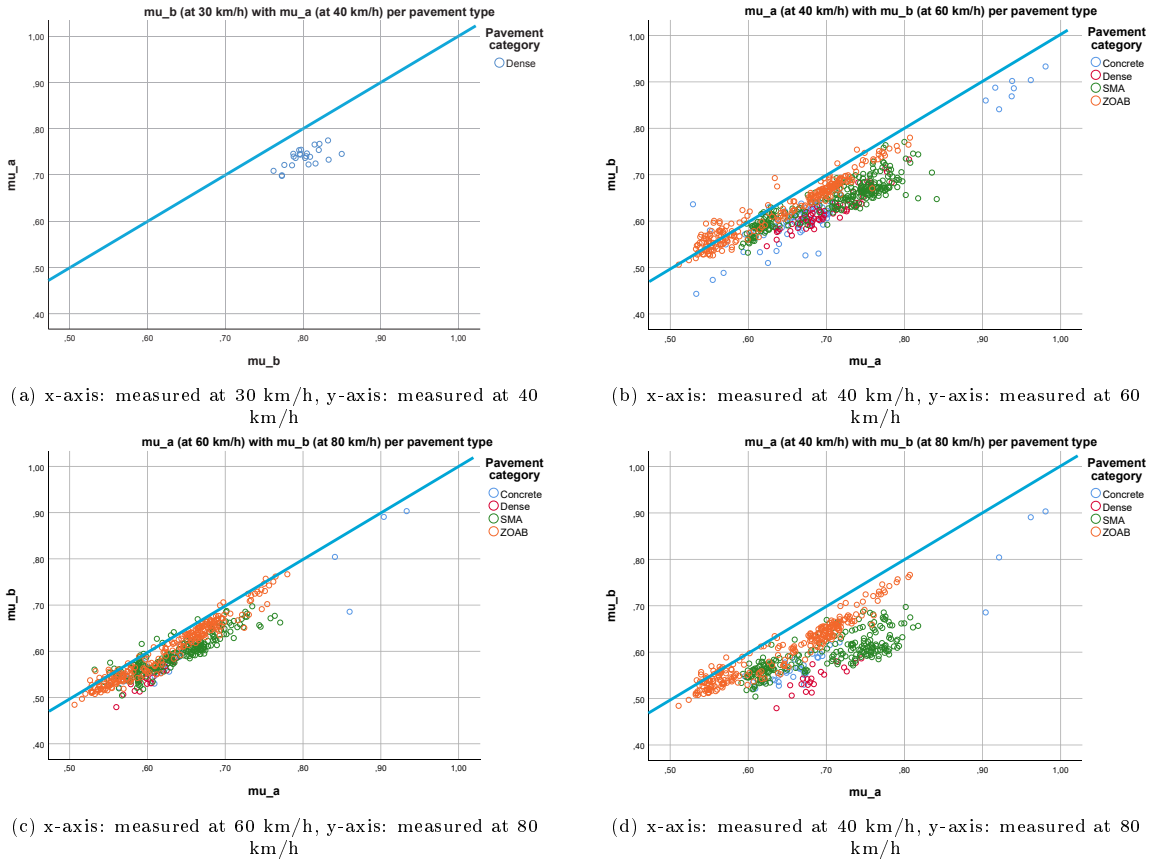

(a) x-axis: measured at 30 km/h, y-axis: measured at 40 km/h

(b) x-axis: measured at 40 km/h, y-axis: measured at 60 km/h

(c) x-axis: measured at 60 km/h, y-axis: measured at 80 km/h

(d) x-axis: measured at 40 km/h, y-axis: measured at 80 km/h

Figure C.5: Plots of two skid resistance measurements at different speeds. The lower speed is plotted on the x-axis, thus all the data points under the blue lines indicate a decline in skid resistance, whereas datapoints above the plotted line indicate an increase in skid resistance with increasing speed.

Most datapoints are situated below the line, which indicates a decline in skid resistance with increasing speed. Some datapoints are situated above the line, this happens mainly on pavements with ZOAB. Since MPD-values on ZOAB are usually high and are associated with less speed dependency of the skid resistance, another round of measurements at a slightly higher speed might in some case lead to a higher skid resistance value purely because of uncertainties and random variation in the test results. For the majority of the cases a higher speed leads to lower skid resistance values.

Figures C.6a to C.6c show the percentage of change in skid resistance for increasing the measuring speed from respectively 40 to 60, 60 to 80, and 40 to 80.

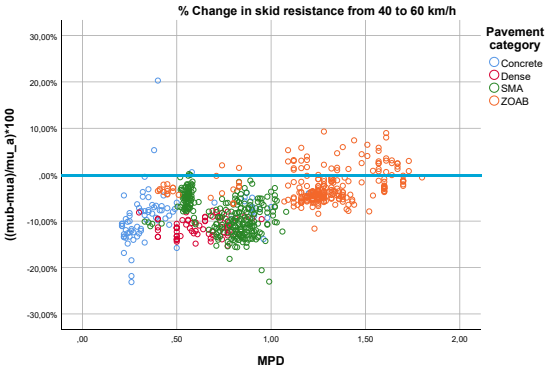

(a) % change in skid resistance with an increase in measuring speed from 40 to 60 km/h

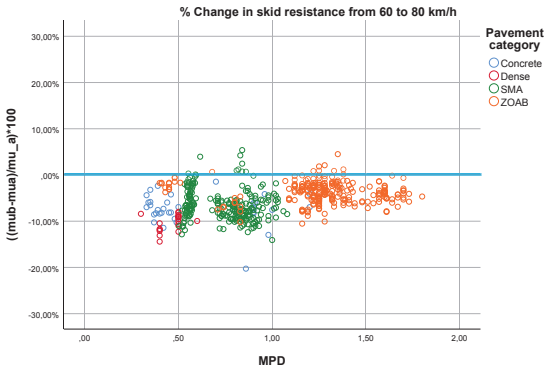

(b) % change in skid resistance with an increase in measuring speed from 60 to 80 km/h

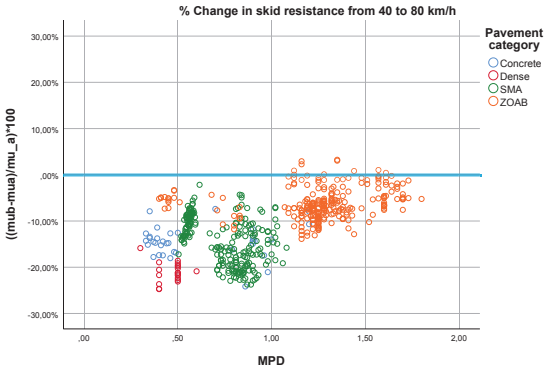

(c) % change in skid resistance with an increase in measuring speed from 40 to 80 km/h

Figure C.6: Percentage of change in skid resistance for increasing the measuring speed from respectively 40 to 60, 60 to 80, and 40 to 80. A positive percentage (above the blue line) indicates an increase in skid resistance with an increasing speed, whereas a negative percentage (below the blue line) indicates a decreasing skid resistance with increasing speed.

Figures C.6a to C.6c show that from 40 to 60 km/h, much of the measured skid resistances increase for ZOAB pavements, and also few measurements of concrete and SMA show an increased skid resistance. From 60 to 80 km/h, even more of the measurements performed on SMA show an increase in skid resistance. However, the majority of the sections with SMA show a declining skid resistance with increasing speed. Overall, from 40 to 80 km/h, only some sections with a ZOAB pavement show an increasing skid resistance with increasing speed. Furthermore, in Figure C.6c one could see that a lower MPD in general leads to a larger % change in skid resistance.

C.4. Repeatability

Repeatability can be defined as 'the ability of a measurement device to produce the same measured value when measurement runs are repeated on the same surface under the same conditions' (Vos and Groenendijk, 2009). Because the friction coefficient is a result of tyre-pavement interaction, the measured friction coefficient is an indicator of the interaction process. The repeatability for one device for one pavement, may not apply for the same device on another pavement.

The repeatability is calculated as follows:

1. The standard deviations of the measured friction coefficients are calculated per road section.
2. The variance per road section is calculated by quadrating the standard deviations.
3. The repeatability for one road and one measuring speed is calculated by:

$$r = 2.77 \cdot \sqrt{\frac{\sum_1^n (VAR_n)}{n}} \tag{C.1}$$

The repeatability is the value that will not be exceeded by the difference between two successive measurements, with a 95% probability (Vos and Groenendijk, 2009). A small repeatability therefore indicates better performance than a larger repeatability. In this research the repeatability is calculated based on two measurements (measurements are performed twice per measuring speed), more measurements would give better estimations of the repeatability.

Table C.4 show the repeatability for the different road sections of which data will be used in this research, Figure C.7 visualises the table.

Table C.4: Repeatability of different road sections

Name of excel file	**40 km/h**	**60 km/h**	**80 km/h**
I_1800501-uitgebreid_per_100m_ N302_ DAB	0.021	0.060	0.068
I_1800501-uitgebreid per 100m N344 DGD	0.037	0.017	0.023
I_1800501-uitgebreid per 100m Oost Veluwe weg Beton	0.012	0.024	0.029
181217 N224 DGAD	0.052	0.045	0.084
181217 N304 DGAD	0.035	0.039	0.057
181217 N304 DGAD2	0.044	0.048	-
181217 N338 2ZOAB	0.046	0.065	0.054
181217 N344 ZOAB11	0.050	0.092	0.065
181217 RW015 ZOAB	0.061	0.038	0.025
SMA 11 type 2	0.058	0.053	0.052
181213 N310 SMA 8G+	0.044	0.032	
181213 N311 AC 16 Surf	0.041	0.027	
181213 N320 SMA 8	0.040	0.032	0.040
181213 N795 SMA 8G+	0.034	0.046	0.032
181213 N804 AC 11 Surf	0.082	0.135	
181213 RW015 A18ZOAB	0.046	0.045	0.033
190401 HOV1 BetonC35	0.017	0.066	

	30 km/h	**40 km/h**
190301 Gildenlaan	0.090	0.035
190301 Kanaal	0.061	

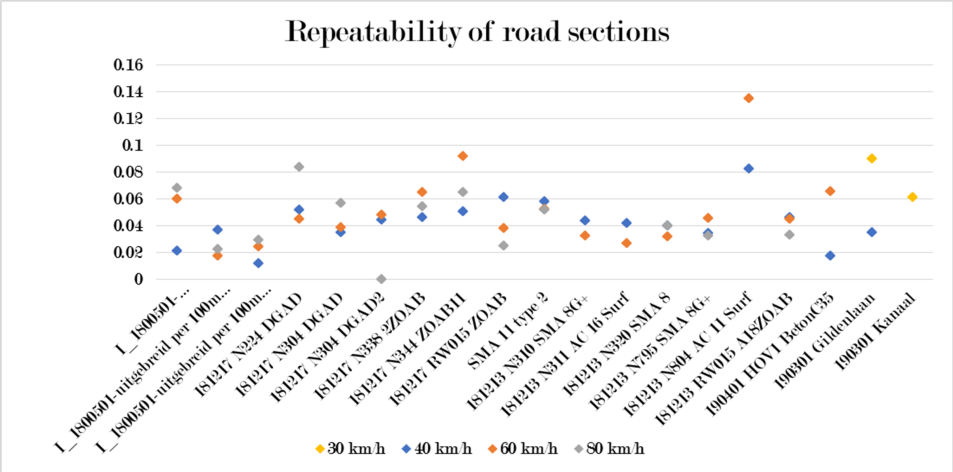

Figure C.7: Repeatability of different road sections

As one can see, the repeatability for N804 AC 11 Surf at 60 km/h is high. These measurements are deviating much from each other.

D

Syntaxes for regressions performed in SPSS

D.1. Determination of hierarchical structure for multilevel model

This code given below shows syntax for the regressions to detect the optimal hierarchical structure as given in Section 5.4.2, Table 5.9.

```
**Regression 1: 1 level, V_100.
MIXED ln_mu WITH V_100
/CRITERIA=CIN(95) MXITER(100) MXSTEP(10) SCORING(1) SINGULAR(0.000000000001) HCONVERGE(0,
ABSOLUTE) LCONVERGE(0, ABSOLUTE) PCONVERGE(0.000001, ABSOLUTE)
/FIXED= V_100 | SSTYPE(3)
/METHOD=ML
/PRINT=CORB COVB G LMATRIX R SOLUTION TESTCOV.

**Regression 2: 1 level, V_100 MPD_V_100.
MIXED ln_mu WITH V_100 MPD_V_100
/CRITERIA=CIN(95) MXITER(100) MXSTEP(10) SCORING(1) SINGULAR(0.000000000001) HCONVERGE(0,
ABSOLUTE) LCONVERGE(0, ABSOLUTE) PCONVERGE(0.000001, ABSOLUTE)
/FIXED= V_100 MPD_V_100 | SSTYPE(3)
/METHOD=ML
/PRINT=CORB COVB G LMATRIX R SOLUTION TESTCOV.

**Regression 3: 2 levels, V_100.
MIXED ln_mu WITH V_100
/CRITERIA=CIN(95) MXITER(100) MXSTEP(10) SCORING(1) SINGULAR(0.000000000001) HCONVERGE(0,
ABSOLUTE) LCONVERGE(0, ABSOLUTE) PCONVERGE(0.000001, ABSOLUTE)
/FIXED= V_100 | SSTYPE(3)
/random intercept | subject(Zoekcode) covtype(ID)
/repeated=Measurement | subject(Zoekcode) COVTYPE (DIAG)
/METHOD=ML
/PRINT=CORB COVB G LMATRIX R SOLUTION TESTCOV.

**Regression 4: 2 levels, V_100 MPD_V_100.
MIXED ln_mu WITH V_100 MPD_V_100
/CRITERIA=CIN(95) MXITER(100) MXSTEP(10) SCORING(1) SINGULAR(0.000000000001) HCONVERGE(0,
ABSOLUTE) LCONVERGE(0, ABSOLUTE) PCONVERGE(0.000001, ABSOLUTE)
/FIXED= INTERCEPT V_100 MPD_V_100 | SSTYPE(3)
/random INTERCEPT | subject(Zoekcode) covtype(ID)
/repeated=Measurement | subject(Zoekcode) COVTYPE (DIAG)
/METHOD=ML
/PRINT=CORB COVB G LMATRIX R SOLUTION TESTCOV.

**Regression 5: 3 levels, V_100.
MIXED ln_mu WITH V_100
/CRITERIA=CIN(95) MXITER(100) MXSTEP(10) SCORING(1) SINGULAR(0.000000000001) HCONVERGE(0,
ABSOLUTE) LCONVERGE(0, ABSOLUTE) PCONVERGE(0.000001, ABSOLUTE)
/FIXED= V_100 | SSTYPE(3)
/random intercept | subject(Excel_file) covtype(ID)
/random intercept | subject(Excel_file*Zoekcode) covtype(ID)
/repeated=Measurement | subject(Excel_file*Zoekcode) COVTYPE (DIAG)
/METHOD=ML
/PRINT=CORB COVB G LMATRIX R SOLUTION TESTCOV.
```

```
**Regression 6: 3 levels, V_100 MPD_V_100.
MIXED ln_mu WITH V_100 MPD_V_100
/CRITERIA=CIN(95) MXITER(100) MXSTEP(10) SCORING(1) SINGULAR(0.000000000001) HCONVERGE(0,
ABSOLUTE) LCONVERGE(0, ABSOLUTE) PCONVERGE(0.000001, ABSOLUTE)
/FIXED= V_100 MPD_V_100 | SSTYPE(3)
/random intercept | subject(Excel_file) covtype(ID)
/random intercept | subject(Excel_file*Zoekcode) covtype(ID)
/repeated=Measurement | subject(Excel_file*Zoekcode) COVTYPE (DIAG)
/METHOD=ML
/PRINT=CORB COVB G LMATRIX R SOLUTION TESTCOV.
```

D.2. Determination of predictive variables for multilevel model

```
**7: 3 levels V_100 lnMPD_V_100.
MIXED ln_mu WITH V_100 LN_MPD_V_100
/CRITERIA=CIN(95) MXITER(100) MXSTEP(10) SCORING(1) SINGULAR(0.000000000001) HCONVERGE(0,
ABSOLUTE) LCONVERGE(0, ABSOLUTE) PCONVERGE(0.000001, ABSOLUTE)
/FIXED= V_100 LN_MPD_V_100 | SSTYPE(3)
/random intercept | subject(Excel_file) covtype(ID)
/random intercept | subject(Excel_file*Zoekcode) covtype(ID)
/repeated=Measurement | subject(Excel_file*Zoekcode) COVTYPE (DIAG)
/METHOD=ML
/PRINT=CORB COVB G LMATRIX R SOLUTION TESTCOV.

**8: 3 levels, MPD_V_100.
MIXED ln_mu WITH MPD_V_100
/CRITERIA=CIN(95) MXITER(100) MXSTEP(10) SCORING(1) SINGULAR(0.000000000001) HCONVERGE(0,
ABSOLUTE) LCONVERGE(0, ABSOLUTE) PCONVERGE(0.000001, ABSOLUTE)
/FIXED= MPD_V_100 | SSTYPE(3)
/random intercept | subject(Excel_file) covtype(ID)
/random intercept | subject(Excel_file*Zoekcode) covtype(ID)
/repeated=Measurement | subject(Excel_file*Zoekcode) COVTYPE (DIAG)
/METHOD=ML
/PRINT=CORB COVB G LMATRIX R SOLUTION TESTCOV.

**9: 3 levels ln_V_100 MPD_V_100.
MIXED ln_mu WITH ln_V_100 MPD_V_100
/CRITERIA=CIN(95) MXITER(100) MXSTEP(10) SCORING(1) SINGULAR(0.000000000001) HCONVERGE(0,
ABSOLUTE) LCONVERGE(0, ABSOLUTE) PCONVERGE(0.000001, ABSOLUTE)
/FIXED= ln_V_100 MPD_V_100 | SSTYPE(3)
/random intercept | subject(Excel_file) covtype(ID)
/random intercept | subject(Excel_file*Zoekcode) covtype(ID)
/repeated=Measurement | subject(Excel_file*Zoekcode) COVTYPE (DIAG)
/METHOD=ML
/PRINT=CORB COVB G LMATRIX R SOLUTION TESTCOV.

**10: 3 levels, MPD_V_100, MPDRMS_V_100.
MIXED ln_mu WITH MPD_V_100 MPD_RMS_V_100
/CRITERIA=CIN(95) MXITER(100) MXSTEP(10) SCORING(1) SINGULAR(0.000000000001) HCONVERGE(0,
ABSOLUTE) LCONVERGE(0, ABSOLUTE) PCONVERGE(0.000001, ABSOLUTE)
/FIXED= MPD_V_100 MPD_RMS_V_100 | SSTYPE(3)
/random intercept | subject(Excel_file) covtype(ID)
/random intercept | subject(Excel_file*Zoekcode) covtype(ID)
/repeated=Measurement | subject(Excel_file*Zoekcode) COVTYPE (DIAG)
/METHOD=ML
/PRINT=CORB COVB G LMATRIX R SOLUTION TESTCOV.

**11: 3 levels lnMPD_V_100.
MIXED ln_mu WITH LN_MPD_V_100
/CRITERIA=CIN(95) MXITER(100) MXSTEP(10) SCORING(1) SINGULAR(0.000000000001) HCONVERGE(0,
ABSOLUTE) LCONVERGE(0, ABSOLUTE) PCONVERGE(0.000001, ABSOLUTE)
/FIXED= LN_MPD_V_100 | SSTYPE(3)
/random intercept | subject(Excel_file) covtype(ID)
/random intercept | subject(Excel_file*Zoekcode) covtype(ID)
/repeated=Measurement | subject(Excel_file*Zoekcode) COVTYPE (DIAG)
/METHOD=ML
/PRINT=CORB COVB G LMATRIX R SOLUTION TESTCOV.


**12: 3 levels, lnMPD_V_100, MPDRMS_V_100.
MIXED ln_mu WITH LN_MPD_V_100 MPD_RMS_V_100
/CRITERIA=CIN(95) MXITER(100) MXSTEP(10) SCORING(1) SINGULAR(0.000000000001) HCONVERGE(0,
ABSOLUTE) LCONVERGE(0, ABSOLUTE) PCONVERGE(0.000001, ABSOLUTE)
/FIXED= LN_MPD_V_100 MPD_RMS_V_100 | SSTYPE(3)
/random intercept | subject(Excel_file) covtype(ID)
/random intercept | subject(Excel_file*Zoekcode) covtype(ID)
/repeated=Measurement | subject(Excel_file*Zoekcode) COVTYPE (DIAG)
/METHOD=ML
/PRINT=CORB COVB G LMATRIX R SOLUTION TESTCOV.
```